Investigating Molecular Mechanisms of Drug Resistance in a 3D Cell Culture Model of Pancreatic Cancer

by

Arthur Lee Brannon III

A dissertation submitted in partial fulfillment
of the requirements for the degree of
Doctor of Philosophy
(Cellular and Molecular Biology)
in the University of Michigan
2017

Doctoral Committee

Associate Professor Marina Pasca di Magliano, Chair
Assistant Professor Benjamin L. Allen
Professor Howard C. Crawford
Professor Ronald J. Koenig
Associate Professor Elizabeth R. Lawlor

Arthur Lee Brannon III

abiii@umich.edu

ORCID iD: 0000-0001-5419-3192

Dedication

To Solange

Acknowledgements

Thank you, Jesus! Five years ago, I could not have imagined the challenges, accomplishments, and overall growth I would experience during this time. I am in great appreciation of my mentor, Dr. Marina Pasca di Magliano as well as those who served on my dissertation committee: Dr. Benjamin Allen, Dr. Howard Crawford, Dr. Ronald Koenig, Dr. Elizabeth Lawlor, and Dr. Andrew Rhim. Their guidance was instrumental completion of this work. They have challenged me to cultivate a deeper understanding of my work and its limitations; furthermore, they have fostered my growth as a scientist and helped me develop skills I will utilize throughout my entire career.

I would also like to thank the many friends who have supported me throughout my journey. Shaza Al-Holou, Chris Alexander, Michael Babbish, Joe Baldwin, Ken Baker, Chris Becker, Andrew Bleeda, Amy Caldwell, Rachel Cherny, Patrick Cooper-McCann, Jooho Chung, Anup Das, Corey Dorris, Xixi Du, Andrew Freddo, Adam Gainsley, Erin Golger, Wayne Gilbert, John Greco, Laurie Beth Griffin, Andrew Guy, Chris Halbrook, Arthur Hartnett, Zach Harvanek, Don Knill, Mangala Iyengar, David Lorberbaum, Germanuel Landfair, Gulrez Mahmood, Aaron Mondry, Jon Mowers, Steve Oliver, Beth Pedersen, Carons, Phillips, Bobby Poulson-Houser, Karen Rodriguez, Gillian Ream Gainsley, David Rogawski, Jake Russell, Trisha Saha, Feodies Shipp III, Travis Sims, Ethan Sperry, Josh Steverman, Ken Takeuchi, Julian Tolesism, Wenpu Trim,

Brian Walsh, Annie Weldon, Corey Williams, Matt Windisch, and Julia Young: all of you have had a profound impact on my well-being, and I am absolutely blessed to know you.

The role that the Pasca lab members played in completion of this work cannot possibly be overstated. Thank you to past and present members: Maeva Adoumie, Dr. Fil Bednar, Esther Chen, Dr. Meredith Collins, Annachiara del Vecchio, Kevin Flannagan, Paloma Garcia, Taylor Harrell, Kevin Kane, Dr. Esha Mathew, Rosa Menjivar, Samantha Saylor, Michael Scales, Dr. Heather Schofield, Marsha Thomas, Dr. Joyce Thompson, Ashley Valez, and Dr. Wei Yan. In particular, I would like to highlight the contributions of Donovan Drouillard and Dr. Yaqing Zhang. Donovan has worked diligently and has made tremendous strides in his growth as a student. His intelligence, passion for science, and assertiveness in presenting his ideas were of great contribution to this work (as well as my sanity). Yaqing has been one of the most encouraging individuals whom I have ever had the pleasure of meeting. She has been a great friend, and she helped me master complicated protocols, troubleshoot antibodies, and was always willing to engage in critical discussion that helped move my project forward.

I would like to express how grateful I am to have a family that is loving, caring, supportive, and resilient. I am so fortunate to have so many examples of amazing people, after whom I model my behavior. Without my family (which has grown considerably since 2012), none of this would have been possible. I would like to thank my grandparents, Arthur Sr. & Betty Jean; my great-aunt Earlene Williams; my aunts and

uncles Terry Brannon, Michelle Williams Miles, Lisa Gowdy, Steve Gowdy, Sheri Owens, Kim & Eric Brannon, Lisa Berkery; and all of my cousins and extended family. I love you all dearly and depend on you a great deal. Thank you to my new in-laws Catherine & Kent Bieberich and their parents Carolyn & Jim and Bob & Lil; as well as Caiti Bieberich & Zack Cagley. Your family is so very blessed, and you all share your love so freely and generously. I would like to thank my parents Trena & Arthur Jr. Your love and lives have been inspirational and essential to my personhood. I cannot imagine my life without you. To my sister Allison; you are one of the most intelligent, most caring people I have ever met. You have so much faith in me, it's overwhelming. I am so fortunate and blessed by our friendship. I wish you and Anthonie the best in your lives together. And to my wife, Valerie: knowing you has transformed my life. At every moment I've doubted myself, you've been there to tell me that I am more than equal the task. You're my best friend, and I can't wait to spend my life with you. I'm so proud of our many accomplishments, and this is just the beginning.

Finally, this dissertation is dedicated to Solange. Her art communicates complex ideas and feelings in a way that resonates with the spirit. When I was working late in the lab, it was her voice and her albums' perfection that motivated me to continue. Furthermore, "Cranes in the Sky" is one of the greatest music videos of all time. If not for Solange, this piece of writing would not exist.

Table of Contents

List of Figures

List of Tables

List of Abbreviations

2D	Two-dimensional
3D	Three-dimensional
ADM	Acinar to ductal metaplasia
AKT	Protein Kinase B
αPKC	The alpha subunit of Protein Kinase C
ANOVA	Analysis of variance
AREG	Amphiregulin
BRAF	v-Raf murine sarcoma viral oncogene homolog B
CA 19-9	Carbohydrate antigen 19-9
CC3	Cleaved Caspase 3
CCL5	C-C Motif Chemokine Ligand 5
Col4	Type IV Collagen
CK19	Cytokeratin-19
DOX	Doxycycline
ECM	Extracellular matrix
EGF	Epidermal growth factor
EREG	Epiregulin
FAKi	Small molecule that inhibits FAK activity
FBS	Fetal Bovine Serum
FU	Fluorouracil
GEMM	Geneticallly engineered mouse model
GM-CSF	Granulocyte macrophage colony-stimulating factor
HB-EGF	Heparin-binding EGF-like growth factor
HBSS	Hank's Balanced Salt Solution
HRP	Horseradish peroxidase
iKras* mouse	p48Cre; TetO-KrasG12D; Rosa26rtTa-IRES-EGFP
ikras*p53* mouse	p48Cre; TetO-KrasG12D; Rosa26rtTa-IRES-EGFP; TP53R172H
IMDM	Iscove's Modified Dulbecco's Medium
IRF3	Interferon Regulatory Transcription Factor-3
JAK	Janus Kinase
KC mouse	p48Cre; LSL-KrasG12D
KPC mouse	p48Cre; LSL-KrasG12D; TP53R172H
KRAS	Kristen rat sarcoma virus, p21 GTPase
LPS	Lipopolysaccharides

MAPK	Mitogen-activated protein kinase
MCP-1	Monocyte chemoattractant protein-1
MEK	MAPK Kinase
MEKi	Small molecule that inhibits MEK activity
MEKi-P	PD325901
MEKi-T	Trametinib aka GSK1120212
MKK	Map kinase kinase
MTT	3-(4,5-dimethylthiazol-2-yl)-2,5-diphenyltetrazolium bromide
NF-kB	Nuclear factor kappa-light-chain-enhancer of activated B cells
PanIN	Pancreatic intraepithelial neoplasia
PBS	Phosphate-buffered saline
PCR	Polymerase Chain Reaction
PDAC	Pancreatic ductal adenocarcinoma
PF	P573228 (FAK inhibitor)
PI3K	Phosphoinositie 3 Kinase
qPCR	Quantitative Polymerase Chain Reaction
SD	Standard deviation
SEM	Standard Error Mean
SEER	Surveillance, epidemiology, and end results program
TBK1	Tank Binding Kinase 1
TGF-β	Transforming growth factor beta

Abstract

Pancreatic cancer is the fourth leading cause of malignancy-related mortality in the United States. Despite decades of intensive research, patient 5-year survival following diagnosis remains below 10%. The high mortality rate can be attributed to lack of effective therapies, and pancreatic cancer resistance to traditional cancer treatment modalities. The goal of this study was to identify molecular mechanisms of pancreatic cancer resistance to treatment and ideally characterize novel drug targets, which may prove efficacious in combating this devastating disease. To achieve this, we optimized a 3D culture model system that utilized Matrigel as a basement membrane mimetic, facilitating cell-to-cell adhesion as well as cell-to-extracellular-matrix interactions, similar to tumor signaling dynamics *in vivo*. In this cell culture system, pancreatic cancer cells recapitulated oncogene addiction and other *in* vivo characteristics of disease. We chose to study the molecular mechanism of MAPK blockade in this 3D culture system and found that pancreatic cancer cells relied on β1 integrin signaling to mediate resistance in the context of MAPK blockade. Furthermore, β1 integrin signaling was found to be necessary for upregulation of MAPK signaling in the absence of extracellular matrix signaling. These findings reveal a novel role for β1 integrin in pancreatic cancer pathogenesis and give insight into the molecular mechanisms that drive disease.

Chapter 1. Introduction to Pancreatic Ductal Adenocarcinoma and Molecular Drivers of Disease

Pancreatic cancer is the third leading cause of malignancy-related mortality in the United States (Siegel et al. 2017). Despite decades of intensive research, the 5-year survival remains below 10%. This high mortality rate can be attributed to lack of effective therapies, and pancreatic cancer resistance to traditional cancer treatment modalities. The goal of my thesis was to identify molecular mechanisms of pancreatic cancer resistance to treatment and to characterize novel drug targets, which may prove efficacious in combating this devastating disease.

Normal Pancreas Physiology

The normal pancreas is a partially retroperitoneal organ, situated posterior to the distal part of the stomach. The head of the pancreas is adjacent to the C-loop of the duodenum, and is connected to duodenum via the pancreatic duct, which excretes digestive molecules into the gastrointestinal tract(Robbins 1994). Normal pancreatic function is required for efficient digestion of food as well as maintenance of blood glucose, mediated by the exocrine pancreas and the endocrine pancreas, respectively. The bulk of pancreatic tissue is comprised of components of the exocrine pancreas (80-85%), which consists mainly of acinar cells and ductal cells(Robbins 1994).

Acinar cells are polarized epithelial cells that produce and secrete digestive enzymes in response to hormonal signals, which are upregulated during feeding and digestion. Digestive enzymes including amylases, lipases, peptidases, and nucleases are packaged in granules, and during fasting, these granules are maintained near the apical membrane (Robbins 1994; Pandol 2012). Acinar cell stimulation by hormonal activation (e.g. secretin or cholecystokinin) induces calcium-mediated granule-membrane fusion at the apical surface and subsequent emptying of the digestive enzymes into pancreatic ducts(Petersen 2009). These ducts form a branched network of tubes that originate at acinar cluster bulbs and merge to form larger ducts, finally terminating in the anatomic pancreatic duct, which joins with the duodenum at the major duodenal papilla. This ductal network is comprised of cuboidal, epithelial pancreatic ductal cells which secrete bicarbonate to neutralize duodenal acidity that occurs during gastric emptying(Grapin-Botton 2005).

The human endocrine pancreas is comprised of approximately 1 million clusters of cells known as the islets of Langerhans, which contain four major cell types: α, β, δ, and PP (pancreatic polypeptide). These cells are differentiated largely in part by their secretory products. The α cells secrete glucagon, a hormone responsible for increasing blood glucose via stimulating liver gluconeogenesis (Quesada et al. 2008); β cells secrete insulin, which induces glucose uptake in muscle and adipose and decreases liver gluconeogenesis, resulting in overall to decreased blood glucose(Bilous & Donnelly 2010); δ cells produce and secrete somatostatin which regulates insulin and glucagon secretion(Jain & Lammert 2009); PP cells express pancreas-specific protein (pancreatic

polypeptide, PP) and their function is largely unknown but thought to play a role in neuronal/vagal regulation of the exocrine pancreas(Katschinski et al. 1992).

Pancreatic Ductal Adenocarcinoma epidemiology and risk factors

The most common malignant neoplasm of the pancreas, and the focus of this study, is Pancreatic Ductal Adenocarcinoma (PDAC), which accounts for approximately 85% of pancreatic neoplasms and 95% of new cases of pancreatic malignancy(Yeo 2015). PDAC is currently the third-leading cause of cancer-related death in the United States, and if recent trends continue, it is projected to become the second-leading cause by 2030(Thall et al. 2017; Rahib et al. 2014). This projection relies on multiple observations, namely: increasing incidence and prevalence of PDAC cases as a result of expanding medical care to previously underserved populations and an increase in number of the aging population; as well as a paucity of effective treatment options for PDAC(Rahib et al. 2014).

Approximately 53,000 patients are diagnosed with PDAC each year, with a median age of diagnosis of approximately 70 years of age(Becker 2014). An estimated 10% of PDAC cases are attributed to genetic/hereditary factors(Bartsch et al. 2012),(Klein 2011; Hoskins et al. 2014). In terms of modifiable risk factors, smoking is the greatest, as it accounts for an estimated 20-35% of PDAC cases (Iodice et al. 2008). Multiple studies suggest alcohol intake correlates with increased risk, and this risk is compounded in heavy drinkers who are more susceptible to chronic pancreatitis, which itself is a risk factor for developing PDAC(Yeo 2015; Raimondi et al. 2010; Pandol & Raraty 2007).

Other risk factors include obesity and diabetes types 1 and 2 (Becker 2014). The median survival following diagnosis is 6 months, and the 5-year survival rate is 6-10% (compared to five year survival of breast cancer: 90%; colorectal cancer: 65%; and lung cancer: 18%) [NIH SEER Database: https://seer.cancer.gov/statfacts/html/pancreas.html]. PDAC is considered especially deadly, and its abysmal 5-year survival rate can be attributed to various factors, including late diagnosis, early metastasis, and a paucity of efficacious treatment options.

Unique Problems in treating pancreatic cancer

There are many clinical aspects of PDAC that contribute to challenges in effective treatment, stemming from unique biology and clinical presentation. The majority of PDAC cases (about 80%) patients present to the clinic with invasive or metastatic disease that precludes the option for potentially curative surgery(Vincent et al. 2011). Early detection of PDAC would theoretically lead to increased survival in a greater number of patients; however diagnosis of early PDAC is difficult to achieve due to the relatively nonspecific symptoms patients experience(Wolfgang et al. 2013). A subset of PDAC patients present to the clinic with painless jaundice with a history of steatorrhea (the presence of excess fatty deposits passed in feces) and weight loss, as PDAC tumors arising in the head of the pancreas can obstruct bile flow, leading to inefficient bilirubin excretion and fat digestion. However, the most common symptoms experienced by PDAC patients largely overlap with those of normal aging: asthenia (general weakness), weight loss, anorexia, and abdominal/epigastric pain(Guillén-Ponce et al. 2017).

Moreover, the methods and practices for screening for PDAC are highly controversial, given the relatively low incidence of PDAC and nonspecific markers of disease.

Currently, screening is primarily recommended in 2 patient sub-populations: patients considered "high-risk" and patients who have been surgically treated for PDAC. Patients who are considered at "high-risk" for PDAC present with recurring bouts of chronic pancreatitis earlier in life (teenage-20s), strong family history of PDAC (diagnosis of two first-degree relatives), or harbor mutation in common tumor suppressors (e.g. CDKN2A, BRCA1, BRCA2)(Das & Early 2017). Screening for these individuals has been found to effectively identify asymptomatic, invasive PDAC (Al-Sukhni et al. 2012). However, screening in these populations has not contributed to an increase in overall long-term survival (Al-Sukhni et al. 2012; Kim et al. 2011). Also, endoscopic methods of screening expose patients to procedural risks and complications that can result in decreased quality of life(Andrew Kistler et al. 2017). These observations taken together contribute to controversy and variability in the field, regarding implementation of screening as a preemptive measure in the treatment of PDAC in the "high risk" population.

Biomarker screening, specifically serum levels of carbohydrate antigen 19-9 (CA 19-9), is not specific for pancreatic disease, as high CA 19-9 levels (>37 U/mL) have been observed in healthy patients and patients with non-malignant disease, leading to low overall positive predictive value (e.g. interstitial fibrosis, biliary tract obstruction, cholangitis, pancreatitis)(Kim et al. 2009; Kim et al. 2004). These results contraindicate

CA 19-9 screening in the healthy, asymptomatic population. Conversely, serum CA 19-9 in newly diagnosed patients can predict tumor invasiveness and overall survival, regardless of treatment modality and can also be used to accurately reflect relapse in patients who have undergone surgery for tumor resection (Poruk et al. 2013; Ballehaninna & Chamberlain 2011). So in these select populations serum CA 19-9 is a useful clinical metric.

Newly diagnosed PDAC patients may qualify for surgical resection. Unfortunately, surgical intervention is an option for only 15-20% of patients due to late-stage diagnosis as well as a stringent set of requirements that involve both tumor progression and patient status(Cascinu et al. 2010). Tumors are clinically characterized on a "spectrum of resectability," which intends to predict the potential for curative surgery. Among the factors that affect resectability, the most impactful are tumor invasion of local nerve tissue and vasculature as well as the presence or absence of metastatic lesions(Windsor & Barreto 2017; Tamburrino et al. 2014; Lopez 2014). Generally, patients who qualify for surgery are those whose primary tumors do not involve critical elements of surrounding nerves or arteries and those who lack metastatic PDAC foci. Following surgery, prognosis is changed significantly but modestly. Median survival of PDAC patients receiving surgical resection is increased from 6 months (untreated) to as much as 11 months with adjuvant chemotherapy (Andrew Kistler et al. 2017; Ueno et al. 2009). In terms of survival, analysis of SEER database from 1973-2009 indicated surgical intervention increased the 5-year survival rate from 6% to 30%(Chakraborty & Singh 2013).

For PDAC patients who present to the clinic with invasive and metastatic disease, chemotherapy is considered a first-line treatment (Yip et al. 2006; Kleeff et al. 2016). Investigation of clinical trials across decades shows that chemotherapy versus supportive care alone significantly increased one-year survival (Yip et al. 2006). The pyrimidine analog fluorouracil (FU) is widely considered a first-line agent, and when in combination with folic acid, irinotecan (topoisomerase inhibitor(Pommier et al. 1994)) and oxaliplatin (platinum-based cytotoxic agent(Raymond et al. 1998)), the treatment regimen is known as FOLFIRINOX, which has been shown to significantly increase survival versus chemotherapy with a single agent(Conroy et al. 2011). However, this combination of chemotherapy causes considerable adverse effects including diarrhea, nausea, and myelosuppression, and it is contraindicated in older patients or patients with various comorbidities. Gemcitabine, a nucleoside analog, is often prescribed for patients who are not candidates for FU treatment. Gemcitabine monotherapy has some clinical benefit, as it decreases patient pain and improves general quality of life, although survival benefit is minimal (Yip et al. 2006; Kleeff et al. 2016; Rothenberg et al. 1996). However, combination of gemcitabine with albumin-bound paclitaxel (abraxane) improves survival in PDAC patients with advanced disease when compared to gemcitabine monotherapy (one year survival 35% vs. 22%, n=861)(Goldstein et al. 2015). While combination gemcitabine/abraxane therapy improved survival, patients also experienced significant adverse effects including neutropenia, leukopenia, and neuropathy(Thota et al. 2014). The overall lack of effective chemotherapy options primarily contributes to the lack of consensus standard-of-care for treating metastatic PDAC.

Due to the clinical failure of chemotherapeutics in the treatment of PDAC, the evaluation of small molecules targeting specific signaling pathways that drive PDAC has become a subject of extensive research. The vast majority of these small molecules target some form of KRAS signaling, a GTPase mutated in 95% of PDAC cases. During development and normal physiology, highly regulated growth factor signaling activates KRAS signaling, facilitating KRAS recruitment and interaction of various effector proteins. In its inactive state, KRAS noncovalently binds guanosine diphosphate (GDP). Upon activation by upstream tyrosine kinases, KRAS undergoes a conformational change that results in exchange of GDP for guanosine triphosphate (GTP) (Cox & Der 2010a). When bound to GTP, KRAS recruits and activates effector substrates at the site of the plasma membrane (Schmick et al. 2014; Rajalingam et al. 2007). The result of effector activation is propagation and amplification of cell signaling that promotes cell growth, survival, and proliferation. With the aid GTPase-activating proteins (GAPs), KRAS enzymatic activity then hydrolyzes GTP, reverting KRAS to its inactive, GDP-bound state. In PDAC, mutations in KRAS lead to improper, dysregulated over-activation of pro-tumorigenic cell signaling programs, leading to neoplasia and malignancy(di Magliano & Logsdon 2013). Activating mutations in KRAS (the most prevalent in PDAC being KRASG12D) impair KRAS-GAP interactions as well as the intrinsic GTPase activity of KRAS, leading to constitutive, aberrant activation of KRAS and subsequent neoplasia (Prior et al. 2012). Although this theory is currently untestable in humans, genetically engineered mouse models (GEMMs) offer insight into the role of KRAS in PDAC pathophysiology(Westphalen & Olive 2012; Gopinathan et al. 2015). Inactivation

of KRAS in various murine species have leads to tumor regression in vivo (Yin et al. 2015; Drosten et al. 2017).Small molecules targeting KRAS molecular signaling at multiple nodes have been developed and tested in PDAC; however, no single-agent administration has led to a significant increase in survival across patient subpopulations(Zeitouni et al. 2016). Thus, an active area of intense research focuses on characterizing the molecular drivers of PDAC, which would ideally reveal feasible targets for effective treatment.

Pancreatic Ductal Adenocarcinoma pathophysiology and current models of disease

PDAC is thought to arise from a stepwise progression of premalignant, neoplastic lesions referred to as pancreatic intraepithelial neoplasias (PanINs)(Brat et al. 1998; Brockie et al. 1998). PanINs are graded histologically by morphologic characteristics, and increasing grade represents increasing prevalence of cellular atypia (e.g. metaplasia, anaplasia, loss of polarization) in the absence of epithelial cell local invasion (Hruban et al. 2008). While these lesions are thought to represent precursors to PDAC disease, PanINs can be found in as high as 50% of the aging population through autopsy analysis, independent of malignancy(Lüttges et al. 1999; Andea et al. 2003). An activating mutation in the GTPase KRAS is found in the vast majority of high-grade PanINs, as well as over 90% of frank PDAC (Löhr et al. 2005; Zeitouni et al. 2016). Higher-grade lesions are associated with an increase in somatic mutations, frequently loss of tumor suppressors such as CDKN2A, TP53, and SMAD4 (Kanda et al. 2012; Hong et al. 2011). A combination of reverse-genetics in mouse modeling of disease as well as in vitro and

xenograft analyses have been used to funcitonally determine which genetic aberrations may play a functional role in PDAC development.

The implementation of genetically engineered mouse models (GEMMs) of PDAC have allowed for experimental investigation into the molecular drivers of disease. Since KRAS was found to be mutated in over 95% of PDAC cases, researchers sought to use reverse-genetics techniques to model PDAC. Numerous mouse models that allow for expression of mutant, oncogenic Kras in the pancreas epithelium have shown that Kras expression leads to neoplastic lesions that are histologically similar to PanINs (Murtaugh 2014; Standop et al. 2001; Strimpakos et al. 2009; Hingorani et al. 2003; Hingorani et al. 2005). Furthermore, additional mutations in tumor suppressors leads to formation of metastatic disease in mice (these metastatic lesions often occur in the same pattern as human PDAC metastases, spreading to the liver, lung and peritoneum)(Hingorani et al. 2005; Aguirre et al. 2003).

GEMMs have also been used to been used to investigate the functional role of the inflammation and tumor microenvironment in disease progression. PDAC tumors in humans and mice are comprised of neoplastic cells, inflammatory cells, collagen, and vascular components (Aguirre et al. 2003; Robbins 1994). Data from GEMM studies suggest that this inflammation positively regulates disease, as oncogenic KRAS and pancreatitis synergize to increase tumorigenicity. These data are consistent with clinical evidence that chronic inflammation is a risk factor for developing PDAC and there are some data suggesting that degree of inflammation correlates with poorer

prognosis(Erkan et al. 2008; Jamieson et al. 2011; Lowenfels et al. 1993). However, there is still considerable controversy, regarding the role of inflammation in PDAC pathogenesis: PDAC tumors have considerable heterogeneity, regarding both histology and invasion of various immune components (e.g. T Cells, myeloid-derived cells)(Collisson et al. 2011; Erkan et al. 2012).

Our lab and others have shown that oncogenic Kras expression is necessary for the progression of precursor and malignant lesions and maintenance of disease in vivo (Collins, Bednar, et al. 2012; Ying et al. 2012). To achieve this, a mouse model of inducible and reversible oncogenic KrasG12D was utilized. Mice with the genotype Ptf1aCre/+; Rosa26rtTa/rtTa; Tet-O-KrasG12D allows for the modulation of oncogenic KrasG12D (Kras*) expression in the response to doxycycline administration (this is a "tet-on" system, so adding doxycycline induces Kras* expression, while removing doxycycline from the system inactivates Kras* expression)(Collins, Bednar, et al. 2012; Sun et al. 2007). Following pancreatitis induction, mice that express iKras* as well as a dominant-negative p53R172H (p53*) develop endogenous, invasive PDAC that metastasizes. Primary tumors as well as metastatic lesions were dependent upon oncogenic Kras* expression for their maintenance and progression, as cessation of doxycycline administration led to lesion regression (Collins, Brisset, et al. 2012). Furthermore, this finding was independently discovered by a separate group(Ying et al. 2012). These results are bolstered by findings that knockdown of KRAS in human PDAC commercial cell lines decreases proliferation and cell survival in vitro. These results

taken together suggest that oncogenic Kras* may play a functional, protumorigenic role in PDAC pathogenesis.

The molecular mechanism by which oncogenic Kras* exerts its effects is a point of significant interest in the field. The GTPase Kras is known to activate a variety of distinct effector signaling pathways that can often counter-regulate each other, and the relative importance of these pathways in PDAC pathogenesis is an area of active research. Histologic evidence from human PDAC tumors indicate the Mitogen Activated Protein Kinase (MAPK) pathway as well as the Phosphoinositide 3-kinase (PI3K) pathway are both overactivated, while data from GEMMs suggest that these pathways play functional roles in the development and maintenance of PDAC. Aberrant expression of constitutively active members of either MAPK or PI3K (BRAFV600E and p110αH1047R , respectively) is sufficient to drive the formation of PanIN lesions in GEMMs; in both cases these PanIn lesions are histologically indistinguishable from PanIns derived from mice that express oncogenic Kras*(Eser et al. 2013; Collisson et al. 2012). Furthermore, pharmacologic inhibition of either pathway in human xenograft assays leads to tumor regression and improved survival in mice(Junttila et al. 2015; Alagesan et al. 2014). These data taken together suggest functional, protumorigenic roles for both MAPK and PI3K signaling pathways in PDAC pathogenesis. However, as mentioned above, targeting of these pathways with small molecules has been unsuccessful in affecting human PDAC. The failure of small molecule inhibition compelled us to more deeply investigate the molecular mechanisms of resistance. I chose to focus on resistance in the context of MAPK blockade, as PI3K inhibitors are poorly

tolerated in patients, while the clinically approved MAPK pathway inhibitor, trametinib, has been shown to be well-tolerated in PDAC patients, especially in combination with gemcitabine (Infante et al. 2014; Greenwell et al. 2017; Waldron et al. 2017).

MAPK signaling

The MAPK pathway was originally characterized through a series of experiments that described a set of unknown intracellular proteins between 35kDa and 42kDa (depending on the cell line and assay) as serine/threonine protein kinases that were targets of tyrosine kinases (Avruch 2007; Ray & Sturgill 1988)-(Cooper et al. 1984; Kohno 1985). In response to administration of various soluble mitogens, (e.g. insulin, epidermal growth factor (EGF), fibroblast growth factor (FGF), platelet-derived growth factor (PDGF)), these proteins became phosphorylated on tyrosine residues relatively quickly (in as few as 5 minutes)(Cooper et al. 1984; Kohno 1985), and tyrosine phosphatase administration led to a reversal of protein phosphorylation as well as decreased proliferation, suggesting a functional role for these targets in mammalian cell division(Anderson et al. 1990). This characteristic was of particular interest in the field, as many models had shown that extracellular mitogen signaling had the ability to transform cells and alter their proliferation(Seger & Krebs 1995). In the past 30 years, the MAPK signaling pathway has been thoroughly characterized in many different cellular systems as well as cell signaling networks. However, this characterization is far from complete. Advancement in technology has allowed for deeper analysis of MAPK signaling and has revealed that its function is highly diverse, depending on upstream signaling(Cargnello & Roux 2011), cell type, and MAPK-independent regulation of

MAPK substrates. MAPK-associated proteins, regulation, and how these features are altered in the pathophysiologic context is an area of research currently being actively pursued. Ideally, elucidation of the molecular dynamics of these pathways would allow for manipulation and treatment of a myriad of maladies whose etiology is thought to be derived from MAPK pathway dysregulation.

MAPK signaling is comprised of a highly coordinated network of protein interactions and modifications that interpret and propagate extracellular signaling, which initiates a series of intracellular signaling cascade events that are thought to be sequential and evolutionarily conserved across various species(Li et al. 2011). MAPK signaling components are constitutively expressed in adult quiescent cells; however, their activation relies highly regulated upstream signaling. Generally, small GTPase (e.g. RAS) activation initiates MAPK signaling(Blenis 1993; Cox & Der 2010b) by recruitment of downstream targets to the membrane(Witzel et al. 2012), increasing their effective concentration: in this way, signaling may be regulated spatially and temporally(Rauch & Fackler 2007). Subsequently, sequential propagation of covalent modification (phosphorylation) occurs in the cytosol with the aid of specific adaptor/scaffolding proteins, ultimately resulting in translocation of a downstream effector (e.g. ERK) to the nucleus to activate nuclear targets and induce expression of target genes(Witzel et al. 2012; Brunet et al. 1999). A central element of MAPK signaling is a sequential signaling cascade that includes 3 kinases. The upstream activators and downstream effects of MAPK signaling are mediated by these specific effectors and their interaction with cell-specific signaling partners. Three major families of MAPK signaling have been described

as: ERK (Raf->MEK->ERK), JNK (MLK->MKK->JNK), and p38 (MLK->MKK->p38)(Zhang & Liu 2002); these families are considered distinct due to the difference in ultimate kinase activation as well as alternative activation by specific upstream extracellular ligand-mediated activation. In general, ERK signaling occurs downstream of growth factor signaling(Shaul & Seger 2007); JNK signaling downstream of stress response; p38 signaling downstream of stress response or cytokine signaling (of note, these distinctions are not absolute and there are many examples of one ligand being able to regulate multiple MAPK signaling pathways, highlighting the complexity of this signaling system). Though effector function varies among different species and cell types, major signaling themes have been characterized and their function in normal tissues and injury response may provide insight into the effects of their dysregulation in malignant disease (Fig. 1.1).

MAPK signaling plays a crucial role in the maintenance of multiple tissue types. In the adult mouse, genetic ablation of MEK1/2 leads to epidermal hypoproliferation as well as loss of barrier function, which is ultimately lethal(Scholl et al. 2007). Conversely, constitutive activation of Ras in keratinocytes leads to epidermal hyperplasia and a decrease in cell differentiation in a skin allograft mouse model(Sutter et al. 1991). In adult Drosophila, intestinal stem cells unable to activate MAPK signaling downstream of EGF fail to divide and show decreased survival, especially in the context of bacterial infection(Sutter et al. 1991; Jiang et al. 2011). The requirement for intact MAPK signaling in tissues that require proliferation for homeostasis seems to be relevant in humans as well. Administration of small molecules that inactivate MAPK signaling,

including vemurafenib (BRAF inhibitor; FDA reference ID: 4084937) and cobimetinib (MEK1/2 inhibitor; FDA reference ID: 3845167), leads to skin rash and diarrhea in a subpopulation of human patients. There is no definitive proof that these adverse effects are due specifically to MAPK blockade (any agent administered to patients may induce "off-target" effects)(Manousaridis et al. 2013); however, given the results of animal studies, an assumption that MAPK blockade causes these adverse events experienced by patients is not unfounded.

Integrins

Integrins are transmembrane glycoproteins that act in heterodimers to mediate bidirectional signaling between the cell and surrounding ECM as well as mediate cell adhesion. Integrins form dimers between α and β subunits--currently in 18 distinct α subunits have been discovered, and 8 distinct β subunits (Zhang & Wang 2012; Belkin & Stepp 2000). These subunits can assemble into at least 24 different integrin heterodimers that bind and react with distinct substrates, which are commonly ECM components (e.g. collagens, laminins, fibrinogen, and fibronectin) (Hynes 2002). Due to the large number of α and β subunit heterodimer combinations, integrin signaling is incredibly diverse. Furthermore, cell-intrinsic factors regulate integrin ability to interact with extracellular ligands, as ectopic expression of the same integrin subunits in 2 different cell lines can result in cells acquiring distinct binding affinities for ECM components (Elices & Hemler 1989). Integrin signaling relies on spatial modification of integrin subunits and conformational change that can be mediated by extracellular ligands or intracellular binding partners(Takagi et al. 2002). Through interaction with extracellular ligands,

conformational change, and cytoplasmic interaction with signal-transducing intracellular proteins, integrins are able to exchange information between the cell and its immediate microenvironment to mediate important cellular processes (e.g. survival, polarization, migration, diapedesis) (Takagi et al. 2002; Campbell & Humphries 2011).

Cytoplasmic substrates of integrin signaling are responsible for propagating downstream signaling. Namely, Focal Adhesion Kinase (FAK) and Integrin Linked Kinase (ILK) have been shown to mediate integrin signaling in various cell types. FAK has been shown to be necessary for recruitment and localization of cytoskeletal proteins to the plasma membrane, regulating focal adhesion as well as migration(Serrels & Frame 2012). Further, FAK has also been shown to positively regulate PI3K signaling(Xia et al. 2004). Similarly, ILK has been shown to be important in the activation of PI3K signaling in the context of growth factor signaling(Serrels & Frame 2012; Dedhar et al. 1999). The molecular mechanisms by which these pathways are activated and the effect of downstream signaling are cell and context specific.

Recently, integrins have gained attention for playing significant roles in the pathogenesis of many different malignancies. The observation that integrin signaling mediates apoptosis resistance as well as metastasis in some cells suggests that integrin signaling may be a viable target in attempting to treat certain cancers(Desgrosellier & Cheresh 2010). In human breast cancer, overexpression of β1 integrin is correlated with poor prognosis (dos Santos et al. 2012)(Gonzalez et al. 1999), and in vitro β1 blockade induces apoptosis of malignant cells. In a murine model of pancreatic β cell cancer,

genetic ablation of β1 integrin led to reduced tumor cell proliferation and senescence in(Kren et al. 2007). Also observed, though, was a greater incidence of cancer cell dissemination into lymph nodes; these cells failed to form viable metastatic colonies, but this observation highlights the complexity integrin signaling in regulating important aspects of carcinogenesis. Regarding PDAC, multiple commercial cell lines overexpress integrin α subunits 1-6 and β subunits; moreover the β1 subunit is found to be constitutively active, mediating adhesion and invasiveness in some PDAC lines(Arao et al. 2000).

Outstanding questions and project goals

In 2013, President Barack Obama signed into law the Recalcitrant Cancer Research Act, which calls upon the National Cancer Institute (NCI) to develop a financial and infrastructural plan to improve research and outcomes in particularly devastating malignancies. These efforts aimed to foster the discovery of effective treatments for "recalcitrant cancer," a legal definition which requires a malignancy to have less than 20% 5-year survival and is estimated to cause the death of at least 30,000 individuals in the United States each year(Rahib et al. 2014). As of 2017, PDAC fits this definition [SEER Database]. The devastating and refractory nature of PDAC is clearly a national burden, and eradication of this disease would improve the quality of life for the general public.

Despite extensive characterization of molecular drivers of PDAC, researchers have yet to develop an effective treatment regimen. The goal of this project was to

develop a 3D culture system that allowed for an efficient, reproducible approach to studying the molecular mechanisms underlying PDAC resistance to small molecule inhibition. We found that PDAC survival in the context of MAPK inhibition in vitro relied on active β1 integrin signaling, suggesting that β1 integrin mediates resistance in this context. These findings will hopefully contribute to elucidating druggable molecular targets in the treatment of this insidious disease.

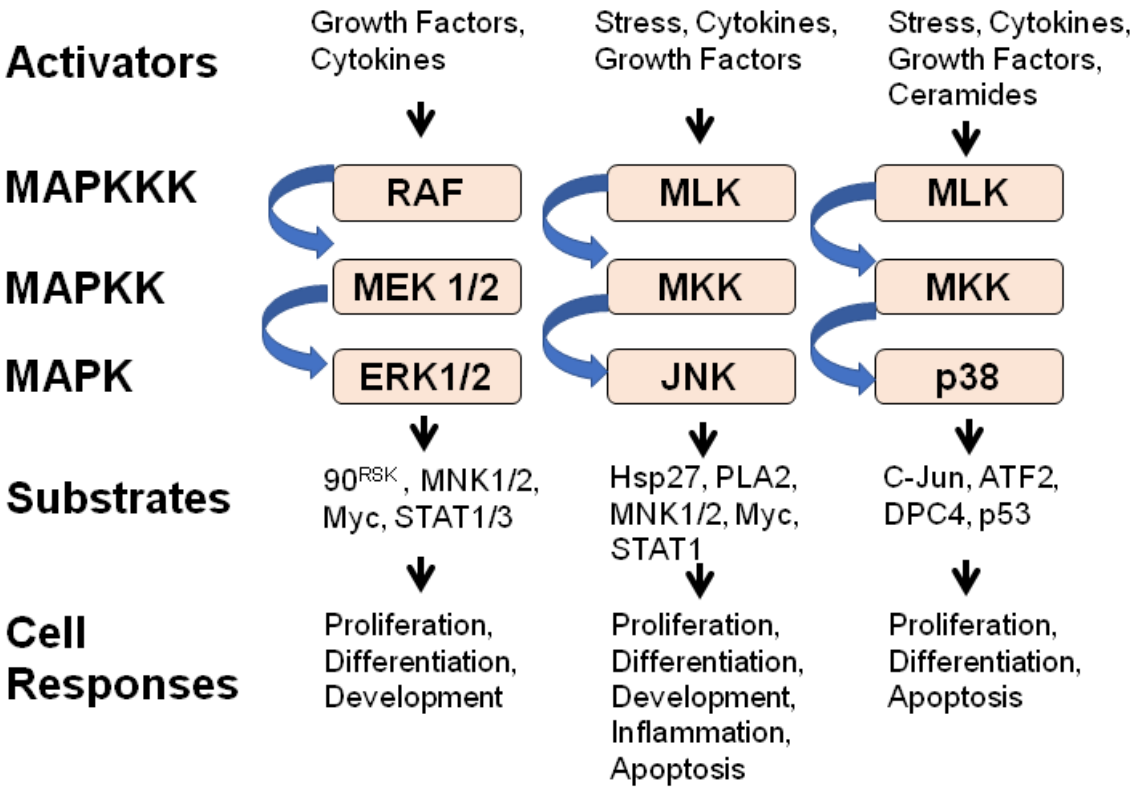

Figure 1.1 MAPK Signaling
Shown here is a simplified schematic of the three major MAPK pathways with activating factors and downstream effectors. MAPK signaling is initiated by a variety of upstream factors, including growth factors, cytokines, and stress signaling. A phosphorylation cascade of downstream effectors (blue, curved arrows) then propagates this signal. Effector signaling terminates in modifying biologic function, including inducing proliferation, differentiation, apoptosis, and others. (Adapted from

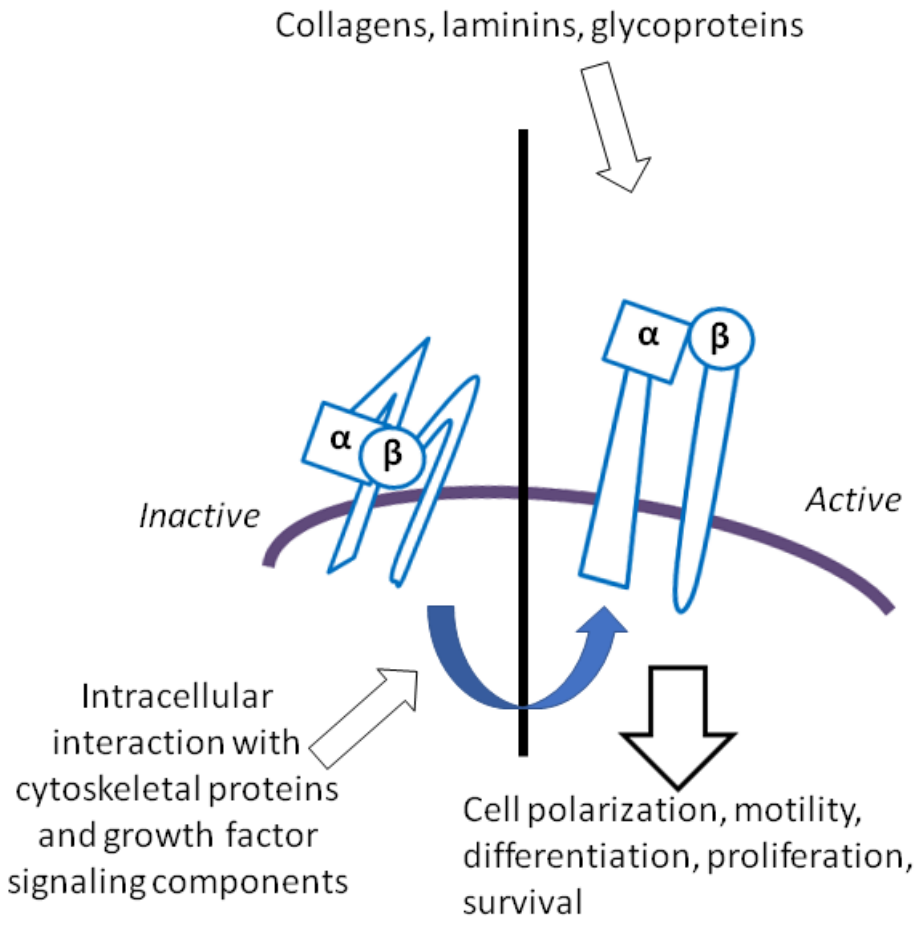

Figure 1.2 Integrin Signaling
Integrins are comprised of two signaling subunits that act as obligate heterodimers to mediate signaling from the extracellular matrix, leading to activation of intracellular targets. Alpha and beta subunits are expressed on the surface of the plasma membrane and must be activated, usually via internal signaling. Upon activation, integrins change conformation, exposing binding sites for extracellular ligands. Integrin interaction with extracellular proteins (e.g. collagens, laminins, glycoproteins) leads to activation of cytoplasmic targets and propagation of downstream signaling, ultimately leading to change in cell function (e.g. polarization, motility, differentiation, proliferation, survival).

References

Aguirre, A.J. et al., 2003. Activated Kras and Ink4a/Arf deficiency cooperate to produce metastatic pancreatic ductal adenocarcinoma. Genes & development, 17(24), pp.3112–3126.

Alagesan, B. et al., 2014. Combined MEK and PI3K Inhibition in a Mouse Model of Pancreatic Cancer. Clinical cancer research: an official journal of the American Association for Cancer Research, 21(2), pp.396–404.

Al-Sukhni, W. et al., 2012. Screening for pancreatic cancer in a high-risk cohort: an eight-year experience. Journal of gastrointestinal surgery: official journal of the Society for Surgery of the Alimentary Tract, 16(4), pp.771–783.

Andea, A., Sarkar, F. & Adsay, V.N., 2003. Clinicopathological correlates of pancreatic intraepithelial neoplasia: a comparative analysis of 82 cases with and 152 cases without pancreatic ductal adenocarcinoma. Modern pathology: an official journal of the United States and Canadian Academy of Pathology, Inc, 16(10), pp.996–1006.

Anderson, N.G. et al., 1990. Requirement for integration of signals from two distinct phosphorylation pathways for activation of MAP kinase. Nature, 343(6259), pp.651–653.
Andrew Kistler, C. et al., 2017. Complications of Upper Endoscopy and Their Management. In Upper Endoscopy for GI Fellows. pp. 105–123.

Arao, S., Masumoto, A. & Otsuki, M., 2000. Beta1 integrins play an essential role in adhesion and invasion of pancreatic carcinoma cells. Pancreas, 20(2), pp.129–137.

Avruch, J., 2007. MAP kinase pathways: the first twenty years. Biochimica et biophysica acta, 1773(8), pp.1150–1160.

Ballehaninna, U.K. & Chamberlain, R.S., 2011. Serum CA 19-9 as a Biomarker for Pancreatic Cancer—A Comprehensive Review. Indian journal of surgical oncology, 2(2), pp.88–100.

Bartsch, D.K., Gress, T.M. & Langer, P., 2012. Familial pancreatic cancer—current knowledge. Nature reviews. Gastroenterology & hepatology, 9(8), pp.445–453.

Becker, A.E., 2014. Pancreatic ductal adenocarcinoma: Risk factors, screening, and early detection. World journal of gastroenterology: WJG, 20(32), p.11182.

Belkin, A.M. & Stepp, M.A., 2000. Integrins as receptors for laminins. Microscopy research and technique, 51(3), pp.280–301.

Bilous, R. & Donnelly, R., 2010. Handbook of Diabetes

Blenis, J., 1993. Signal transduction via the MAP kinases: proceed at your own RSK. Proceedings of the National Academy of Sciences of the United States of America, 90(13), pp.5889–5892.

Brat, D.J. et al., 1998. Progression of pancreatic intraductal neoplasias to infiltrating adenocarcinoma of the pancreas. The American journal of surgical pathology, 22(2), pp.163–169.

Brockie, E., Anand, A. & Albores-Saavedra, J., 1998. Progression of atypical ductal hyperplasia/carcinoma in situ of the pancreas to invasive adenocarcinoma. Annals of diagnostic pathology, 2(5), pp.286–292.

Brunet, A. et al., 1999. Nuclear translocation of p42/p44 mitogen-activated protein kinase is required for growth factor-induced gene expression and cell cycle entry. The EMBO journal, 18(3), pp.664–674.

Campbell, I.D. & Humphries, M.J., 2011. Integrin structure, activation, and interactions. Cold Spring Harbor perspectives in biology, 3(3). Available at: http://dx.doi.org/10.1101/cshperspect.a004994.

Cargnello, M. & Roux, P.P., 2011. Activation and function of the MAPKs and their substrates, the MAPK-activated protein kinases. Microbiology and molecular biology reviews: MMBR, 75(1), pp.50–83.

Cascinu, S. et al., 2010. Pancreatic cancer: ESMO Clinical Practice Guidelines for diagnosis, treatment and follow-up. Annals of oncology: official journal of the European Society for Medical Oncology / ESMO, 21 Suppl 5, pp.v55–8.

Chakraborty, S. & Singh, S., 2013. Surgical resection improves survival in pancreatic cancer patients without vascular invasion- a population based study. Annales de gastroenterologie et d'hepatologie, 26(4), pp.346–352.

Collins, M.A., Brisset, J.-C., et al., 2012. Metastatic pancreatic cancer is dependent on oncogenic Kras in mice. PloS one, 7(12), p.e49707.

Collins, M.A., Bednar, F., et al., 2012. Oncogenic Kras is required for both the initiation and maintenance of pancreatic cancer in mice. The Journal of clinical investigation, 122(2), pp.639–653.

Collisson, E.A. et al., 2012. A central role for RAF→MEK→ERK signaling in the genesis of pancreatic ductal adenocarcinoma. Cancer discovery, 2(8), pp.685–693.

Collisson, E.A. et al., 2011. Subtypes of pancreatic ductal adenocarcinoma and their differing responses to therapy. Nature medicine, 17(4), pp.500–503.

Conroy, T. et al., 2011. FOLFIRINOX versus Gemcitabine for Metastatic Pancreatic Cancer. The New England journal of medicine, 364(19), pp.1817–1825.

Cooper, J.A., Sefton, B.M. & Hunter, T., 1984. Diverse mitogenic agents induce the phosphorylation of two related 42,000-dalton proteins on tyrosine in quiescent chick cells. Molecular and cellular biology, 4(1), pp.30–37.

Cox, A.D. & Der, C.J., 2010a. Ras history. Small GTPases, 1(1), pp.2–27.

Cox, A.D. & Der, C.J., 2010b. Ras history: The saga continues. Small GTPases, 1(1), pp.2–27.

Das, K.K. & Early, D., 2017. Pancreatic Cancer Screening. Current treatment options in gastroenterology. Available at: http://dx.doi.org/10.1007/s11938-017-0149-8.

Dedhar, S., Williams, B. & Hannigan, G., 1999. Integrin-linked kinase (ILK): a regulator of integrin and growth-factor signalling. Trends in cell biology, 9(8), pp.319–323.

Desgrosellier, J.S. & Cheresh, D.A., 2010. Integrins in cancer: biological implications and therapeutic opportunities. Nature reviews. Cancer, 10(1), pp.9–22.

Drosten, M., Guerra, C. & Barbacid, M., 2017. Genetically Engineered Mouse Models of K-Ras-Driven Lung and Pancreatic Tumors: Validation of Therapeutic Targets. Cold Spring Harbor perspectives in medicine. Available at: http://dx.doi.org/10.1101/cshperspect.a031542.

Elices, M.J. & Hemler, M.E., 1989. The human integrin VLA-2 is a collagen receptor on some cells and a collagen/laminin receptor on others. Proceedings of the National Academy of Sciences of the United States of America, 86(24), pp.9906–9910.

Erkan, M. et al., 2008. The activated stroma index is a novel and independent prognostic marker in pancreatic ductal adenocarcinoma. Clinical gastroenterology and hepatology: the official clinical practice journal of the American Gastroenterological Association, 6(10), pp.1155–1161.

Erkan, M. et al., 2012. The role of stroma in pancreatic cancer: diagnostic and therapeutic implications. Nature reviews. Gastroenterology & hepatology, 9(8), pp.454–467.

Eser, S. et al., 2013. Selective requirement of PI3K/PDK1 signaling for Kras oncogene-driven pancreatic cell plasticity and cancer. Cancer cell, 23(3), pp.406–420.

Goldstein, D. et al., 2015. nab-Paclitaxel plus gemcitabine for metastatic pancreatic cancer: long-term survival from a phase III trial. Journal of the National Cancer Institute, 107(2). Available at: http://dx.doi.org/10.1093/jnci/dju413.

Gonzalez, M.A. et al., 1999. An immunohistochemical examination of the expression of E-cadherin, alpha and beta/gamma-catenins, and alpha2- and beta1-integrins in invasive breast cancer. The Journal of pathology, 187(5), pp.523–529.

Gopinathan, A. et al., 2015. GEMMs as preclinical models for testing pancreatic cancer therapies. Disease models & mechanisms, 8(10), pp.1185–1200.

Grapin-Botton, A., 2005. Ductal cells of the pancreas. The international journal of biochemistry & cell biology, 37(3), pp.504–510.
Greenwell, I.B. et al., 2017. Clinical use of PI3K inhibitors in B-cell lymphoid malignancies: today and tomorrow. Expert review of anticancer therapy, 17(3), pp.271–279.

Guillén-Ponce, C. et al., 2017. Diagnosis and staging of pancreatic ductal adenocarcinoma. Clinical & translational oncology: official publication of the Federation of Spanish Oncology Societies and of the National Cancer Institute of Mexico. Available at: http://dx.doi.org/10.1007/s12094-017-1681-7.

Hingorani, S.R. et al., 2003. Preinvasive and invasive ductal pancreatic cancer and its early detection in the mouse. Cancer cell, 4(6), pp.437–450.

Hingorani, S.R. et al., 2005. Trp53R172H and KrasG12D cooperate to promote chromosomal instability and widely metastatic pancreatic ductal adenocarcinoma in mice. Cancer cell, 7(5), pp.469–483.

Hong, S.-M. et al., 2011. Molecular signatures of pancreatic cancer. Archives of pathology & laboratory medicine, 135(6), pp.716–727.

Hoskins, J., Jia, J. & Amundadottir, L.T., 2014. Genetic Susceptibility and Risk of Pancreatic Cancer. In Molecular Diagnostics and Treatment of Pancreatic Cancer. pp. 169–194.

Hruban, R.H., Maitra, A. & Goggins, M., 2008. Update on pancreatic intraepithelial neoplasia. International journal of clinical and experimental pathology, 1(4), pp.306–316.
Hynes, R.O., 2002. Integrins: bidirectional, allosteric signaling machines. Cell, 110(6), pp.673–687.

Infante, J.R. et al., 2014. A randomised, double-blind, placebo-controlled trial of trametinib, an oral MEK inhibitor, in combination with gemcitabine for patients with untreated metastatic adenocarcinoma of the pancreas. European journal of cancer, 50(12), pp.2072–2081.

Iodice, S. et al., 2008. Tobacco and the risk of pancreatic cancer: a review and meta-analysis. Langenbeck's archives of surgery / Deutsche Gesellschaft fur Chirurgie, 393(4), pp.535–545.

Jain, R. & Lammert, E., 2009. Cell-cell interactions in the endocrine pancreas. Diabetes, obesity & metabolism, 11 Suppl 4, pp.159–167.

Jamieson, N.B. et al., 2011. A Prospective Comparison of the Prognostic Value of Tumor- and Patient-Related Factors in Patients Undergoing Potentially Curative Surgery for Pancreatic Ductal Adenocarcinoma. Annals of surgical oncology, 18(8), pp.2318–2328.

Jiang, H. et al., 2011. EGFR/Ras/MAPK signaling mediates adult midgut epithelial homeostasis and regeneration in Drosophila. Cell stem cell, 8(1), pp.84–95.

Junttila, M.R. et al., 2015. Modeling targeted inhibition of MEK and PI3 kinase in human pancreatic cancer. Molecular cancer therapeutics, 14(1), pp.40–47.

Kanda, M. et al., 2012. Presence of somatic mutations in most early-stage pancreatic intraepithelial neoplasia. Gastroenterology, 142(4), pp.730–733.e9.

Katschinski, M. et al., 1992. Cephalic stimulation of gastrointestinal secretory and motor responses in humans. Gastroenterology, 103(2), pp.383–391.

Kim, E.R. et al., 2011. Is health screening beneficial for early detection and prognostic improvement in pancreatic cancer? Gut and liver, 5(2), pp.194–199.

Kim, H.-R. et al., 2009. Increased CA 19-9 level in patients without malignant disease. Clinical chemistry and laboratory medicine: CCLM / FESCC, 47(6), pp.750–754.

Kim, J.-E. et al., 2004. Clinical usefulness of carbohydrate antigen 19-9 as a screening test for pancreatic cancer in an asymptomatic population. Journal of gastroenterology and hepatology, 19(2), pp.182–186.

Kleeff, J. et al., 2016. Pancreatic cancer. Nature reviews. Disease primers, 2, p.16022.
Klein, A.P., 2011. Genetic susceptibility to pancreatic cancer. Molecular carcinogenesis, 51(1), pp.14–24.

Kohno, M., 1985. Diverse mitogenic agents induce rapid phosphorylation of a common set of cellular proteins at tyrosine in quiescent mammalian cells. The Journal of biological chemistry, 260(3), pp.1771–1779.

Kren, A. et al., 2007. Increased tumor cell dissemination and cellular senescence in the absence of β1-integrin function. The EMBO journal, 26(12), pp.2832–2842.

Li, M., Liu, J. & Zhang, C., 2011. Evolutionary history of the vertebrate mitogen activated protein kinases family. PloS one, 6(10), p.e26999.

Löhr, M. et al., 2005. Frequency of K-ras mutations in pancreatic intraductal neoplasias associated with pancreatic ductal adenocarcinoma and chronic pancreatitis: a meta-analysis. Neoplasia , 7(1), pp.17–23.

Lopez, N.E., 2014. Borderline resectable pancreatic cancer: Definitions and management. World journal of gastroenterology: WJG, 20(31), p.10740.

Lowenfels, A.B. et al., 1993. Pancreatitis and the risk of pancreatic cancer. International Pancreatitis Study Group. The New England journal of medicine, 328(20), pp.1433–1437.

Lüttges, J. et al., 1999. Duct changes and K-ras mutations in the disease-free pancreas: analysis of type, age relation and spatial distribution. Virchows Archiv: an international journal of pathology, 435(5), pp.461–468.

di Magliano, M.P. & Logsdon, C.D., 2013. Roles for KRAS in pancreatic tumor development and progression. Gastroenterology, 144(6), pp.1220–1229.

Manousaridis, I. et al., 2013. Cutaneous side effects of inhibitors of the RAS/RAF/MEK/ERK signalling pathway and their management. Journal of the European Academy of Dermatology and Venereology: JEADV, 27(1), pp.11–18.

Murtaugh, L.C., 2014. Pathogenesis of pancreatic cancer: lessons from animal models. Toxicologic pathology, 42(1), pp.217–228.

Pandol, S.J., 2012. The Exocrine Pancreas, San Rafael (CA): Morgan & Claypool Life Sciences.

Pandol, S.J. & Raraty, M., 2007. Pathobiology of alcoholic pancreatitis. Pancreatology: official journal of the International Association of Pancreatology ... [et al.], 7(2-3), pp.105–114.

Petersen, O.H., 2009. Ca2+ signaling in pancreatic acinar cells: physiology and pathophysiology. Brazilian journal of medical and biological research = Revista brasileira de pesquisas medicas e biologicas / Sociedade Brasileira de Biofisica ... [et al.], 42(1), pp.9–16.

Pommier, Y., Tanizawa, A. & Kohn, K.W., 1994. Mechanisms of topoisomerase I inhibition by anticancer drugs. Advances in pharmacology, 29B, pp.73–92.

Poruk, K.E. et al., 2013. The clinical utility of CA 19-9 in pancreatic adenocarcinoma: diagnostic and prognostic updates. Current molecular medicine, 13(3), pp.340–351.

Prior, I.A., Lewis, P.D. & Mattos, C., 2012. A comprehensive survey of Ras mutations in cancer. Cancer research, 72(10), pp.2457–2467.

Quesada, I. et al., 2008. Physiology of the pancreatic -cell and glucagon secretion: role in glucose homeostasis and diabetes. The Journal of endocrinology, 199(1), pp.5–19.

Rahib, L. et al., 2014. Projecting cancer incidence and deaths to 2030: the unexpected burden of thyroid, liver, and pancreas cancers in the United States. Cancer research, 74(11), pp.2913–2921.

Raimondi, S. et al., 2010. Pancreatic cancer in chronic pancreatitis; aetiology, incidence, and early detection. Best practice & research. Clinical gastroenterology, 24(3), pp.349–358.

Rajalingam, K. et al., 2007. Ras oncogenes and their downstream targets. Biochimica et Biophysica Acta (BBA) - Molecular Cell Research, 1773(8), pp.1177–1195.

Rauch, S. & Fackler, O.T., 2007. Viruses, lipid rafts and signal transduction. Signal transduction, 7(1), pp.53–63.

Ray, L.B. & Sturgill, T.W., 1988. Insulin-stimulated microtubule associated protein kinase is detectable by analytical gel chromatography as a 35-kDa protein in myocytes, adipocytes, and hepatocytes. Archives of biochemistry and biophysics, 262(1), pp.307–313.

Raymond, E. et al., 1998. Oxaliplatin: mechanism of action and antineoplastic activity. Seminars in oncology, 25(2 Suppl 5), pp.4–12.

Robbins, S.L., 1994. Robbins Pathologic Basis of Disease, W.B. Saunders Company.

Rothenberg, M.L. et al., 1996. A phase II trial of gemcitabine in patients with 5-FU-refractory pancreas cancer. Annals of oncology: official journal of the European Society for Medical Oncology / ESMO, 7(4), pp.347–353.

dos Santos, P. et al., 2012. Beta 1 integrin predicts survival in breast cancer: a clinicopathological and immunohistochemical study. Diagnostic pathology, 7(1), p.104.
Schmick, M. et al., 2014. KRas localizes to the plasma membrane by spatial cycles of solubilization, trapping and vesicular transport. Cell, 157(2), pp.459–471.

Scholl, F.A. et al., 2007. Mek1/2 MAPK kinases are essential for Mammalian development, homeostasis, and Raf-induced hyperplasia. Developmental cell, 12(4), pp.615–629.

Seger, R. & Krebs, E.G., 1995. The MAPK signaling cascade. FASEB journal: official publication of the Federation of American Societies for Experimental Biology, 9(9), pp.726–735.

Serrels, B. & Frame, M.C., 2012. FAK and talin: who is taking whom to the integrin engagement party? The Journal of cell biology, 196(2), pp.185–187.

Shaul, Y.D. & Seger, R., 2007. The MEK/ERK cascade: from signaling specificity to diverse functions. Biochimica et biophysica acta, 1773(8), pp.1213–1226.

Siegel, R.L., Miller, K.D. & Jemal, A., 2017. Cancer Statistics, 2017. CA: a cancer journal for clinicians, 67(1), pp.7–30.

Standop, J. et al., 2001. Experimental animal models in pancreatic carcinogenesis: lessons for human pancreatic cancer. Digestive diseases , 19(1), pp.24–31.

Strimpakos, A.S., Hoimes, C. & Saif, M.W., 2009. Pancreatic cancer: translating lessons from mouse models. JOP: Journal of the pancreas, 10(2), pp.98–103.

Sun, Y., Chen, X. & Xiao, D., 2007. Tetracycline-inducible expression systems: new strategies and practices in the transgenic mouse modeling. Acta biochimica et biophysica Sinica, 39(4), pp.235–246.

Sutter, C. et al., 1991. v-Ha-ras-induced mouse skin papillomas exhibit aberrant expression of keratin K13 as do their 7,12-dimethylbenz[a]anthracene/12-O-tetradecanoylphorbol-13-acetate -induced analogues. Molecular carcinogenesis, 4(6), pp.467–476.

Takagi, J. et al., 2002. Global conformational rearrangements in integrin extracellular domains in outside-in and inside-out signaling. Cell, 110(5), pp.599–511.

Tamburrino, D. et al., 2014. Selection criteria in resectable pancreatic cancer: a biological and morphological approach. World journal of gastroenterology: WJG, 20(32), pp.11210–11215.

Thall, P.F. et al., 2017. Bayesian nonparametric statistics: A new toolkit for discovery in cancer research. Pharmaceutical statistics. Available at: http://dx.doi.org/10.1002/pst.1819.

Thota, R., Pauff, J.M. & Berlin, J.D., 2014. Treatment of metastatic pancreatic adenocarcinoma: a review. Oncology , 28(1), pp.70–74.

Ueno, H. et al., 2009. A randomised phase III trial comparing gemcitabine with surgery-only in patients with resected pancreatic cancer: Japanese Study Group of Adjuvant Therapy for Pancreatic Cancer. British journal of cancer, 101(6), pp.908–915.

Vincent, A. et al., 2011. Pancreatic cancer. The Lancet, 378(9791), pp.607–620.

Waldron, M., Winter, A. & Hill, B.T., 2017. Pharmacokinetic and Pharmacodynamic Considerations in the Treatment of Chronic Lymphocytic Leukemia: Ibrutinib, Idelalisib, and Venetoclax. Clinical pharmacokinetics. Available at: http://dx.doi.org/10.1007/s40262-017-0529-1.

Westphalen, C.B. & Olive, K.P., 2012. Genetically engineered mouse models of pancreatic cancer. Cancer journal , 18(6), pp.502–510.

Windsor, J.A. & Barreto, S.G., 2017. The concept of “borderline resectable” pancreatic cancer: limited foundations and limited future? Journal of gastrointestinal oncology, 8(1), pp.189–193.

Witzel, F., Maddison, L. & Blüthgen, N., 2012. How scaffolds shape MAPK signaling: what we know and opportunities for systems approaches. Frontiers in physiology, 3, p.475.

Wolfgang, C.L. et al., 2013. Recent progress in pancreatic cancer. CA: a cancer journal for clinicians, 63(5), pp.318–348.

Xia, H. et al., 2004. Focal Adhesion Kinase Is Upstream of Phosphatidylinositol 3-Kinase/Akt in Regulating Fibroblast Survival in Response to Contraction of Type I Collagen Matrices via a β1Integrin Viability Signaling Pathway. The Journal of biological chemistry, 279(31), pp.33024–33034.

Yeo, T.P., 2015. Demographics, epidemiology, and inheritance of pancreatic ductal adenocarcinoma. Seminars in oncology, 42(1), pp.8–18.

Ying, H. et al., 2012. Oncogenic Kras maintains pancreatic tumors through regulation of anabolic glucose metabolism. Cell, 149(3), pp.656–670.

Yin, X. et al., 2015. K-ras-driven engineered mouse models for pancreatic cancer. Discovery medicine, 19(102), pp.15–21.

Yip, D. et al., 2006. Chemotherapy and radiotherapy for inoperable advanced pancreatic cancer. In Cochrane Database of Systematic Reviews.

Zeitouni, D. et al., 2016. KRAS Mutant Pancreatic Cancer: No Lone Path to an Effective Treatment. Cancers, 8(4). Available at: http://dx.doi.org/10.3390/cancers8040045.

Zhang, W. & Liu, H.T., 2002. MAPK signal pathways in the regulation of cell proliferation in mammalian cells. Cell research, 12(1), pp.9–18.

Zhang, Y. & Wang, H., 2012. Integrin signalling and function in immune cells. Immunology, 135(4), pp.268–275.

Chapter 2. Development of a 3D Culture Model of Pancreatic Cancer

Introduction

The technique of maintaining cells in culture to study their behavior has transformed our understanding of cell function as well as cell response to a host of stimuli. In cancer biology, the method has been used to discover fundamental aspects of pathophysiology as well as test the potential effectiveness of a myriad of therapies. Traditional cell culture experiments take advantage of cells' ability to survive ex vivo when supplemented with specific nutrients in a regulated environment. In these assays, cells are grown in a monolayer atop a clear glass or plastic plate to allow for optical clarity. As these techniques were being optimized, it was noticed that cells lacking the ability to adhere to the plate failed to thrive, so cell culture plates were coated with synthetic and biologic material to allow for cell adherence via connection with extracellular, structural proteins(Mitchell et al. 2006; Curtis 1983). While these systems promote cell to survival and proliferation, they do not allow for growth in 3 dimensions (3D). 3D growth is a phenomenon that is near-universal in tissue cells in vivo, and mounting evidence suggests that the cell:cell and cell:ECM interactions that occur play an important role in cell signaling and response to external stimuli (Simian & Bissell 2017; Ravi et al. 2014).

In order to more accurately reflect in vivo characteristics of ultrastructural tissues, 3D culture techniques have been utilized(Vinci et al. 2012). In cancer, recent evidence suggests 3D culture more accurately reflects cancer cell biology and may lead to better prediction of drug action in vivo (Vinci et al. 2012; Imamura et al. 2015). This characteristic is likely due to 3D growth facilitating cell:cell and cell:ECM interactions--these physical, adhesive interactions are known to modulate important aspects of tumorigenesis such as differentiation, proliferation, and resistance to chemotherapy(Farahani et al. 2014; Aoudjit & Vuori 2012; Seguin et al. 2015). This question is of great interest in the field of PDAC, wherein cancer cells are especially resistant to therapy, and efficient, reproducible study of PDAC would ideally lead to better prediction of successful treatment options.

PDAC patient lines have been successfully explanted, grown and passaged in 3D culture and have been shown to recapitulate fundamental aspects of disease (Boj et al. 2015; Longati et al. 2013). In order to study PDAC biology in vitro, we set out to develop and optimize a 3D culture system that would better recapitulate in vivo hallmarks of PDAC; allow for inducible oncogenic Kras* expression; and also allow for efficient, timely study. In order to achieve this, we adapted protocols from in vitro 3D models of breast cancer/development as well as 3D growth of normal acinar explants(Pinto et al. 2011; Lee et al. 2007; Myers et al. 2006; Debnath et al. 2003).

In our system, PDAC cells maintained and passaged in 2D culture are trypsinized and resuspended in single-cell suspension, then plated atop a basement mimetic: Matrigel. Matrigel is a biologic gel product containing elements of the basement membrane that allow for cell:ECM interaction and facilitate cell:cell adhesion and subsequent 3D growth. Using this system, we found that PDAC cells recapitulated fundamental aspects of PDAC biology, including oncogenic Kras* necessity. Thus, we chose to optimize this assay for further investigation and biological characterization of PDAC pathophysiology.

Reagents & Methods

MTT Assay

Cells maintained in 2D were plated 3x103 cells per well in a 96-well plate **Corning Cat# 3595** in Iscove's Modified Dulbecco's Media (IMDM Gibco Cat# 12440053) +10% Fetal Bovine Serum, and specific experimental groups were supplemented with 1µg/mL doxycycline **Sigma Cat# D989**. 48 hours following plating, media was aspirated and discarded. MTT reagent diluted 1:30 in IMDM was added to each well, then the plate was incubated at 37°C for 2 hours. At which point the MTT+media was aspirated and discarded. 120µL dimethyl sulfoxide (DMSO) was added to each well to induce cell lysis. Plates were covered with aluminum foil (this reaction is light-sensitive) then slowly rocked at room temperature for 2 hours. Absorbance at 570nm was detected using a Spectra Max plate reader and quantified with the Spectra Max software. Statistical analysis was performed using Prism software, and two-tailed student's t test was utilized to compare experimental groups.

3D culture assay: "embedded"

Growth-factor-reduced Matrigel is a basement membrane mimetic that is produced by Engelbreth-Holm-Swarm (EHS) sarcoma cells maintained in culture; it is comprised primarily of Type IV collagen, laminins, and entactin(Benton et al. 2011). All 3D culture experiments utilized in this group of studies involve use of growth-factor-reduced Matrigel, so for simplicity, from here on, growth-factor-reduced Matrigel will be referred to as "Matrigel." This gelatinous protein solution is liquid at 4°C and solid at 22°C, and after purchase arrives frozen and is maintained at -20°C. Before use, it is important to thaw on ice or overnight at 4°C--thawing at room temperature or above may lead to premature solidification and subsequent complications in use.

Briefly, in the 3D "embedded" assay, cells were resuspended in single-cell suspension in 1:3 (cell culture media:Matrigel) atop a surface of agarose to prevent invasion and 2D growth (Fig. 2.2A). At the start, Matrigel was thawed overnight at 4°C. Also 1 day prior to plating cells, 0.4% agarose **Sigma Cat# A9539** was boiled and plated 300µL per well in a 24 well plate Sigma **Cat# CLS3526** then cooled at 4°C overnight.

Cells of interest were maintained in 2D in Iscove's Modified Dulbecco's Media aka IMDM **Gibco Cat# 12440053** +10% Fetal Bovine Serum +1µg/mL doxycycline **Sigma Cat# D9891** (if iKras*p53* PDAC cell line). Media from cells in 2D was aspirated and discarded. Then, cells were washed with Hank's Balanced Salt Solution (HBSS) **Gibco Cat# 14025092** (2x2 minutes; of note, phosphate buffered saline (PBS)

can also work here, but the presence of glucose in HBSS likely improves survival of these cells during handling). HBSS was aspirated and discarded, at which point Trypsin solution **Gibco Cat# 2520056** was added to cells. Following incubation, culture media was added in a 1:1 ratio, trypsin:media to inactivate trypsin. Cells were then centrifuged (5 minutes, 180xg relative centrifugal force). Supernatant was discarded and the tube was subjected to mechanical force (5-10 forceful flicks) to disaggregate cells. Then, cells were resuspended in 7-10mL IMDM+10% FBS and prepared for counting via hemocytometer **Sigma Cat# Z359629** or cell countess machine ThermoFisher Countess II FL Automated Cell Counter Cat# AMQAX1000. After, total cells needed for the assay at hand were centrifuged for 5 minutes at 180xg RCF and their supernatant discarded.

Cells were resuspended in Waymouth's media:Matrigel 1:3. Waymouth's media **Gibco Cat# 11220035** was supplemented: + 10% FBS + 1% penicillin/streptomycin **Gibco Cat# 15140122** +100µg/mL soybean trypsin inhibitor **Sigma Cat# T6522** + 1µg/mL dexamethasone **Sigma Cat# D4902**. After, the cell suspension was added to each well (500µL/well) and incubated 10 minutes at 37°C to induce solidification. 500µL warm (approximately 37°C) Waymouth's (+FBS, penicillin/streptomycin, trypsin inhibitor, dexamethasone) was added on top of the solidified Matrigel plug. Media was changed every 2-3 days. To achieve this, liquid media atop the plug was aspirated via micropipette and discarded. Then, fresh 37°C Waymouth's (+FBS, penicillin/streptomycin, trypsin inhibitor, dexamethasone) was added atop the plug.

3D culture assy: "on-top"

Briefly, in the 3D "on top" assay, cells of interest were plated in single-cell suspension atop a surface of growth-factor-reduced Matrigel (Fig. 2.2B). To begin, Matrigel was thawed overnight and pipetted onto the surface of chamber slides (either 100µL 4-well Corning **Cat# 354114** or 50µL in 8-well Corning **Cat# 354108**). Chamber slides were placed atop ice during plating to ensure even spread of Matrigel. After Matrigel plating, chamber slides were incubated at 37°C, inducing solidification.

During Matrigel solidification, cells were prepared for single-cell suspension as described above. Usually, cells that are 50-80% confluent thrive the best in this assay. The amount of cells needed depended on the number of experimental groups as well as optimum plating density (Fig. 2.3C).

After, cells were resuspended in 37°C Waymouth's media **Gibco Cat# 11220035** + 2% Matrigel + 10% FBS + 1% penicillin/streptomycin **Gibco Cat# 15140122** 100µg/mL soybean trypsin inhibitor **Sigma Cat# T6522** + 1µg/mL dexamethasone **Sigma Cat# D4902**. At which point, the cells in single-cell-suspension were added to chamber wells (900µL in 4-well chamber slides, 540µL in 8-well slides) and maintained at 37°C. After 6 hours, cells settled and became anchored to Matrigel, so changing media was performed relatively easily.

Every 2-3 days, media was changed via P1000 micropipette. Chambers were tipped slightly and media was removed slowly from one corner of the chamber well and discarded. After, fresh 37°C Waymouth's media (+FBS, +penicillin/streptomycin, +trypsin inhibitor, + dexamethasone) was added slowly to the well in the same corner to limit cluster or Matrigel disruption.

Quantification of cluster size

To quantify the area of clusters, low-magnification brightfield images were taken (at least 5 per well in a 4-well chamber slide). Photos and ImageJ software were then used to trace clusters (Fig. 2.4B). In order to be traced, clusters needed to be entirely pictured (for example if a fraction of a cluster was out of the photo frame, it was excluded), and clusters needed to be at least 25μm in diameter in order to prevent the inclusion of cellular debris in calculation. After, ImageJ "analyze particles" function was used to calculate the number of clusters and their respective areas.

Fixation, Paraffin Embedding, and Sectioning of 3D culture samples

At experimental endpoints, media was replaced with 3.7% formaldehyde in in chamber wells. Plates were then incubated for at least 2 hours at 22°C. Afterward, formalin was aspirated, and the chambers were removed via the tool included in the chamber well packaging. Matrigel plugs were added to intermediate-sized cryomolds **Sakura Cat#4566** along with 65°C Histogel **ThermoFisher Cat# HG-4000**. Molds with Matrigel samples and Histogel were incubated at 4°C for 15 minutes to induce

solidification of the mold. Then, the Matrigel/Histogel plugs were placed into tissue processing cassettes and submerged in 70% ethanol. Paraffin processing and embedding was performed at the University of Michigan Microscopy and Image Analysis Laboratory. After, paraffin blocks of samples were sectioned into 5μm-thick slices and placed on slides.

Histochemical analysis

Slides were deparaffinized prior to staining. A heated citra antigen retrieval was then performed with "citra plus" reagent **ThermoFisher Cat#NC9755543**, and tissues were blocked with 1% bovine serum albumin solubilized in 1xPBS. Samples were stained overnight at 4°C with corresponding primary antibodies. After a wash with 1xPBS, fluorophore-conjugated secondary antibodies were incubated at 22°C for 90 minutes. Slides were then mounted with Prolong gold +DAPI ThermoFisher **Cat#P36931**. Slides were imaged using either Nikon A-1 Confocal microscope and NIS elements software or Olympus BX-51 microscope and cellSens software.

Results

iKras*p53* cells in 2D culture poorly reflect in vivo PDAC biology

In order to test whether or not iKras*p53* PDAC cells recapitulate oncogenic Kras* necessity, we utilized a viability assay (MTT). In this assay, cells were plated in the absence or presence of doxycycline to inactivate or induce expression of oncogenic Kras*, respectively. After 2 days, cells were then evaluated for viability via their ability

to reduce the yellow MTT into purple-colored Formazan--this reaction is catalyzed by mitochondrial proteins and thought to only occur in viable cells(Mosmann 1983). Doxycycline addition to the media increased viability in one cell line (1012U); however, in the majority of iKras*p53* cell lines, doxycycline addition failed to affect viability (Fig. 2.1B). PDAC cell lines derived from KPC mice were also not affected by doxycycline presence, which is expected, as in these cells doxycycline does not control oncogenic Kras* expression. These results suggested that iKras*p53* cells in 2D culture fail to recapitulate a key characteristic of PDAC biology, as our lab and others have shown in multiple murine in vivo models that oncogenic Kras* is necessary for PDAC cell survival. We hypothesized that a 3D culture model would more accurately reflect in vivo models, as 3D culture allows for cell:cell and cell:ECM signaling that would theoretically be present in in vivo organs but absent in 2D models.

The "on-top" 3D assay is more practical than the "embedded" 3D assay

In order to accomplish growth in 3D, we first sought to test 2 different models that both utilize Matrigel as the basement membrane mimetic. These models are described above and outlined in Fig 2.2 as "embedded" versus "on-top." In the "embedded" model, cells are fully surrounded and physically suspended by solidified Matrigel. In the "on-top" assay, cells are plated atop a Matrigel surface in media that contains 2% Matrigel. Theoretically, the Matrigel precipitates out of solution upon heating and coats the cells, surrounding them completely with the basement membrane mimetic. We found that the brightfield appearance of iKras*p53* cells grown in "embedded" versus "on-top" assays were indistinguishable (Fig 2.2C,D). Also, despite

the fact that the number of cells plated in each well was the same as well as area of the wells (24 well plates and 4-well chamber slides both have surface areas of approximately 1.8cm2), quantification of clusters was more difficult in "embedded" wells. Clusters in "embedded" wells were suspended stochastically in Matrigel and were not all in the same focal plane (Fig 2.2A). Conversely, clusters in the "on-top" assay were technically easier to image, as these clusters were mostly in the same plane because PDAC cells settled atop a Matrigel surface that was of equal height throughout the well (Fig 2.2B). Also, in the "on-top" assay, discrete PDAC clusters formed efficiently and seeding density could be titrated to increase the number of clusters that could be used for size/biochemical analysis as well as limit size variation (Table 2.1). Furthermore, Matrigel is economically burdensome (approximately $370/10mL), so limiting its use would be of benefit. For these reasons we chose to pursue the "on-top" assay for the bulk of the following studies.

iKras*p53* cells in 3D culture recapitulate oncogenic Kras* dependency as well as characteristic features of primary tumor histology

To test whether iKras*p53* cells recapitulate oncogenic Kras* necessity, doxycycline was withheld or added at the time of 3D plating to inactivate or activate expression of oncogenic Kras*, respectively (cells in 2D are maintained in doxycycline to limit selection for cells that express oncogenic Kras* in a doxycycline-independent manner). Brightfield microscopy was then utilized to monitor cluster growth. Cells that expressed oncogenic Kras* grew into large clusters containing multiple layers of cells (Fig. 2.4A,B), while Kras*-off cells did not form large clusters. This result was quantified via analysis described above (Fig. 2.4B). This Kras* dependency was consistent across 5

different iKras*p53* PDAC cell lines, suggesting that cells in 3D culture more accurately reflect in vivo observations than iKras*p53* cells in 2D culture.

Upon histochemical analysis, PDAC cells in 3D culture maintained a similar differentiation status as epithelial cells present in primary tumors. For example, 4668 and 9805 cells are derived from tumors that are described as relatively well-differentiated due to the fact that neoplastic epithelial cells retain some duct-like structure (Fig. 2.6A,C). These characteristics are echoed in 3D, as these cells adopt a cuboidal appearance and form lumen (Fig 2.6K,M). These similarities are not limited to observations in morphology.

Subsequent biochemical analysis via immunofluorescence, we found that 4668 primary tumor tissue expressed the membrane protein E-cadherin, and this E-cadherin expression was also present in subcutaneous allografts as well as clusters in 3D culture (Fig. 2.7A). Conversely, 4292 primary tumor tissue lacked E-cadherin expression, and this finding was consistent across allograft and 3D culture models (Fig 2.7B). Taken together, these data indicate that PDAC cells in 3D culture recapitulate functional aspects of in vivo findings and suggest that the 3D culture assay may be used to provide insight into molecular drivers of PDAC pathophysiology.

Discussion

In this set of experiments, we aimed to develop and optimize a culture system that more accurately reflects in vivo biological characteristics of PDAC than traditional 2D culture. We found that PDAC cells plated in the "on-top" 3D culture assay 1) formed discrete clusters, whose growth was easily quantified via brightfield microscopy and ImageJ analysis; 2) allowed for reproducible oncogenic Kras* dependency, similar to in vivo models; and 3) recapitulated morphologic and biochemical characteristics of primary tumors. These results taken together make a compelling argument for studying PDAC pathophysiology in this model.

3D culture allows for study of cell-autonomous PDAC behavior, and decreases the complexity of in vivo systems. And even though only epithelial cells are present in this system (this differs from "classical" PDAC tumors, which are known to contain many stromal elements, e.g. immune cells, fibroblasts, and vascular components), the ability to fix, section, and stain for the presence of specific biochemical aspects allows for deep analysis of protein expression. Thus, we used this model to investigate mechanisms of drug resistance with some confidence that results of these assays may reflect fundamental aspects of PDAC pathophysiology. Furthermore, this system is simple and the experiments take place over 6-10 days, allowing for rapid testing and analysis of protein expression and subcellular localization via immunohistochemistry.

However, there are some considerations, regarding the technical difficulty of this assay. For example, cells to be plated in 3D are far more sensitive to trypsin incubation than cells in 2D culture. If cells are exposed to trypsin too long (the optimal length of trypsin incubation must be tested empirically, Table 2.2), they will fail to grow clusters, even in the context of oncogenic Kras* expression. (This observation became apparent when I prepared cells for 2D and 3D in the same cohort and found that cells in 2D were unaffected by long trypsin incubation, while cells in 3D failed to thrive.) This observation is likely due to cell reliance on adhesion protein function, as trypsin digests extracellular proteins required for cell:cell and cell:ECM interaction(Akiyama & Yamada 1985). Technical difficulties notwithstanding, the 3D "on-top" model provides a biologically relevant, efficient, powerful tool for studying PDAC cell biology in vitro.

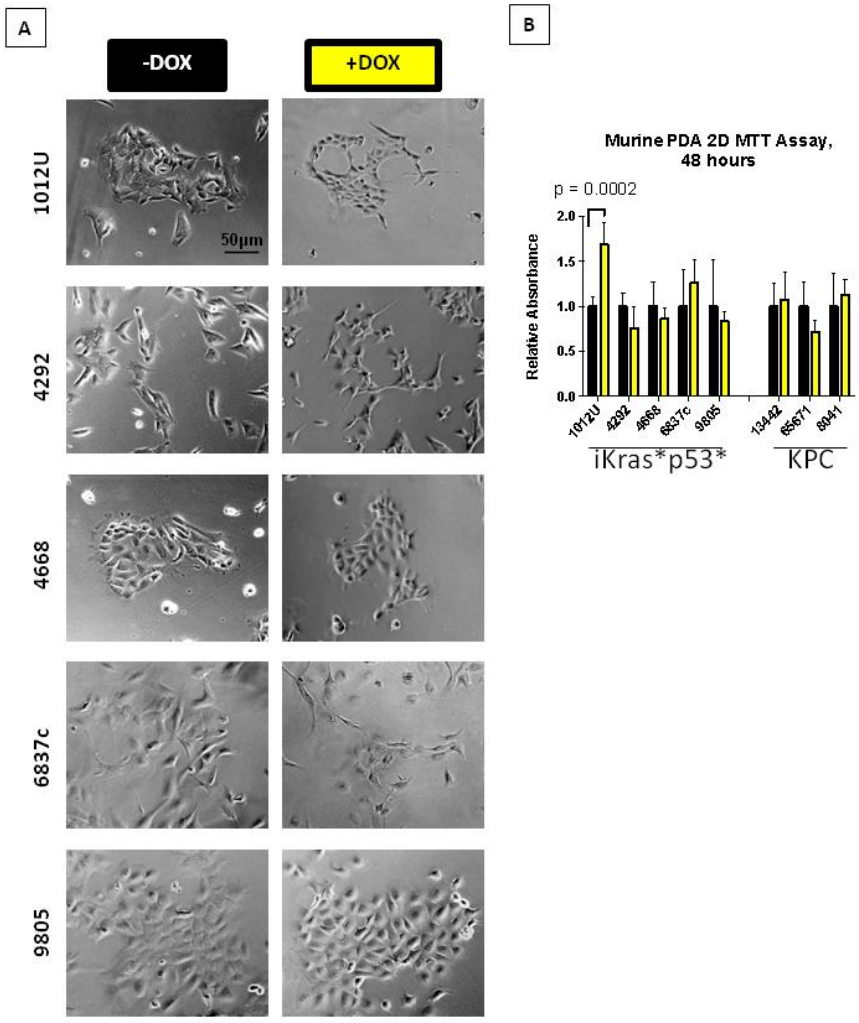

Figure 2.1 iKras*p53* PDAC cell lines fail to recapitulate oncogenic Kras* dependency in 2D.
PDAC cell lines derived from iKras*p53* mice were plated in 2D cell culture in the absence or presence of doxycycline to inactivate or induce expression of oncogenic $Kras^{G12D}$, respectively. 48 hours after plating, cells were evaluated for metabolic activity via MTT assay. (A) Brightfield images of cells in 2D in the absence or presence of doxycycline (1µg/mL) (Kras* off or on, respectively). (B) Quantification of absorbance at a wavelength of 570nm following MTT dye assay. Bars represent relative absorbance mean ± SD of treatment groups plated in technical quintuplicate. Black bars represent no doxycycline (Kras* off) treatment groups; yellow bars represent doxycycline 1µg/mL (Kras* on) treatment groups. "p value" is representative of Student's t test result.

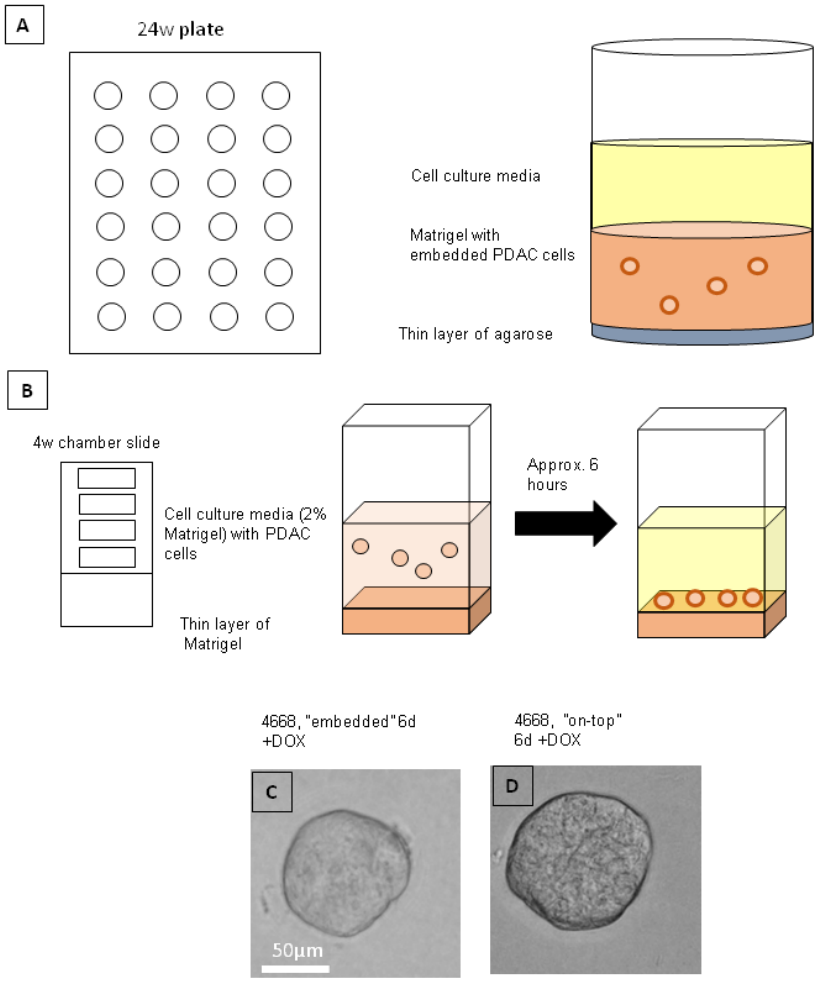

Figure 2.2 Two different cell culture models that facilitate cellular growth in 3D
(A) Top-down view of a 24-well cell culture plate and single well example of the embedded 3D protocol, in which 24-well plates are coated with a thin layer of agarose and topped with PDAC cells in single suspension (1:1, media:Matrigel). Upon solidification of Matrigel, media is added to each well and can subsequently be changed without disturbing cells. (B) Top-down view of 4-well chamber slides and single well example of "on-top" 3D protocol wherein chamber wells are coated with a thin layer of Matrigel and topped with PDAC cells in single suspension (media +2% solubilized Matrigel). In this system, cells sink the bottom of the well in approximately 6 hours and the solubilized Matrigel is thought to coat cells, allowing PDAC cells to become fully surrounded by the basement membrane mimetic. (C,D) Brightfield images of iKras*p53* cells (line 4668) in "embedded" or "on-top" systems, respectively, 6 days post-plating (Kras* on).

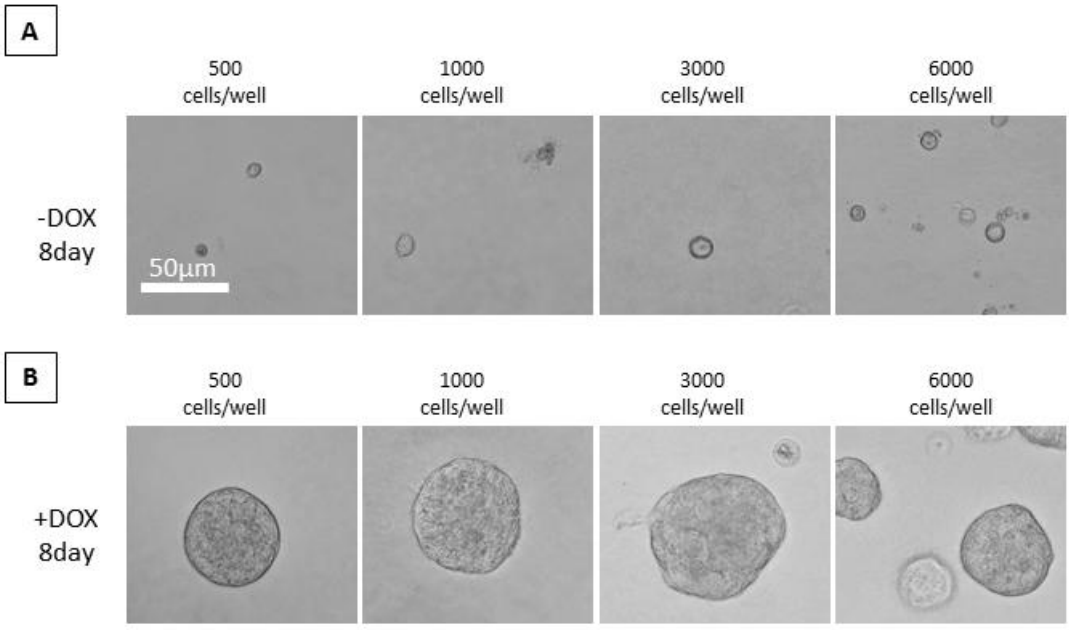

Figure 2.3 Optimizing cell density when plating in a 3D assay
(A,B) Brightfield images of iKras*p53* (9805) cells 8 days after being plated in increasing density in the "on-top" 3D assay in the absence (A) or presence (B) of doxycycline (1µg/mL) to turn Kras* On or Off, respectively. (C) Table of optimum seeding densities of various cell lines in the "on-top" 3D assay in order to achieve discrete cluster formation with limited variation in size, 6-8 days post plating.

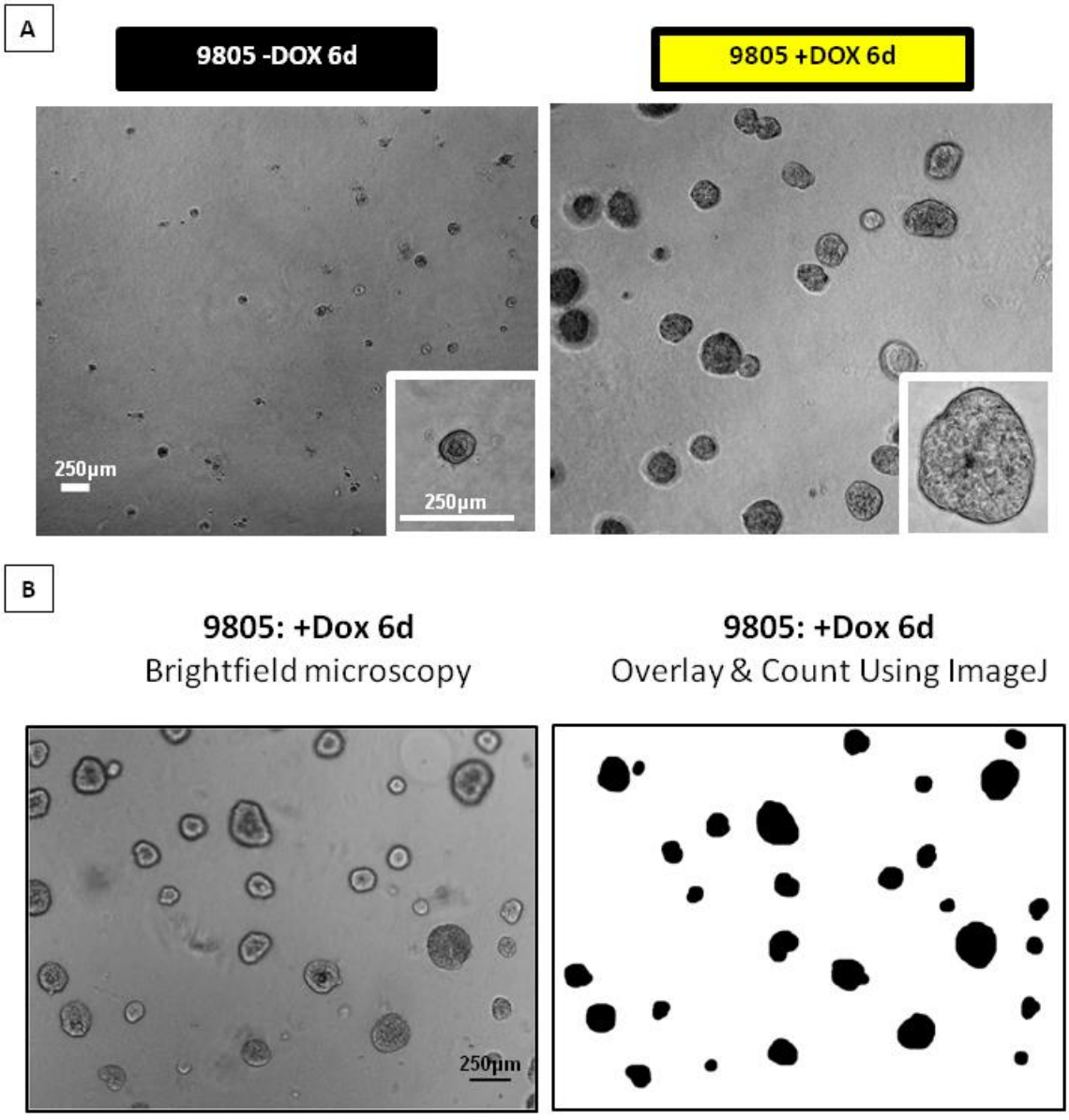

Figure 2.4 iKras*p53* PDAC cells recapitulate oncogenic Kras* dependency *in vitro* in a 3D cell culture model.
(A) Brightfield images of iKras*p53* cells plated in 3D in the absence or presence of doxycycline (1µg/Ml) (Kras* on or off, respectively), 6 days following plating of cells. (B) Example of a tracing overlay of low-magnification images. In quantification of cluster size, a blinded observer (Donovan Drouillard) acquires 5-7 low-magnification images per well and traces clusters in an overlay created in ImageJ (black and white photo). This software can analyze the number and area of each discrete cluster.

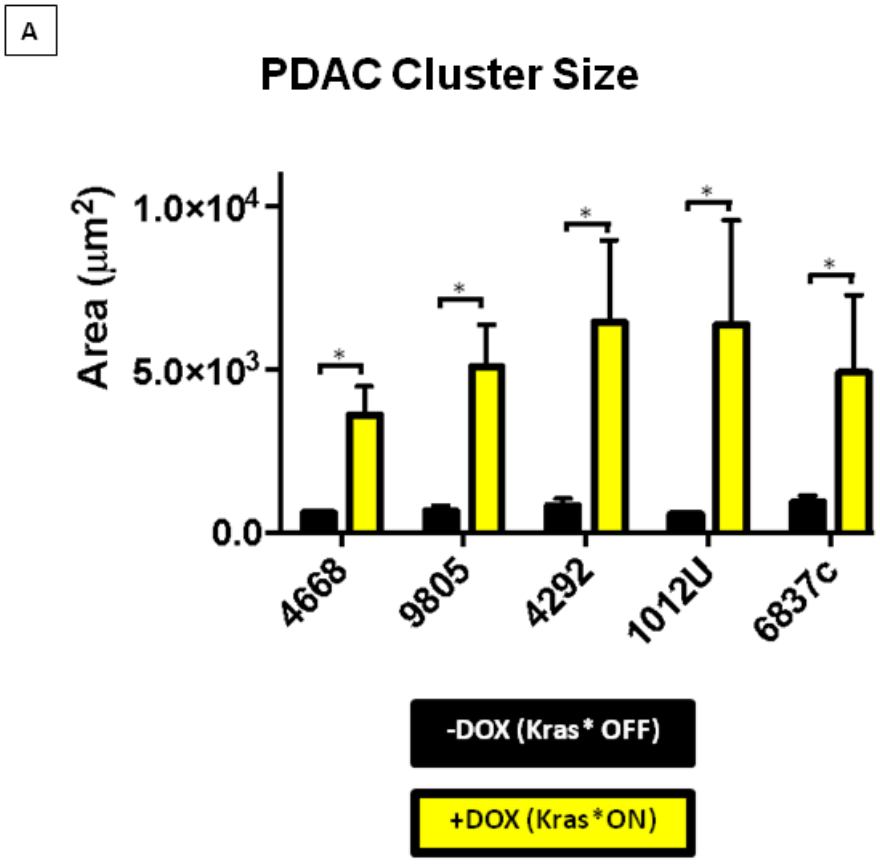

Figure 2.5 Multiple iKras*p53* PDAC cell lines recapitulate oncogenic Kras* dependency *in vitro* in a 3D cell culture model.
Quantification of cluster area size, 6 days following plating thin the absence (black bars) or presence (yellow bars) of doxycycline (1μg/mL). In quantification, at least 100 clusters were traced and quantified in combined duplicate treatment wells. Bars represent average cluster area ± SD. *$p<0.01$ in Student's t test analysis. On the x-axis, each cell line tested has been shown.

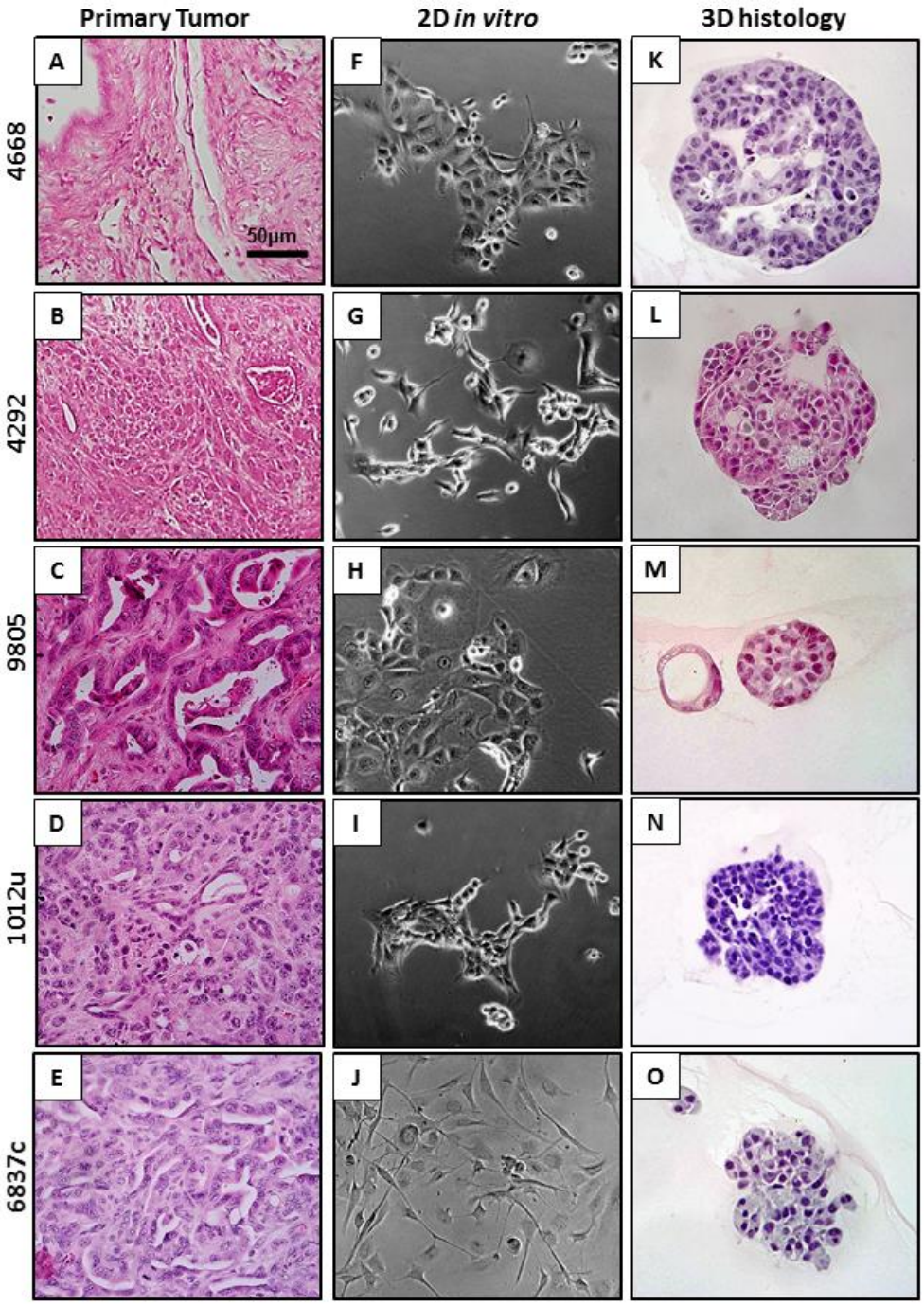

Figure 2.6 PDAC cells harvested from *in vitro* assays display characteristic features of primary tumor histology.
(A-E) Hematoxylin/eosin stain of primary iKras*p53* PDAC tumors. (F-J) Brightfield images of PDAC cell lines in 2D culture, maintained in doxycycline (1µg/mL) (Kras* on). (K-O) Hematoxylin/eosin stain of iKras*p53* PDAC cell cross sections, 6 days following plating in the "on-top" 3D system (cells were also maintained in doxycycline (1µg/mL).

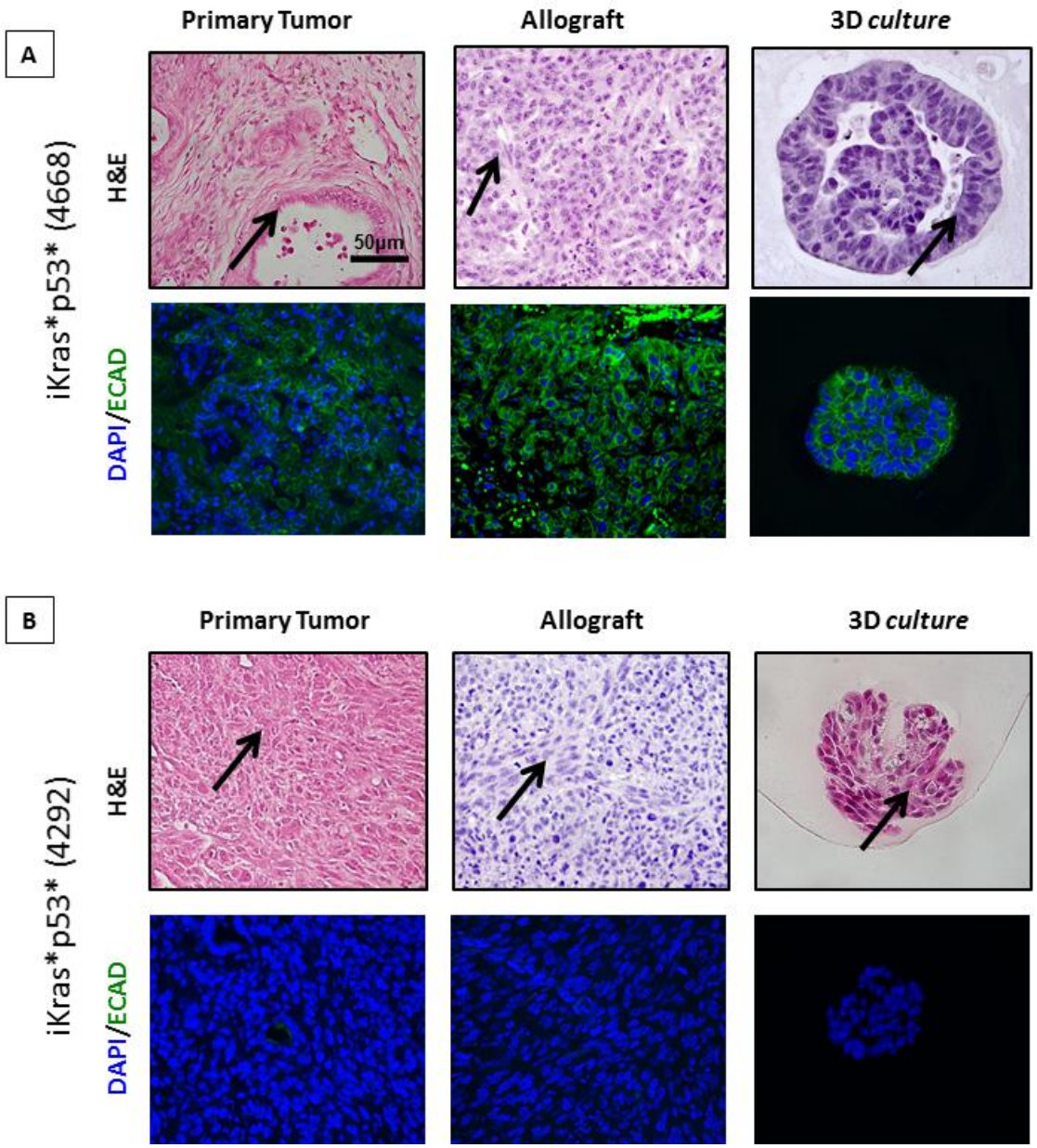

Figure 2.7 PDAC cells *in vitro* biochemically recapitulate *in vivo* expression of plasma membrane protein E-cadherin.
(A) Hematoxylin/eosin and E-cadherin immunofluorescence of iKras*p53* **mouse 4668** primary tumors, subcutaneous tumor allografts, or PDAC cells plated in 3D culture with Kras* on 6 days. (B) Hematoxylin/eosin and E-cadherin immunofluorescence of iKras*p53* **mouse 4292** primary tumors, subcutaneous tumor allografts, or PDAC cells plated in 3D culture with Kras* on 6 days. Arrows point to epithelial cells, highlighting the difference in differentiation/maturation of neoplastic cells in each context.

Cell line	Cell Origin	Optimum Seeding Density ($x10^3$ cells/cm^2)
1012U	iKras*;p53*	4.4
13442	KPC	9.0
4292	iKras*;p53*	4.4
4668	iKras*;p53*	11.8
65671	KPC	3.0
6837c	iKras*;p53*	3.0
7940B	KPC	12.0
8041	KPC	11.8
9805	iKras*;p53*	11.8
UM-5	Human Patient	7.1

Table 2.1 Optimum cell seeding density for 3D assays
Table of optimum seeding densities of various cell lines in the "on-top" 3D assay in order to achieve discrete cluster formation with limited variation in size, 6-8 days post plating.

A

Cell line	Cell Origin	Trypsin Incubation Time (min)	Trypsin Incubation Temperature (°C)
1012U	iKras*;p53*	3	22
13442	KPC	5	22
4292	iKras*;p53*	2	22
4668	iKras*;p53*	7	37
65671	KPC	3	22
6837c	iKras*;p53*	5	22
7940B	KPC	5	22
8041	KPC	5	22
9805	iKras*;p53*	5	22
UM-5	Human Patient	8-10	37

Table 2.2 Optimal incubation parameters for different cell types
(A) Table of optimal trypsin incubation time and temperature, specific to each cell line in order to achieve single-cell suspension and avoid cellular death when transferring cells from a 2D system to a 3D system.

References

Akiyama, S.K. & Yamada, K.M., 1985. The interaction of plasma fibronectin with fibroblastic cells in suspension. The Journal of biological chemistry, 260(7), pp.4492–4500.

Aoudjit, F. & Vuori, K., 2012. Integrin signaling in cancer cell survival and chemoresistance. Chemotherapy research and practice, 2012, p.283181.

Benton, G. et al., 2011. Multiple uses of basement membrane-like matrix (BME/Matrigel) in vitro and in vivo with cancer cells. International journal of cancer. Journal international du cancer, 128(8), pp.1751–1757.

Boj, S.F. et al., 2015. Organoid models of human and mouse ductal pancreatic cancer. Cell, 160(1-2), pp.324–338.

Curtis, A.S., 1983. Adhesion of cells to polystyrene surfaces. The Journal of cell biology, 97(5), pp.1500–1506.

Debnath, J., Muthuswamy, S.K. & Brugge, J.S., 2003. Morphogenesis and oncogenesis of MCF-10A mammary epithelial acini grown in three-dimensional basement membrane cultures. Methods , 30(3), pp.256–268.

Farahani, E. et al., 2014. Cell adhesion molecules and their relation to (cancer) cell stemness. Carcinogenesis, 35(4), pp.747–759.

Imamura, Y. et al., 2015. Comparison of 2D- and 3D-culture models as drug-testing platforms in breast cancer. Oncology reports, 33(4), pp.1837–1843.

Lee, G.Y. et al., 2007. Three-dimensional culture models of normal and malignant breast epithelial cells. Nature methods, 4(4), pp.359–365.

Longati, P. et al., 2013. 3D pancreatic carcinoma spheroids induce a matrix-rich, chemoresistant phenotype offering a better model for drug testing. BMC cancer, 13, p.95.

Mitchell, S.A., Davidson, M.R. & Bradley, R.H., 2006. Glow discharge modified tissue culture polystyrene: role of surface chemistry in cellular attachment and proliferation. Surface Engineering, 22(5), pp.337–344.

Mosmann, T., 1983. Rapid colorimetric assay for cellular growth and survival: application to proliferation and cytotoxicity assays. Journal of immunological methods, 65(1-2), pp.55–63.

Myers, C. et al., 2006. Three-Dimensional Cultures of Normal and Malignant Human Breast Epithelial Cells to Achieve in vivo-like Architecture and Function. In Cell Biology. pp. 139–149.

Pinto, M.P., Jacobsen, B.M. & Horwitz, K.B., 2011. An immunohistochemical method to study breast cancer cell subpopulations and their growth regulation by hormones in three-dimensional cultures. Frontiers in endocrinology, 2, p.15.

Ravi, M. et al., 2014. 3D Cell Culture Systems: Advantages and Applications. Journal of cellular physiology, 230(1), pp.16–26.

Seguin, L. et al., 2015. Integrins and cancer: regulators of cancer stemness, metastasis, and drug resistance. Trends in cell biology, 25(4), pp.234–240.

Simian, M. & Bissell, M.J., 2017. Organoids: A historical perspective of thinking in three dimensions. The Journal of cell biology, 216(1), pp.31–40.

Vinci, M. et al., 2012. Advances in establishment and analysis of three-dimensional tumor spheroid-based functional assays for target validation and drug evaluation. BMC biology, 10, p.29.

Chapter 3. β1 Integrin Signaling Mediates Pancreatic Ductal Adenocarcinoma Cell Resistance to MAPK Inhibition in a 3D Cell Culture Model

Introduction

Pancreatic Ductal Adenocarcinoma (PDAC) accounts for 85% of pancreatic neoplasms, and if the death-to-incidence rates follow recent trends, pancreatic cancer is projected to become the 2nd leading cause of malignancy-related death in the US by 2030 (Smith et al. 2009),(Rahib et al. 2014). Despite extensive research and advancements in the understanding of molecular drivers of disease, the abysmal 5-year survival rate has remained below 10% for over 60 years (Ilic & Ilic 2016). Low survival may be attributed to a paucity of effective treatment options. Surgery, the only potentially curative option (Khorana et al. 2017), improves prognosis modestly (from 5% 5-year survival to 30% (Chakraborty & Singh 2013)). Furthermore, only 10-20% of patients qualify for these procedures due to the high rate of late-stage diagnosis. Radiation therapy and chemotherapy are also largely unsuccessful in eradicating disease. Due to the refractory nature of PDAC to these treatment modalities, molecularly targeted therapy is an alternative that is being actively pursued in the field. A deep understanding of the molecular pathways that govern PDAC pathogenesis would ideally reveal effective targets in the treatment of this devastating disease.

Over 95% of PDAC cases express a mutated form of the GTPase KRAS, a protein whose function requires localization to the inner-leaflet of the plasma membrane (Vincent et al. 2011; Morris et al. 2010). During development and normal physiology, highly regulated growth factor signaling activates KRAS signaling, facilitating KRAS binding to GTP and subsequent activation and recruitment of various effector proteins, ultimately upregulating cell survival, growth, and proliferation. KRAS intrinsic GTPase activity leads to GTP hydrolysis and inactive KRAS. Activating mutations in KRAS (the most prevalent being KRASG12D) impair intrinsic GTPase activity of KRAS, leading to constitutive, aberrant activation of KRAS and subsequent neoplasia (Prior et al. 2012).GEMMs in various species have shown that inactivation of oncogenic Kras leads to tumor regression in vivo (Yin et al. 2015; Drosten et al. 2017). Further, cell culture models isolating both mouse and human patient PDAC lines demonstrate that knockdown of oncogenic KRAS leads to decreased tumor cell proliferation, survival, and metastatic capability (Collins et al. 2012; Ying et al. 2012). These data, taken with the high prevalence of activating KRAS mutations in PDAC, make KRAS an attractive target for therapy.

Unfortunately, efforts to directly inhibit KRAS function have been ineffectual. Because membrane association is necessary for KRAS signaling, early attempts to inactivate mutant KRAS aimed to prevent its localization to the plasma membrane (Appels & M.G.M. Appels 2005). In normal physiology, immediately after synthesis, KRAS undergoes a series of lipid modifications to become tethered to the plasma membrane through farnesylation (Appels & M.G.M. Appels 2005; Casey et al. 1989).

Researchers hypothesized that inhibiting farnesylation through inactivation of the enzyme farnesyltransferase would downregulate KRAS trafficking to the membrane and subsequently downregulate KRAS function. However, results from these studies revealed that KRAS can be directed to the membrane through alternative lipid modification (geranylgeranylation) and can thus bypass farnesyltransferase inhibition (Whyte et al. 1997). The lack of effective KRAS targeting strategies offers a compelling argument for targeting downstream effector pathways of KRAS in the treatment of PDAC.

The relative roles of specific KRAS effector pathways in PDAC pathogenesis is highly controversial and remains to be fully elucidated. Immunohistologic stainings of human PDAC tissues indicate overexpression of the Mitogen-activated protein kinase (MAPK) pathway, as well as the Phosphoinositide Kinase-3 (PI3K) pathway(Ji et al. 2015; Eser et al. 2013). These pathways are both suggested to play a functional and protumorigenic role, as overactivation of either pathway predicts poorer prognosis(Yamamoto et al. 2004; Chadha et al. 2006). Also, in GEMMs, constitutive activation of either MAPK or PI3K specific kinases (BRAF or p110a, respectively), induces the formation of PDAC precursor lesions that are histologically indistinguishable from those that arise via constitutive oncogenic Kras activation(Collisson et al. 2012; Eser et al. 2013). Furthermore, inhibition of either pathway leads to decreased cell proliferation and survival in vitro and in vivo in xenograft models(Williams et al. 2012; Cao et al. 2009). Inhibition of both pathways in conjunction leads to additive anti-tumor effects in GEMMs, as well as increased cell death in in vitro assays that use patient

lines(Roy et al. 2010; Zhong et al. 2015). These data suggest that targeting effector pathways may potentially be successful in treating human PDAC patients.

However, despite early success in PDAC cell culture and xenograft models, small molecule inhibition of the MAPK pathway, the PI3K pathway, or both fail to improve patient outcomes in the clinic due to a number of factors, most of which remain unclear(Barati Bagherabad et al. 2017; Infante et al. 2014). Because the clinically available MEK inhibitor, trametinib, has been found to be well-tolerated in the PDAC patient population, we sought to determine the mechanism by which PDAC cells can survive trametinib treatment. To study cell autonomous mechanisms of resistance, we utilized a three dimensional (3D) in vitro model of PDAC, adapted from similar cell culture models used to study breast cancer. The primary component of this assay is Matrigel, a basement membrane mimetic, comprised of extracellular matrix (ECM) proteins: laminins, Type IV collagen (Col4), and entactin. Matrigel facilitates 3D proliferation and adhesion of cells, similar to those formed in a tumor in vivo; these characteristics of the assay are important, as it's been shown that cell interactions with adjacent cells and adjacent basement membrane can regulate crucial aspects of cancer molecular pathogenesis. One of the signaling molecules that has been found to play a central role in ECM:cell signaling is β1 integrin, a transmembrane, bi-directional signaling molecule that interacts with ECM components and intracellular signaling molecules to engage in outside-in and inside-out signaling. Its function in cancer remains controversial and unclear, as β1 integrin signaling seems to play protumorigenic and anti-tumorigenic roles, depending on cancer type: overexpression of β1 integrin in breast

cancer relates to poor prognosis (dos Santos et al. 2012), while loss of β1 integrin in prostate cancer is associated with poor prognosis and an increased likelihood of disease progression(dos Santos et al. 2012; Pontes-Júnior et al. 2013). Commercial PDAC cell lines express constitutively active β1 integrin, and knockdown leads to decreased tumor growth and metastasis in mice(Grzesiak et al. 2011; Arao et al. 2000).

In this study, we discovered a novel relationship between MAPK and β1 integrin signaling. In a 3D culture system, oncogenic Kras* effector blockade led to decreased cluster growth. Strikingly, upon MEK inhibition PDAC cells adjacent to Matrigel displayed a survival advantage, suggesting that perhaps ECM:cell signaling was responsible for survival in the context of MEK inhibition. We hypothesized that β1 integrin signaling was responsible for mediating this signal, as in the normal pancreas, β1 integrin signaling is necessary to maintain epithelial polarity and survival. Interestingly, we found that β1 integrin blockade decreased oncogenic Kras* effector signaling in non-matrigel adjacent PDAC cells, suggesting a novel role for both β1 integrin signaling and ECM signaling, regarding mediation of oncogenic Kras* effector activation. Furthermore, MEK inhibition synergized with β1 integrin blockade, inducing significantly increased apoptosis. These results taken together suggest β1 integrin plays an active, protumorigenic role in oncogenic Kras* signaling and mediates PDAC cell resistance in the context of MEK inhibition.

Methods

Murine PDAC model and establishment of primary cell cultures

PDAC tumor cell lines from iKras*p53* mice were established(Collins et al. 2012). p48-Cre (Ptf1a-Cre) mice were crossed with TetO-KrasG12D, Rosa26rtTa/rtTa and p53R172H/+ mice to generate p48Cre(Kawaguchi et al. 2002); TetO-KrasG12D(Kawaguchi et al. 2002; Fisher et al. 2001); Rosa26rtTa/+(Kawaguchi et al. 2002; Fisher et al. 2001; Belteki et al. 2005); p53R172H/+(Kawaguchi et al. 2002; Fisher et al. 2001; Belteki et al. 2005; Olive et al. 2004) (iKras*p53*) mice. In adult mice, DOX was administered through the drinking water, at a concentration of 0.2g/L in a solution of 5% sucrose, and replaced every 3–4 days. Three days following DOX administration, pancreatitis was induced through two series of eight hourly intraperitoneal injections of caerulein **Sigma Cat# C9206**, at a concentration of 75 μg/kg, over a 48-hour period, as previously described. Following endogenous tumor formation, tissue was harvested from the primary tumor, minced, and digested with 1 mg/ml collagenase V **Sigma Cat# C9263** at 37°C for 15 minutes. RPMI-1640 **Gibco Cat# 11875** +10% Fetal Bovine Serum +1% penicillin/streptomycin was used to halt digestion and cells were isolated by filtration through a 100 um cell strainer and plated in complete medium containing DOX at 1 μg/mL(Collins et al. 2012).

Cell culture

iKras*p53* PDAC cells were maintained and passaged in 2D culture in IMDM media +10%FBS +DOX 1μg/mL. The 3D assay used was adapted from multiple models. Chamber slides were coated with 50-100μL Matrigel. Afterward, the slides were

incubated for 10 minutes at 37°C to induce solidification of GFR Matrigel. PDAC cells were trypsinized and centrifuged. Pellets were resuspended in single-cell-suspension in Waymouth's media **Gibco Cat# 11220035** + 2% Matrigel + 10% FBS + 1% penicillin/streptomycin Gibco Cat# 15140122 100µg/mL soybean trypsin inhibitor **Sigma Cat# T6522** + 1µg/mL dexamethasone **Sigma Cat# D4902** and the solution was added atop the Matrigel surface. Every 2-3 days, media was changed. In experiments using small molecule inhibitors, inhibitors were solubilized in DMSO or 1xPBS, and vehicle or drug treatment groups were administered in either technical duplicate or triplicate.

Fixation and staining

PDAC clusters were fixed in formalin at 22°C for at least 2 hours. After fixation, chambers from chamber slides were removed, and PDAC clusters in GFR Matrigel were collected and placed in a cryomold with Histogel. These samples were then processed and embedded in paraffin, and cut into 5μm-thick sections. Histology and immunofluorescence were performed as described in Chapter 2.

Imaging and quantification

Brightfield and fluorescent images were acquired with an Olympus BX-51 microscope DP71 digital camera/software as well as Pannoramic SCAN II slide scanner and software. Brightfield, low-magnification images of clusters growing in chamber slides were used to quantify PDAC cluster area. Pictures of at least 5 non-overlapping areas were taken and a blinded observer (Donovan Drouillard) used ImageJ to trace and

measure cluster area. Results indicate the average area of at least 100 unique clusters per treatment group. To quantify cleaved-caspase 3 positivity, a blinded observer (Donovan Drouillard) analyzed cross sections of fixed, sectioned, and stained PDAC clusters. The number of nuclei as well as positive and negative staining was recorded in at least 50 cross sections of unique PDAC cell clusters from 3 biological replicate experiments.Graphpad PRISM software was used to statistically analyze quantification.

Results

Small molecule blockade of Kras* effector pathways decreases Kras*-mediated PDAC growth

Given that PDAC cells in 3D recapitulate oncogenic Kras* dependency (Fig 2.5A), we sought to test whether Kras* downstream effector pathways, specifically MAPK and PI3K, played a functional role in PDAC growth in 3D. In order to test this question, iKras*p53*-derived PDAC cells were grown in 3D for 6 days and then administered small molecule inhibitors that target Kras* effector pathways (Fig 3.1A). Administration of MEK inhibitor PD325901 or PI3K/mTOR inhibitor BEZ235 decreased Kras*-mediated growth in 2 separate iKras*p53* cell lines (4668 and 9805, Fig 3.1B). This growth inhibition was exacerbated by dual inhibition (Fig. 3.1B). These data suggest that in our 3D system, iKras*p53* PDAC cells rely on MAPK and PI3K signaling to induce growth and proliferation, similar to previous findings by many other groups. Strikingly, upon histologic examination, we found that MEK inhibition specifically induced formation of apoptotic lumen, indicated by a disruption of cell membranes in the center of clusters as well as lack of intact nuclei and presence of hyperchromatic debris.

Further, these results were consistent across cell lines and this lumen formation was present in the dual-inhibited clusters (Fig. 3.1D,F). We found that lumen formation was reproducible and dose-dependent, as increasing concentrations of MEK inhibitor PD325901 were associated with increased prevalence of PDAC cross sections with single-layered morphology and lumen that accounted for >75% of the cluster cross section area. These results suggest that MEK inhibition abrogates Kras*-mediated cluster growth as a result of increased apoptosis and perhaps lumen formation is protective for a subset of PDAC cells. To test whether this morphologic phenotype was specific to PD325901 or MEK inhibition, in general, we repeated this experimental setup with a clinically available MEK inhibitor: trametinib.

MEK inhibition via trametinib induces apoptotic lumen formation in iKras*p53* PDAC cells in vitro

To determine whether this apoptotic lumen phenotype was consistent across multiple MEK inhibitors, PDAC cells were grown for 1 week and administered clinically available MEK inhibitor, trametinib (MEKi-T) for 4 days (Fig. 3.3). To visualize any morphologic changes induced by MEK inhibition, PDAC clusters were fixed, sectioned, and stained for hematoxylin and eosin. Similar to clusters treated with MEKi-P, MEKi-T treated clusters were found to have apoptotic lumen--this is evidenced by unorganized hyaline aggregation as well hyperchromatic debris, which indicates nuclear fragmentation, features consistent with cells that undergo programmed cell death (Fig. 3.3C). For a biochemical analysis of apoptosis, sections of PDAC clusters were stained to visualize cleaved caspase-3 (CC3) (Fig. 3.3A,B), as CC3 has been shown to play a pro-apoptotic

role in multiple cell systems. The prevalence of clusters with apoptotic debris that occupied >75% of a single lumen was found to be significantly increased approximately 7-fold following MEK-T administration (Fig. 4D). Taken together, these histologic data suggest that PDAC cells undergo programmed cell death in response to MEK inhibition. The prevalence of single-layer cluster morphology suggests that cells adjacent to the Matrigel basement membrane mimetic may display a survival advantage. In this 3D system, Matrigel coats the entire outside of the cluster in vitro, so following fixation and sectioning, the outermost layer of cells in cluster cross-sections are considered adjacent to the Matrigel (Fig. 2.2). This can be visualized by staining for Type IV collagen (Col4), a primary component of Matrigel and the basement membrane in vivo. Staining reveals Col4 enrichment on the outer edge of clusters treated with either drug vehicle (DMSO) or MEKi-T, suggesting that MEK inhibition does not affect interaction with the basement membrane (Fig. 3.4A). Upon quantification of cells adjacent or non-adjacent to Matrigel, the MEK-T treated clusters showed an increased prevalence of cells adjacent to the Matrigel, suggesting that these cells have a survival advantage over cells that lack ECM signaling (Fig. 3.4B). The phenomenon of programmed cell death in response to lack of ECM signaling is often described as anoikis, and we hypothesized that Matrigel-adjacent cells were able to resist anoikis due to their ability to interact and exchange signals with ECM components.

Human and murine PDAC cells have been shown to engage in complex signaling with the surrounding microenvironment, yet the implications of this signaling and their effects on disease pathogenesis are currently poorly understood. In multiple systems, this

ECM signaling is mediated by a cytoskeleton-/ membrane-associated protein Focal Adhesion Kinase (FAK). FAK is responsible for interpreting and propagating ECM and cell adhesion signaling in many different cell types and its overactivation in malignancy is protumorigenic in various models of disease. We originally hypothesized that FAK may have been responsible for mediating survival in Matrigel-adjacent PDAC cells in the context of MEK inhibition.

To test whether FAK was active in our cells we used Western blot analysis to visualize active, phosphorylated FAK in iKras*p53* 9805 cells cultured in 2D (immunostaining for phosphorylated FAK was unsuccessful via immunohistochemistry or immunofluorescence, data not shown). We found that expression of FAK's active, phosphorylated species was present in 9805 cells, but targeting with both FAK inhibitor PF-573228 and Sigma FAK Inhibitor 14 administration were unsuccessful (Fig. 3.5), regarding inhibiting FAK activation (phosphorylated FAK is a target of itself, so successful inhibition would theoretically lead to decreased phosphorylated FAK). Due to the failure of PF-573228 and FAK inhibitor 14 to target FAK in our system, we chose to use a different FAK inhibitor, VS-4718, to test the functional relevance of FAK activity in the context of 3D PDAC growth. iKras*p53* PDAC cells (4668 or 9805) were grown in 3D for 7 days and then treated for 4 days with VS-4718, trametinib, or a combination of the agents.

We found that VS-4718 administration had no effect on 4668 cluster size (Fig. 3.6A) but decreased PDAC cluster growth in 9805 cells (Fig. 3.6B), suggesting that FAK

activity may play a functional role in Kras*-mediated growth in our model. However, upon histologic analysis, we found that FAK inhibition via VS-4718 was unsuccessful in targeting surviving cells in the context of MEK inhibition. Thus, it is unlikely that Matrigel-adjacent PDAC cells utilize FAK signaling as a mechanism of MAPK blockade resistance. Therefore, we shifted our focus to exploring other upstream components of ECM:cell signaling. One of the most attractive targets we chose to explore was β1 integrin, a transmembrane, bidirectional signaling molecule.

β1 integrin has been implicated in coordinating cell-to-cell and cell-to-ECM interactions and is overexpressed in PDAC. Furthermore, in the normal murine pancreas, β1 integrin expression is necessary for maintaining epithelial cell polarity and its ablation leads to decreased epithelial cell survival and tissue deterioration. In our 3D system, we found that iKras*p53* PDAC cells highly express β1 integrin (Fig. 3.7 C,M), and this expression is not affected by administration of MEKi-T (Fig. 3.7 H,R). Given that Matrigel-adjacent PDAC cells show a survival advantage and express β1 integrin, we hypothesized that β1 integrin signaling mediated survival in this population.

Singular B1 integrin blockade affects cell membrane dynamics and decreases KRAS effector signaling in PDAC clusters

The function of β1 integrin is highly dependent upon cell type as well as the cell's immediate microenvironment. To determine the functional importance of β1 integrin signaling in our 3D culture model, PDAC clusters were grown for 7 days and treated with either solubilized immunoglobulin G (IgG) or a β1 integrin neutralizing

antibody for 4 days. Because antibodies are sterically hindered from crossing cell plasma membranes, the β1 integrin neutralizing antibody specifically blocks β1 integrin outside-in signaling. Following administration of either IgG or β1 integrin neutralizing antibody, cells were fixed, sectioned histologically analyzed.

After 4 days of treatment with control IgG, brightfield microscopy of PDAC clusters formed distinct colonies with smooth and ordered interactions with the surrounding Matrigel (Fig. 3.8A). β1 integrin blockade induced structural disorder of PDAC clusters in their interaction with surrounding Matrigel as well as induced some disintegration of clusters, as evidenced by an increase in scattered, single cells (Fig. 3.8B). Upon histological analysis, PDAC clusters treated with IgG formed disorganized colonies with 1 or multiple lumen (Fig. 3.8 C-F); conversely, β1 integrin blockade abrogated lumen formation (Fig. 3.8 G-J), suggesting that β1 integrin outside-in signaling is necessary for PDAC cell:cell adhesion and formation of higher ordered 3D structure.

To evaluate the effects of β1 integrin blockade on Kras* effector signaling, experimental PDAC cluster cross sections were IF-analyzed. Following administration of control IgG, PDAC clusters demonstrated activation of MAPK and PI3K signaling in Matrigel-adjacent and non-Matrigel-adjacent cells indicated by positive staining of pERK and pS6 (Fig. 3.9B, 8L). Strikingly, following β1 integrin blockade, Kras* effector signaling was restricted to Matrigel-adjacent cells (Fig. 3.9G, 8Q). Though β1-integrin-blocked PDAC clusters showed some localization of β1 integrin to the ECM (Fig. 3.9H, 8R), colocalization of β1 integrin and pERK or pS6 signals was rare (Fig. 3.9I, 8S).

These results suggest that β1 integrin signaling is necessary for PDAC upregulation of Kras* downstream signaling in the absence of ECM signaling in our system. Furthermore, β1 integrin outside-in signaling is dispensable for Kras* effector signaling, if cells are physically adjacent to the ECM.

β1 integrin blockade sensitizes cells to MEK inhibition-induced apoptosis

Prior studies have demonstrated that epithelial cell lumen formation is an active process that requires both cell:cell adhesion and cell:ECM signaling. Since lumen formation appears to be protective for PDAC cells in the context of MEK inhibition (Fig. 3.2) and β1 integrin is necessary for lumen formation in our model, we hypothesized β1 integrin signaling blockade would prevent lumen formation and potentiate the ability of MEK inhibition to induce apoptosis. To test this question, PDAC cells were grown in 3D for 7 days and treated for 4 days with vehicle (DMSO+IgG), MEK-T, an anti-β1 integrin neutralizing antibody, or a combination of the compounds. Subsequently, PDAC clusters were fixed, sectioned and prepared for immunofluorescent analysis.

Singular administration of either MEK-T or anti-β1 integrin neutralizing antibody increased apoptosis, as indicated by increased CC3 staining (Fig. 3.10I-L). Results from blinded observer (Donovan Drouillard) quantification of CC3 staining indicates that dual blockade significantly increased apoptosis, compared to either MEK inhibition or β1 integrin singular blockade (Fig. 3.10Q).. These results taken together suggest that β1 integrin signaling mediates PDAC resistance to MEK inhibition; however there is a small,

subpopulation of cells able to withstand dual inhibition, likely due to their physical interaction with the surrounding ECM.

Discussion

The relative importance of cell:cell adhesion and cell:ECM signaling in PDAC pathophysiology are issues being actively addressed in the field, as a growing body of evidence suggests that these signaling networks are vast and important for key functions of tumorigenicity (Senthebane et al. 2017; Venning et al. 2015; Zent & Pozzi 2005; Lu et al. 2012). Comprehensive elucidation of these pathways may provide insight into mechanisms that regulate disease persistence, which would ideally lead to practical, effective molecular targeting and eradication of disease. This study sought to provide insight into molecular mechanisms that regulate PDAC cell resistance to small-molecule inhibition of MAPK signaling, using a 3D culture system that incorporates ECM elements that are present in vivo in both normal and pathologic contexts. Our results show that MEK inhibition induced lumen formation in iKras*p53*-mouse-derived PDAC cells in vitro. Furthermore, the presence of CC3-positive lumen, suggests that MEK inhibition sensitizes PDAC cells to anoikis, programmed cell death in response to detachment from the ECM(Taddei et al. 2012). These results are not surprising, given that (1) constitutive MEK/ERK signaling prevents anoikis in vitro in multiple normal cell types, and (2) MAPK pathway inhibition has been shown to increase apoptosis in human PDAC cell lines in a 2D Poly[2-hydroxyethyl methacrylate] (polyHEMA) model of anoikis, wherein cells are plated atop a cell dish surface that hinders cell:cell and cell:ECM interactions(Galante et al. 2009; Paoli et al. 2013). We also found that lumen

formation as well as PDAC cell survival in the context of MEK inhibition were significantly decreased following β1 integrin neutralizing antibody administration, suggesting that PDAC resistance to MEK inhibition is mediated in some part by β1 integrin signaling.

Strikingly, singular blockade of β1 integrin decreased Kras* effector signaling in cells lacking ECM attachment but failed to decrease MAPK or PI3K signaling pathway activation in Matrigel-adjacent PDAC cells. These data suggest 2 novel findings in relation to iKras*p53* PDAC cell biology in vitro: (1) cells lacking ECM interaction require β1 integrin to upregulate downstream effectors of Kras* and (2) ECM-adjacent cells upregulate Kras*-effector signaling in a β1 integrin-signaling-independent manner. These results are surprising, in light of the fact that β1 integrin is widely known to transmit signals from the ECM rather than cell:cell adhesions. However, the β1 integrin signaling requirement of non-ECM-adjacent cells to activate downstream Kras* signaling may reflect of the importance of membrane dynamics in mutant Kras* signaling, as Kras* effector pathway activation has been found to be dependent upon its ability to recruit signaling substrates to a scaffold complex at the plasma membrane localization, and here we've observed β1 integrin blockade clearly disrupts membrane and cell:cell dynamics (Hancock & Parton 2005).

Alternatively, β1 integrin signaling requirement of non-ECM-adjacent cells may occur due to β1 integrin signaling function in PDAC cell exchange of soluble growth factor signaling. β1 integrin signaling is necessary for sustained MAPK signaling in

fibroblasts, and β1 integrin signaling has been found to play a pivotal role in TGF-β signaling, a factor known to play a role in PDAC pathogenesis(Cabodi et al. 2004; Bhowmick et al. 2001; Truty & Urrutia 2007). Regardless of the mechanism of β1 integrin-mediated activation of Kras* signaling, results from this study suggest that β1 integrin signaling plays a role parallel to upstream of Kras* in activating Kras* effector signaling, as oncogenic Kras* expression is insufficient in activating MAPK or PI3K signaling pathways in the context of β1 integrin blockade.

The fact that β1 integrin signaling is not required to activate ECM-adjacent PDAC cell Kras* effector signaling is puzzling, as β1 integrin has been found to have functional relevance in PDAC adhesion to ECM components and subsequent PDAC tumorigenicity. Our results suggest that ECM signaling, independent of the β1 integrin signaling axis, is responsible for upregulating Kras* effector signaling in vitro.. The role of ECM:PDAC cell signaling has been extensively studied, but remains poorly characterized, especially in the context of drug resistance. In terms of β1 integrin-independent ECM signaling, some groups have found that β3 integrin may regulate ECM:PDAC signaling and important aspects of PDAC pathophysiology, specifically metastasis in vivo(Desgrosellier et al. 2009). These results suggest that subunit-specific signaling my modulate different characteristics of PDAC biology and interaction with the microenvironment. Extensive characterization of integrin subunit expression and activation would ideally reveal the molecular mechanism by which PDAC cells utilize integrin signaling to promote tumorigenesis.

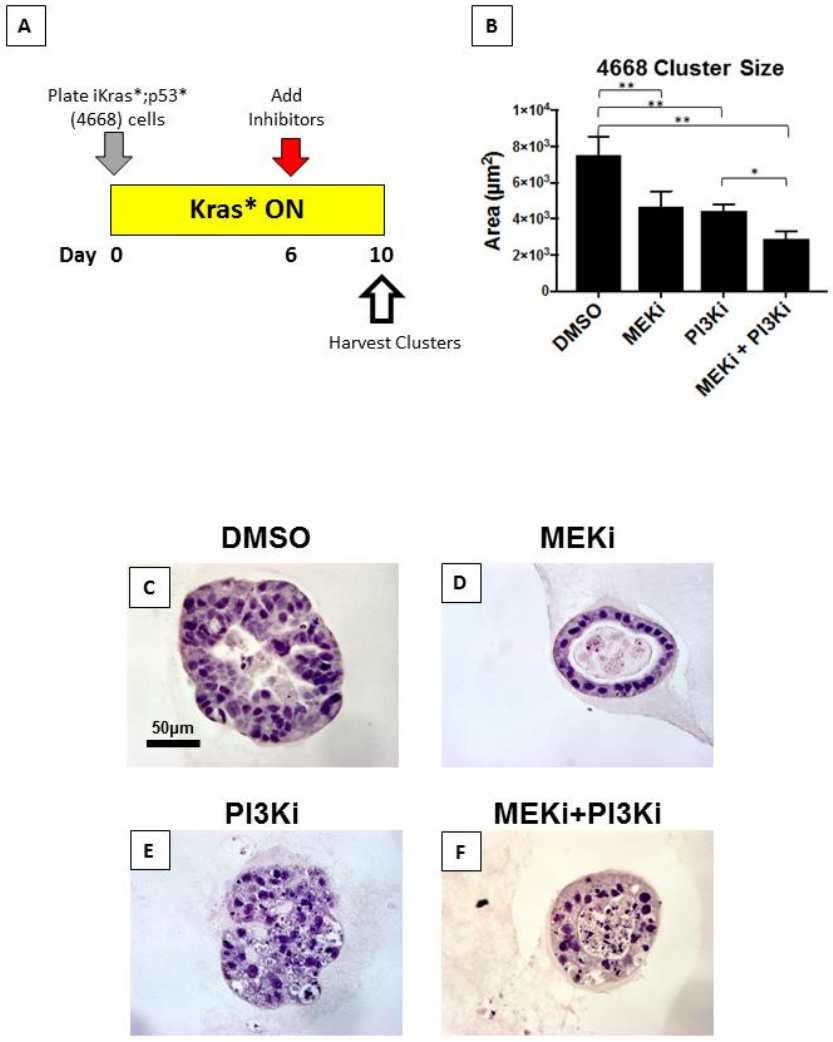

Figure 3.1a Small-molecule-induced blockade of oncogenic Kras* effector pathways in iKra*p53* PDAC cells in a 3D cell culture model (4668 cell line)
(A) Experimental scheme for growing iKras*p53* PDAC cells in 3D culture for 6 days then treating them for 4 days with small molecule inhibitors (MEKi=PD325901; PI3Ki=BEZ235). (B) Quantification of cluster size at day 10. (C-F) Hematoxylin/eosin-stained representative cluster cross sections of experimental groups. *p<0.05, **p<0.01, n.s. not significant, Student's t test.

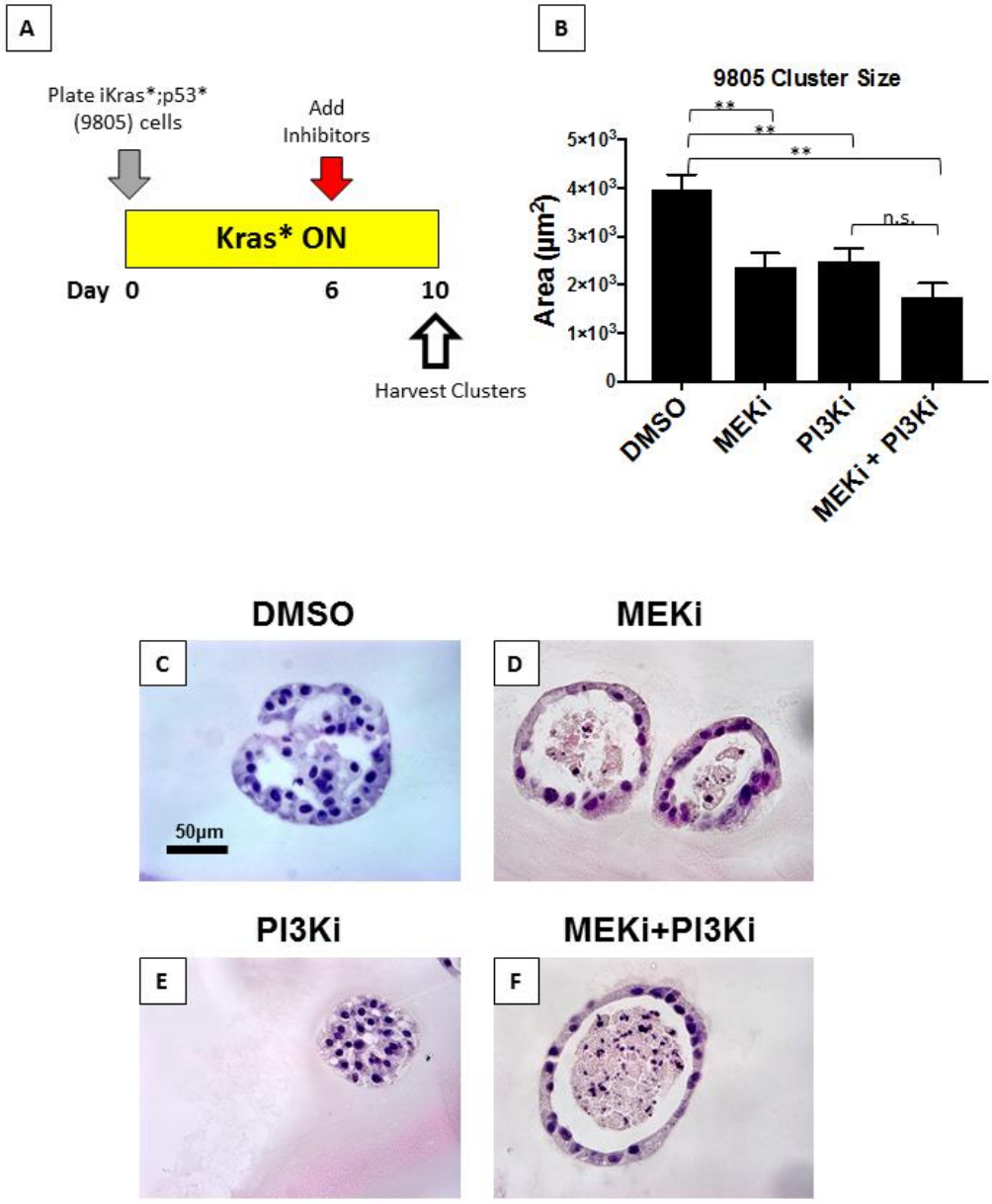

Figure 3.1b Small-molecule-induced blockade of oncogenic Kras* effector pathways in iKra*p53* PDAC cells in a 3D cell culture model (9805)

(A) Experimental scheme for growing iKras*p53* PDAC cells in 3D culture for 6 days then treating them for 4 days with small molecule inhibitors (MEKi=PD325901; PI3Ki=BEZ235). (B) Quantification of cluster size at day 10. (C-F) Hematoxylin/eosin-stained representative cluster cross sections of experimental groups. *p<0.05, **p<0.01, n.s. not significant, Student's t test.

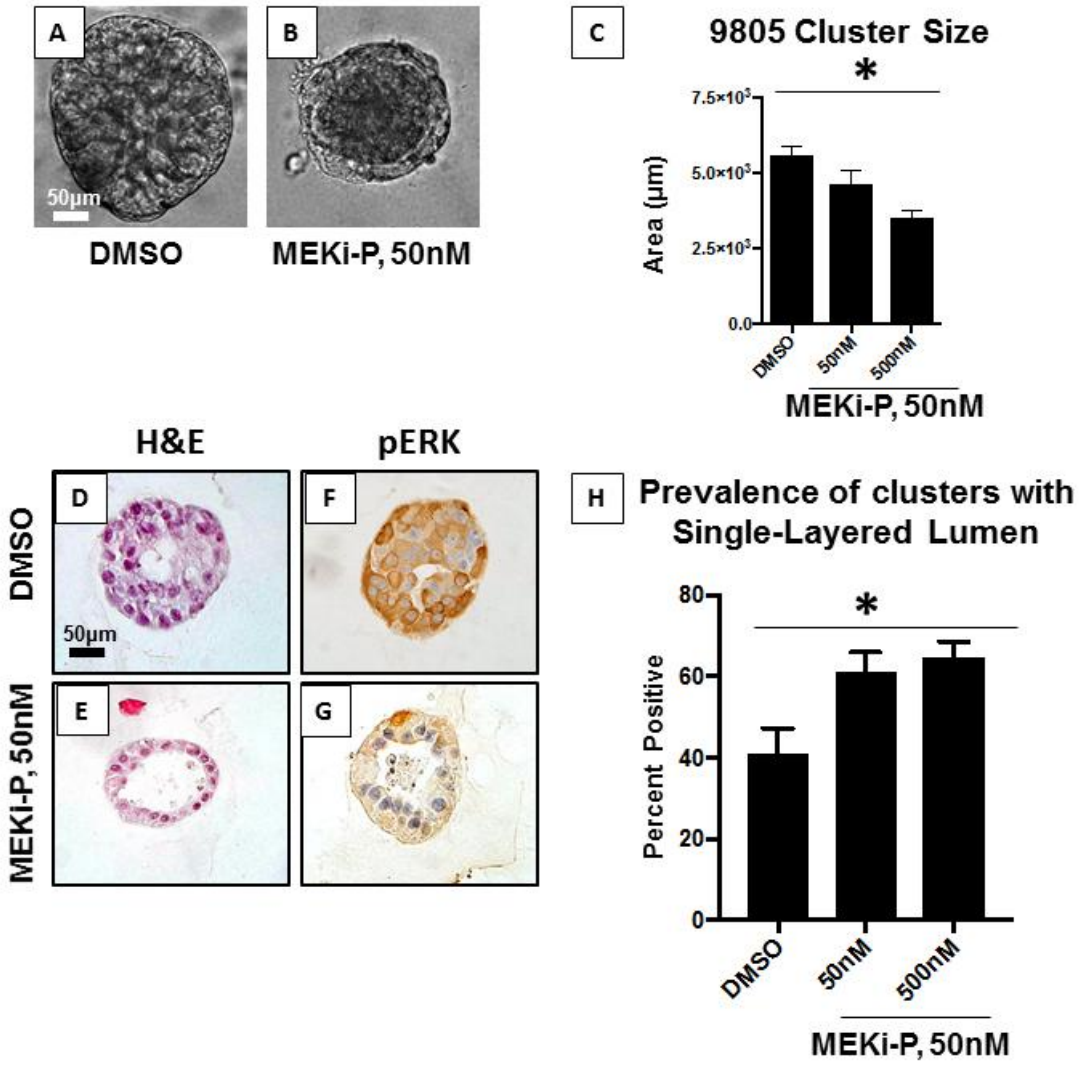

Figure 3.2 MAPK inhibition abrogates Kras*-mediated growth and induces lumen formation.

iKras*p53* PDAC cells (9805) were grown in 3D culture for 6 days and treated with increasing concentrations of MEKi-P (PD325901) for 4 days (Kras*on the entire experiment). (A,B) Brightfield, top-down images of 9805 PDAC cell *in vitro*, 4 days post treatment. (C) Quantification of cluster area, 4 days post treatment; at least 100 clusters per treatment group were analyzed. Bars represent cluster area mean ± SEM. ANOVA statistical analysis; * indicates $p<0.01$. (D,E) Hematoxylin/eosin stains of representative cluster cross sections. (F,G) Immunohistochemical staining of phosphorylated ERK at Thr202 and Tyr204 (pERK); brown dye indicates positive staining. (H) Quantification of cluster cross sections with a single layer of epithelial cells adjacent to the Matrigel as well as lumen that accounts for >75% of the cluster area. Over 50 cluster cross sections per treatment group were analyzed. Bars represent single layer cluster prevalence per technical replicate, mean ± SEM. ANOVA statistical analysis; * indicates $p<0.01$.

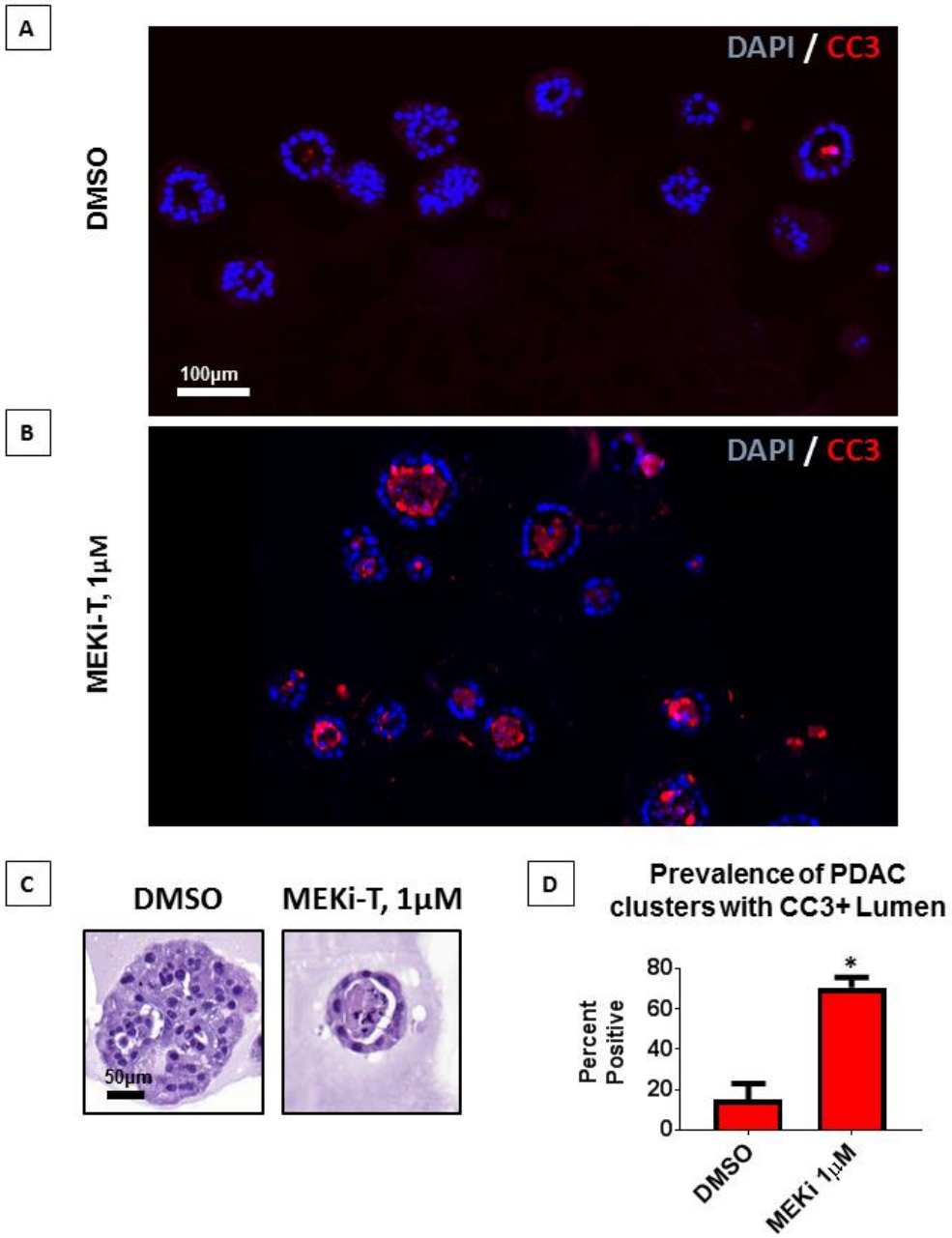

Figure 3.3 MAPK inhibition induces apoptotic lumen formation.
iKras*p53* PDAC cells (9805) were grown in 3D culture for 6 days and then treated with the MEK inhibitor trametinib (MEK-T) for 4 days (Kras*on the entire experiment). (A,B) Immunofluorescence staining of cleaved caspase 3 (CC3) in red, indicating apoptosis. (C) Hematoxylin/eosin staining of representative PDAC cluster cross sections from corresponding treatment groups. (D) Quantification of prevalence of PDAC cluster cross sections wherein the lumen accounts for >75% of the cluster and contains CC3-positive debris. Bars represent mean prevalence ±SEM of over 50 cluster cross sections in 3 grouped biological replicate studies. Statistics: student's t test; * indicates $p<0.001$.

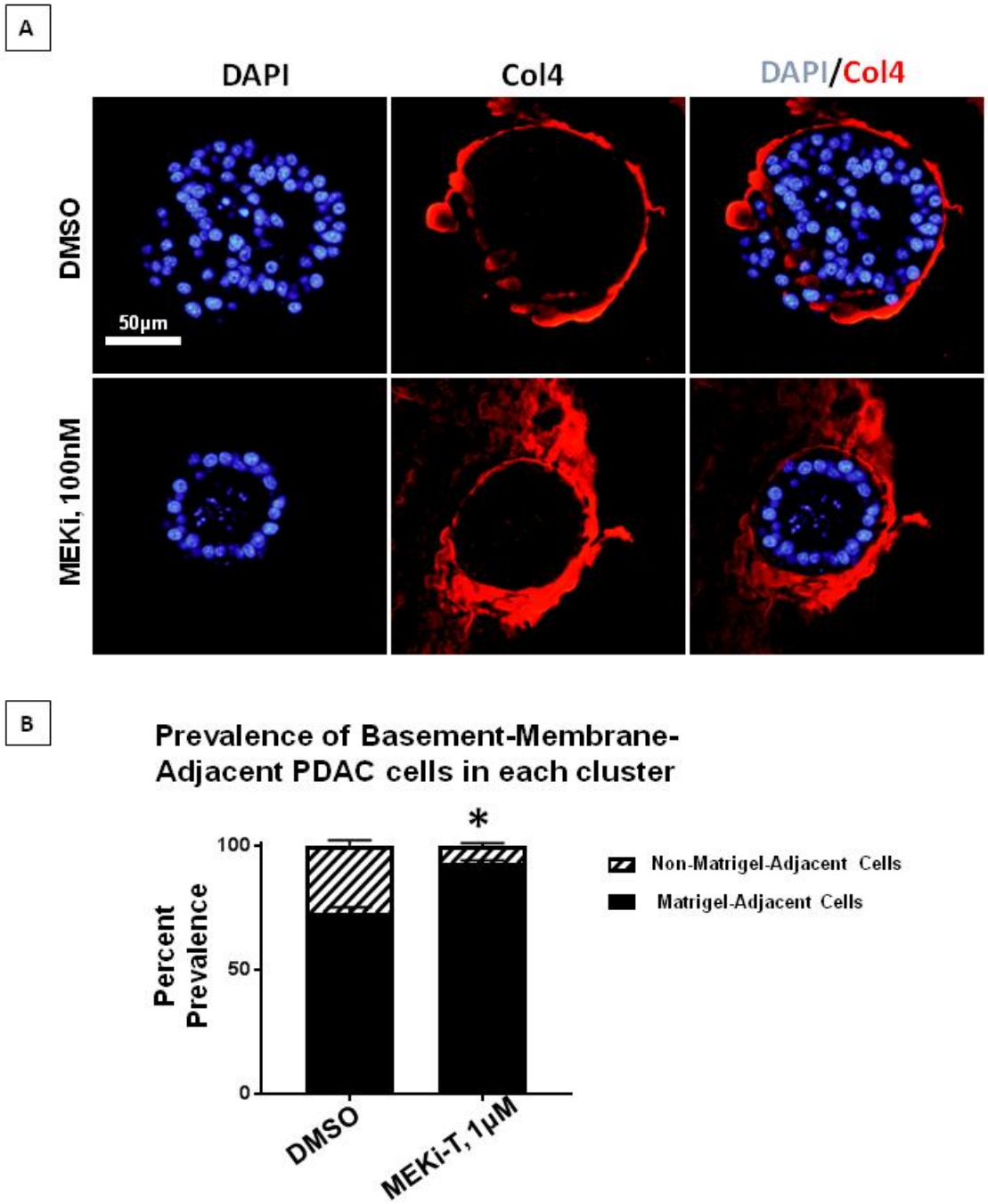

Figure 3.4 Matrigel-adjacent PDAC cells display survival advantage in the context of MAPK inhibition.

iKras*p53* PDAC cells (9805) were grown in 3D culture for 6 days and then treated with the MEK inhibitor trametinib (MEK-T) for 4 days (Kras*on the entire experiment). (A) representative PDCA cluster cross sections, immunofluorescence staining of type IV collagen (Col4) in red. (B) Quantification of the prevalence of non-matrigel-adjacent versus matrigel-adjacent, DAPI-positive nuclei in striped and black bars, respectively. Bars represent mean prevalence ±SEM of over 50 cluster cross sections in 3 grouped biological replicate studies. Statistics: student's t test; * indicates $p<0.001$.

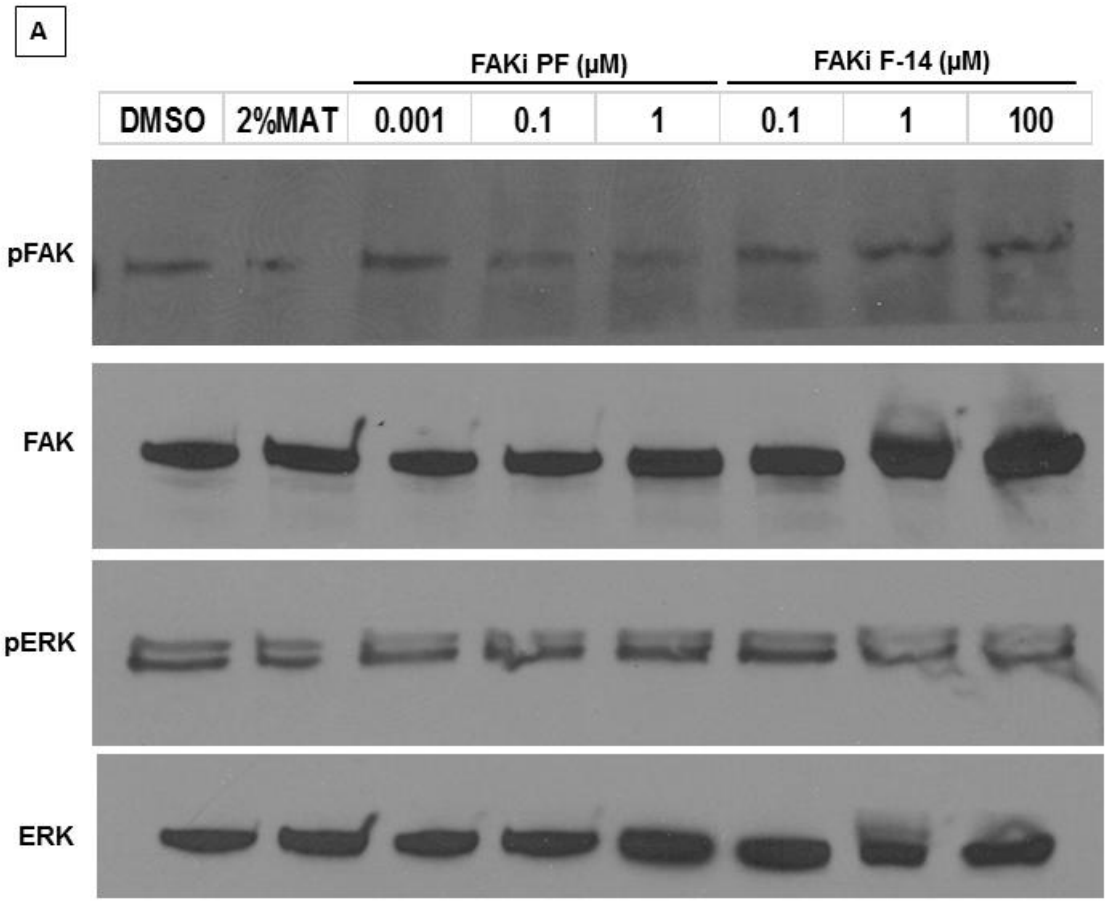

Figure 3.5 PDAC cells activate Focal Adhesion Kinase (FAK) signaling in 2D cell culture.
iKras*p53* PDAC 9805 PDAC cells were maintained in 2D culture, in media containing 10% fetal bovine serum (FBS) and doxycycline (1μg/mL) and grown to approximately 75% confluency. At which point, cells were serum-starved for 16 hours (media+0.5% FBS). After serum starvation, either vehicle, Matrigel, or small molecule inhibitors targeting FAK signaling were administered to experimental groups at corresponding concentrations. After 6 hours of treatment, cells were lysed and prepared for western blot analysis. (A) Western blot displaying protein relative expression in 9805 PDAC cells of phosphorylated and total protein species (phosphorylated species are indicated by "p" preceding probed protein). pFAK=FAK(pTyr397) pERK= ERK1/2 (pThr202/pTyr204)

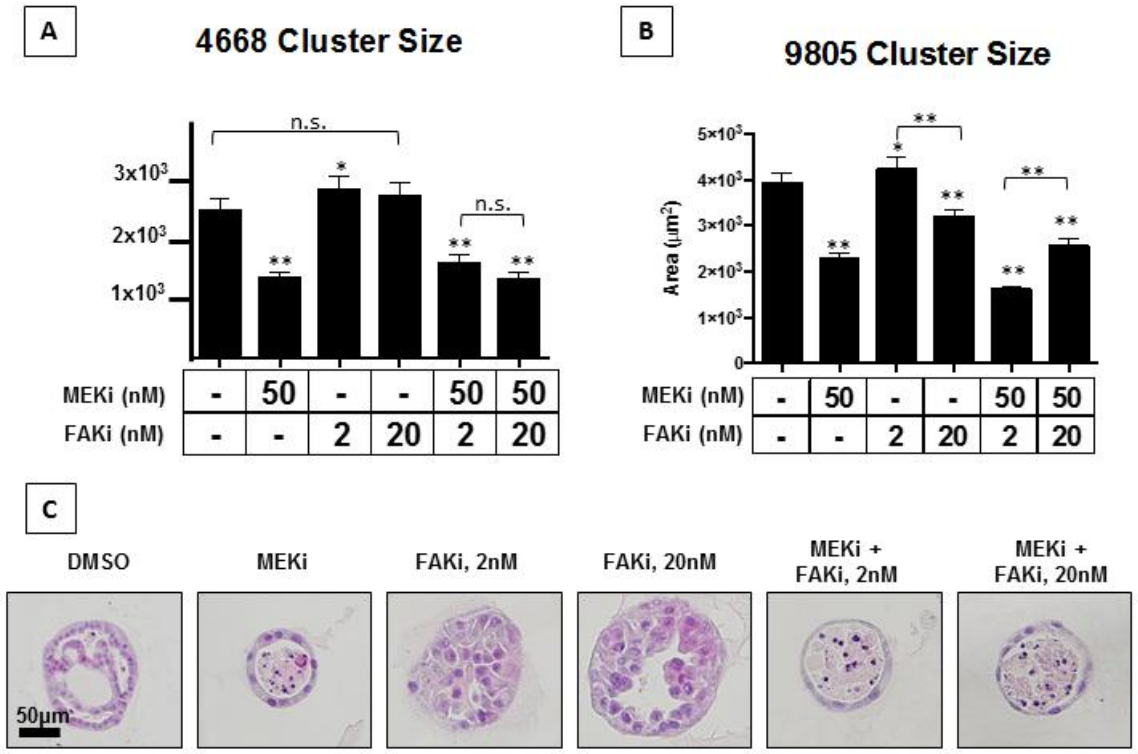

Figure 3.6 FAK inhibition via VS-4718 fails to kill Matrigel-adjacent PDAC cells in the context of MAPK inhibition.
iKras*p53* PDAC cells (4668 or 9805) were grown in 3D for 7 days then treated with MEK inhibitor trametinib (MEKi), FAK inhibitor VS-4718 (FAKi), or both for 4 days. After treatment, experimental group PDAC cluster area was measured/calculated in both 4668 (A) and 9805 (B) cell lines. Bars represent mean cluster area ± SEM. At least 100 clusters per treatment group were analyzed. (C) Shows representative hematoxylin/eosin-stained cross sections of 9805 PDAC clusters from each treatment group. *$p<0.05$, **$p<0.01$, n.s. not significant, Student's t test.

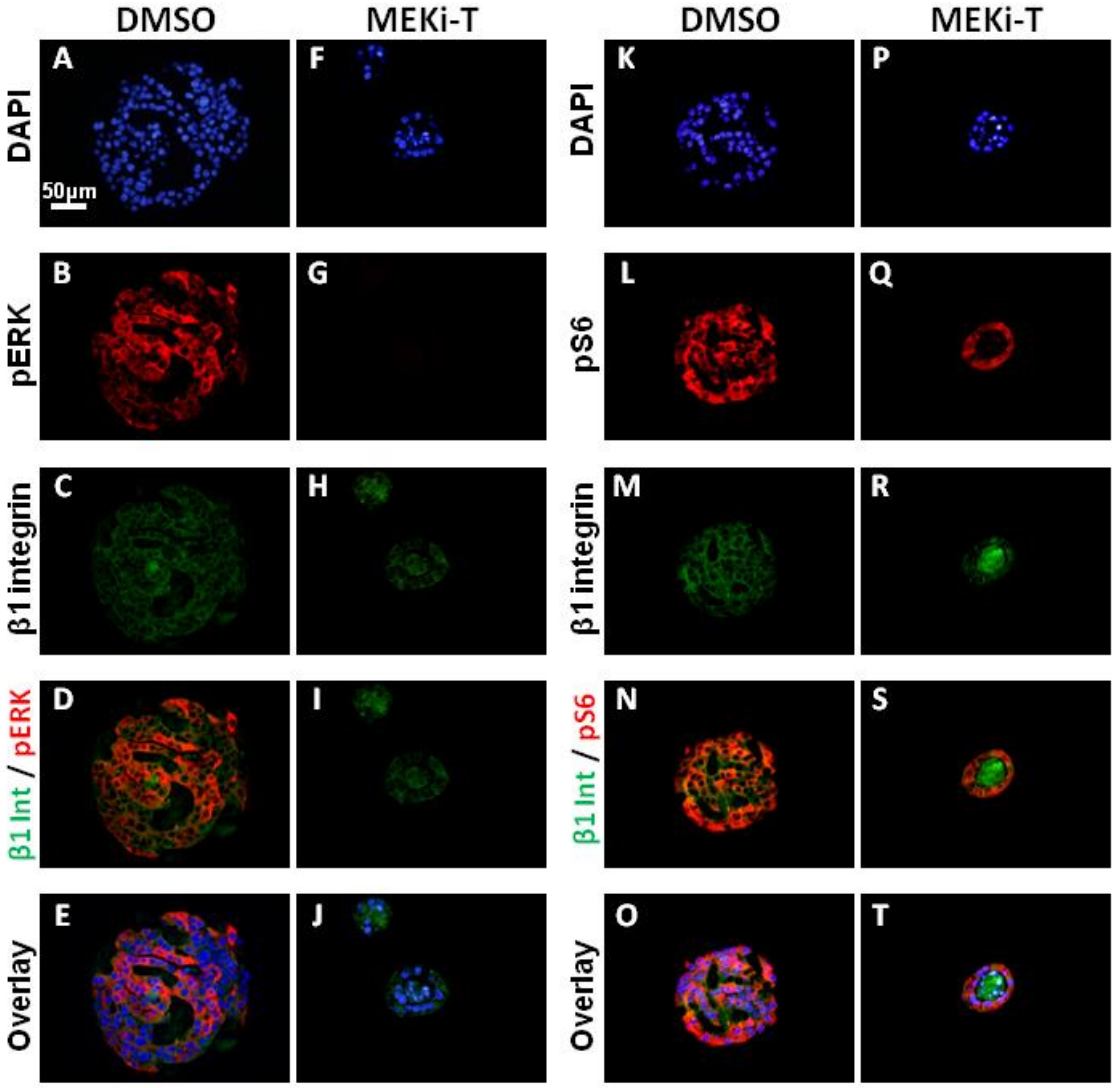

Figure 3.7 PDAC cells *in vitro* express β1 integrin, independent of MAPK activation. iKras*p53* 9805 PDAC cells were grown in 3D for 7 days and treated with either vehicle DMSO (A-E, K-O) or MEK inhibitor (F-J, P-T) trametinib (MEK-T, 100Nm) for 4 days. At which point clusters were fixed, sectioned and stained for immunofluorescence analysis. Pictured here are four unique representative cross sections from corresponding experimental groups, stained for corresponding protein targets as well as a channel overlays. pERK= ERK1/2 (pThr202/pTyr204); pS6= S6 ribosomal protein (pSer235/236); β1 Int= β1 integrin.

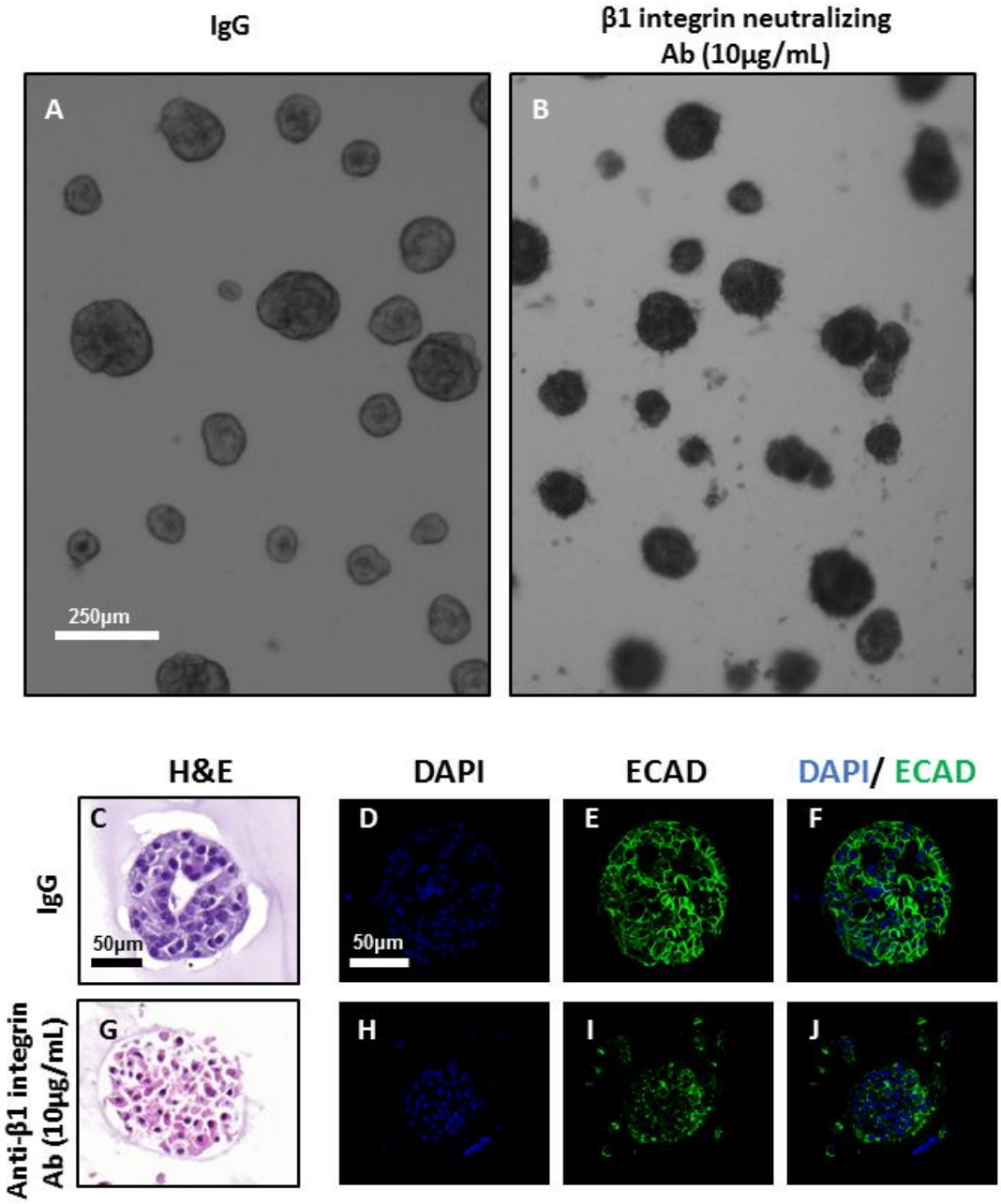

Figure 3.8 β1 integrin blockade disrupts membrane dynamics.
iKras*p53* 9805 PDAC cells were grown in 3D for 7 days and subsequently treated for 4 days with either vehicle IgG or anti-β1 neutralizing antibody (10μg/mL). (A,B) Brightfield, low-magnification microscopy of 9805 PDAC clusters *in vitro*. (C, G) Hematoxylin/eosin staining of PDAC clusters cross sections, treated with either control (IgG) or anti-β1 integrin blocking antibody (G). (D-F, H-J) Immunofluorescence of PDAC cluster cross sections. (D,H) Nuclear visualization with DAPI; (E,I) Stain indicating E-cadherin (ECAD) localization; (F,J) Overlay of DAPI and ECAD channels.

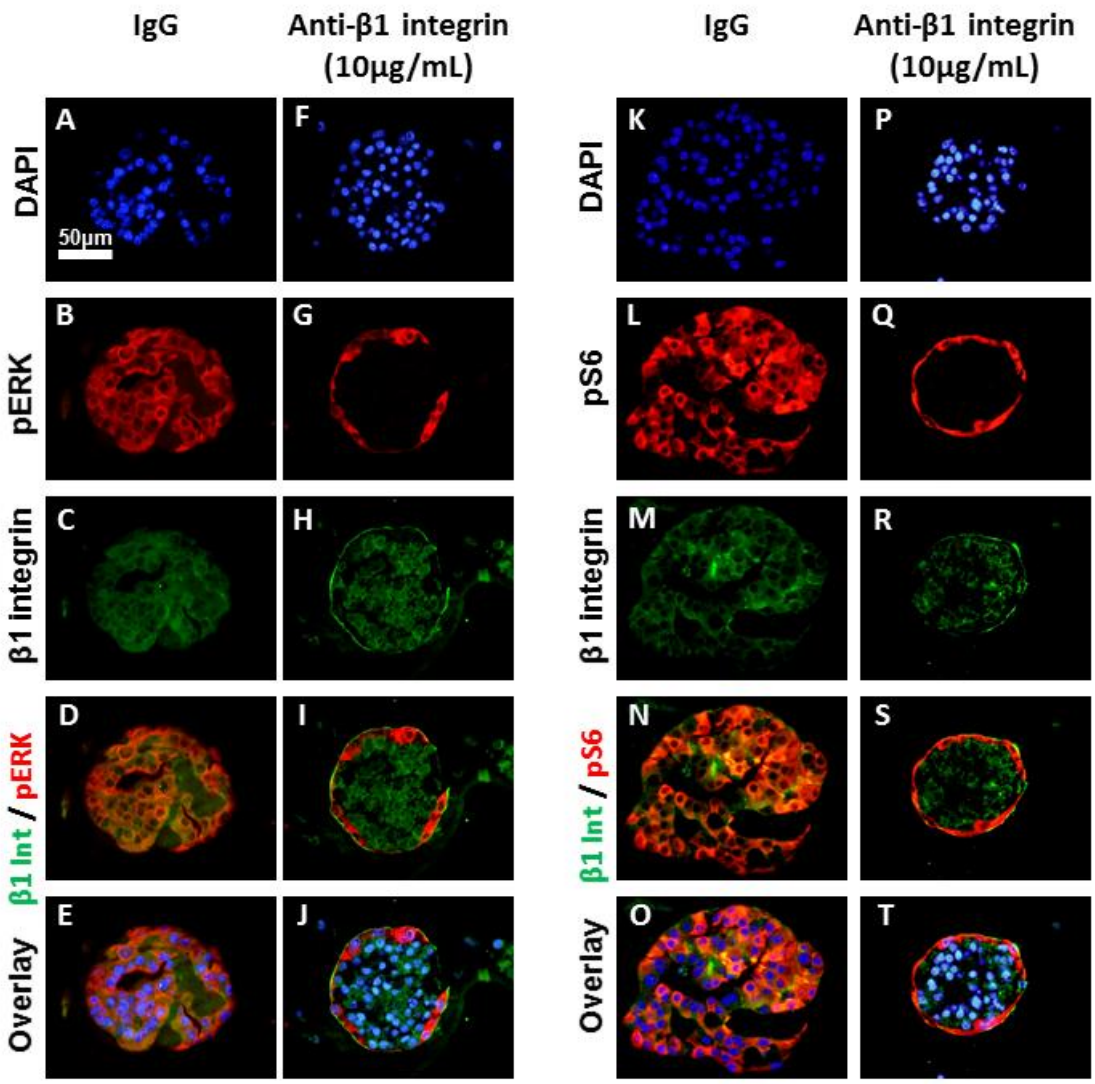

Figure 3.9 β1 integrin blockade decreases Kras* effector signaling in non-Matrigel-adjacent cells

iKras*p53* 9805 PDAC cells were grown in 3D for 7 days and subsequently treated for 4 days with either vehicle IgG or anti-β1 neutralizing antibody (10μg/mL). Pictured are representative PDAC cluster cross sections of control treated (A-E, K-O) or anti-β1 integrin-treated cells. (B,G) Clusters were stained for phosphorylated ERK (pERK) species, indicating MAPK activity. (L,Q) Staining for phosphorylated S6 ribosomal protein (pS6). (C,H,M,R) Staining for β1 integrin. (D,I,N,S) Overlay of red and green channels. (E,J,O,T) Overlay of DAPI, red, and green channels.

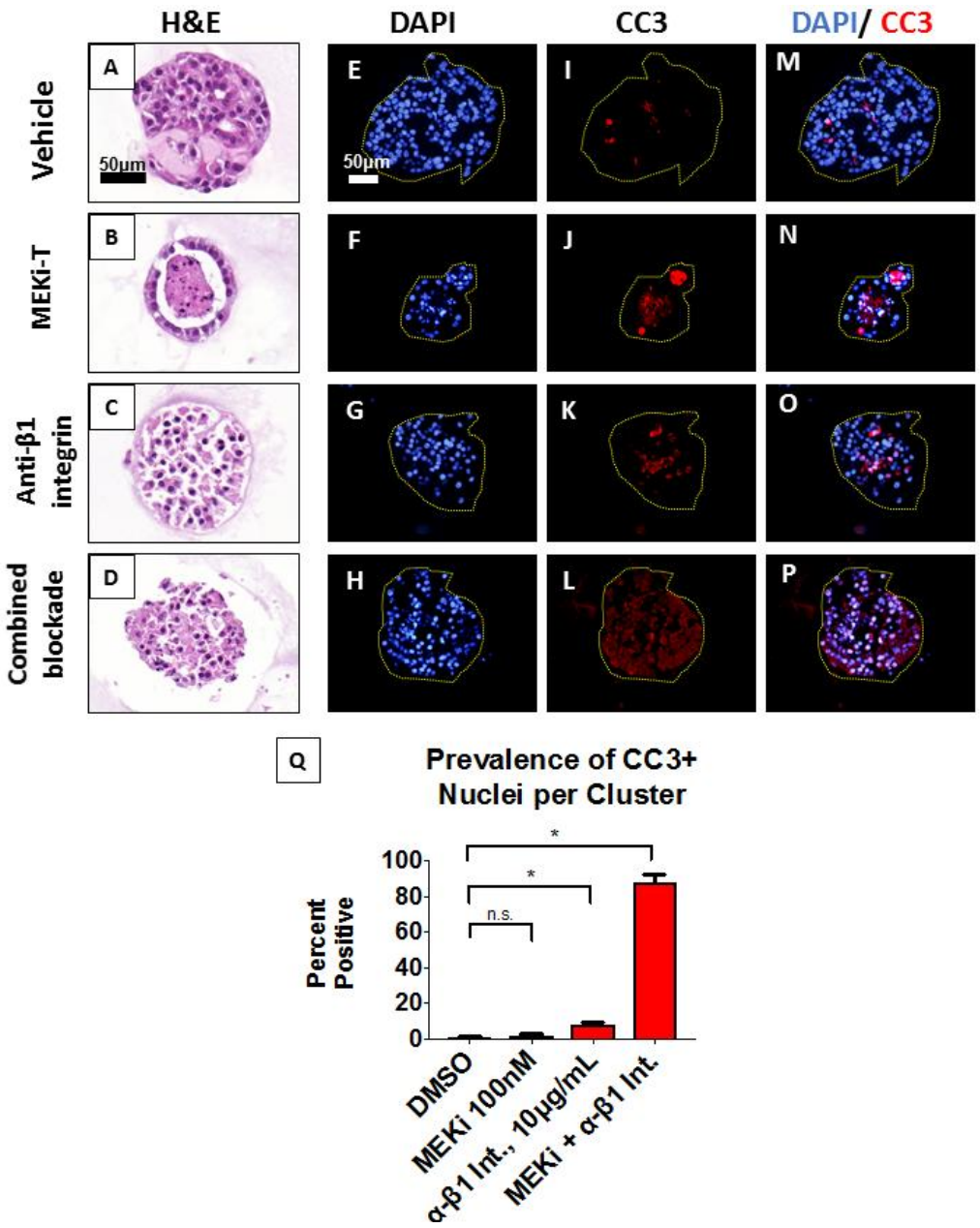

Figure 3.10 Dual blockade of MAPK and β1 Integrin signaling pathways leads to upregulated apoptosis in PDAC cells

iKras*p53* 9805 PDAC cells were grown in 3D for 7 days and subsequently treated for 4 days with either vehicle IgG/DMSO (vehicle), trametinib 100nM (MEKi-T), anti-β1 neutralizing antibody (10μg/mL), or dual trametinib and anti-β1 integrin neutralizing antibody (combined blockade). (A-D) Hematoxylin/eosin stain of representative PDAC cluster cross sections. (E-P) Immunofluorescence data of DAPI (E-H), cleaved caspase 3 or CC3 (I-L) or merged blue and red channels (M-P). (Q) Quantification of CC3-positive nuclei. Bars represent mean prevalence of CC3 positivity per defined nucleus ± SEM. At least 50 unique cluster cross sections from 3 biological replicate experiments were analyzed. Statistical analysis: student's t test. n.s.=$p>0.05$; * indicates $p<0.001$.

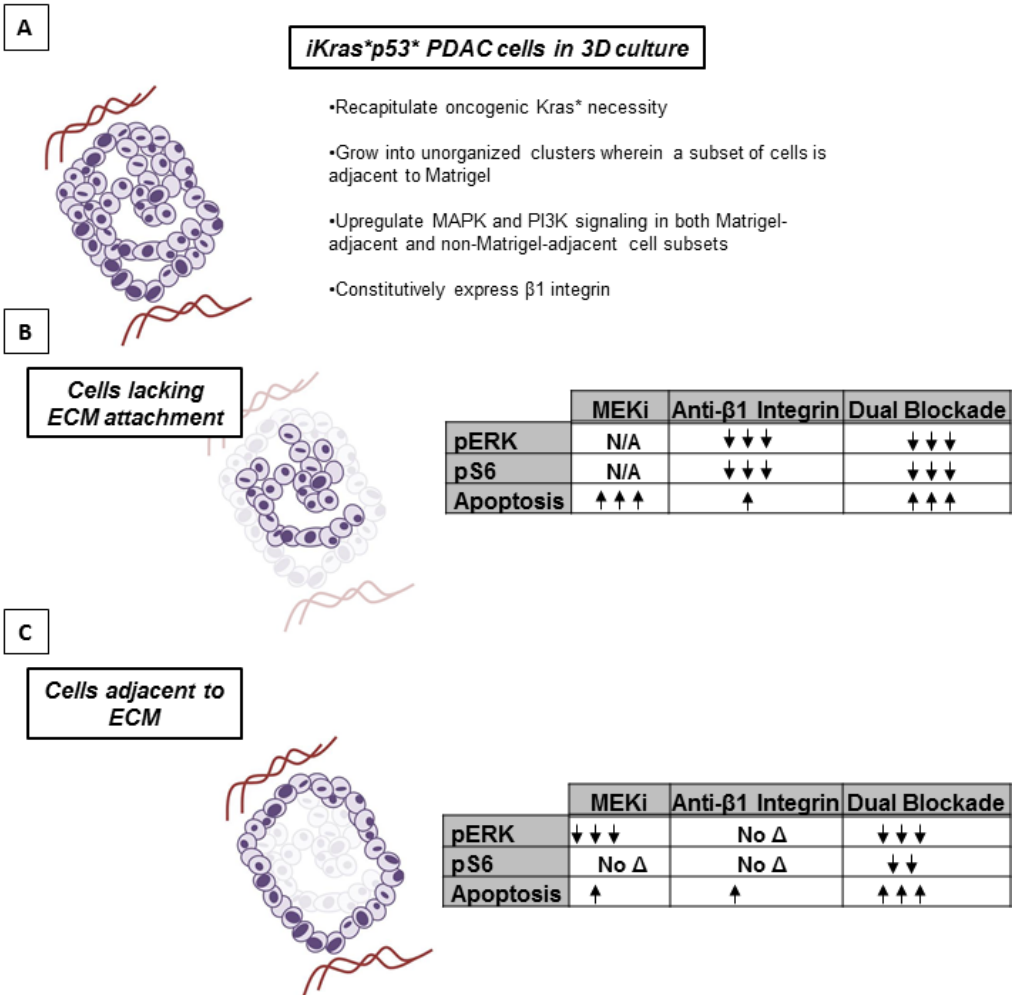

Figure 3.11 Summary of effects of MAPK inhibition, β1 integrin blockade, or both in concert in a 3D cell culture model of PDAC

(A) PDAC clusters in a 3D system recapitulate important aspects of PDAC *in vivo* biology, including oncogenic Kras* necessity and activation of downstream effector pathways, MAPK and PI3K. We found that PDAC cells respond differently to small-molecule-induced-blockade of specific signaling pathways, relative to their position to the basement membrane mimetic. (B) Cells lacking ECM attachment are especially sensitive to MAPK inhibition, as administration of MEK inhibitors leads to increase of apoptosis and an inability to visualize these cells due to nuclear degradation (N/A indicates that effector activation in these cells could not be visualized via immunofluorescence). (C) Conversely, cells adjacent to the ECM displayed a survival advantage in the context of MEK inhibition and were sensitized to apoptosis via dual blockade of MAPK and β1 integrin signaling pathways.

References

Appels, N.M.G.M. & M.G.M. Appels, N., 2005. Development of Farnesyl Transferase Inhibitors: A Review. The oncologist, 10(8), pp.565–578.

Arao, S., Masumoto, A. & Otsuki, M., 2000. Beta1 integrins play an essential role in adhesion and invasion of pancreatic carcinoma cells. Pancreas, 20(2), pp.129–137.

Barati Bagherabad, M. et al., 2017. Targeted Therapies in Pancreatic Cancer: Promises and Failures. Journal of cellular biochemistry. Available at: http://dx.doi.org/10.1002/jcb.26284.

Belteki, G. et al., 2005. Conditional and inducible transgene expression in mice through the combinatorial use of Cre-mediated recombination and tetracycline induction. Nucleic acids research, 33(5), p.e51.

Bhowmick, N.A. et al., 2001. Integrin beta 1 signaling is necessary for transforming growth factor-beta activation of p38MAPK and epithelial plasticity. The Journal of biological chemistry, 276(50), pp.46707–46713.

Cabodi, S. et al., 2004. Integrin regulation of epidermal growth factor (EGF) receptor and of EGF-dependent responses. Biochemical Society transactions, 32(Pt3), pp.438–442.

Cao, P. et al., 2009. Activity of a novel, dual PI3-kinase/mTor inhibitor NVP-BEZ235 against primary human pancreatic cancers grown as orthotopic xenografts. British journal of cancer, 100(8), pp.1267–1276.

Casey, P.J. et al., 1989. p21ras is modified by a farnesyl isoprenoid. Proceedings of the National Academy of Sciences of the United States of America, 86(21), pp.8323–8327.

Chadha, K.S. et al., 2006. Activated Akt and Erk expression and survival after surgery in pancreatic carcinoma. Annals of surgical oncology, 13(7), pp.933–939.

Chakraborty, S. & Singh, S., 2013. Surgical resection improves survival in pancreatic cancer patients without vascular invasion- a population based study. Annales de gastroenterologie et d'hepatologie, 26(4), pp.346–352.

Collins, M.A. et al., 2012. Metastatic pancreatic cancer is dependent on oncogenic Kras in mice. PloS one, 7(12), p.e49707.

Collisson, E.A. et al., 2012. A central role for RAF→MEK→ERK signaling in the genesis of pancreatic ductal adenocarcinoma. Cancer discovery, 2(8), pp.685–693.

Cox, A.D. & Der, C.J., 2010. Ras history. Small GTPases, 1(1), pp.2–27.

Desgrosellier, J.S. et al., 2009. An integrin alpha(v)beta(3)-c-Src oncogenic unit promotes anchorage-independence and tumor progression. Nature medicine, 15(10), pp.1163–1169.

Drosten, M., Guerra, C. & Barbacid, M., 2017. Genetically Engineered Mouse Models of K-Ras-Driven Lung and Pancreatic Tumors: Validation of Therapeutic Targets. Cold Spring Harbor perspectives in medicine. Available at: http://dx.doi.org/10.1101/cshperspect.a031542.

Eser, S. et al., 2013. Selective requirement of PI3K/PDK1 signaling for Kras oncogene-driven pancreatic cell plasticity and cancer. Cancer cell, 23(3), pp.406–420.

Fisher, G.H. et al., 2001. Induction and apoptotic regression of lung adenocarcinomas by regulation of a K-Ras transgene in the presence and absence of tumor suppressor genes. Genes & development, 15(24), pp.3249–3262.

Galante, J.M. et al., 2009. ERK/BCL-2 pathway in the resistance of pancreatic cancer to anoikis. The Journal of surgical research, 152(1), pp.18–25.

Grzesiak, J.J. et al., 2011. Knockdown of the β(1) integrin subunit reduces primary tumor growth and inhibits pancreatic cancer metastasis. International journal of cancer. Journal international du cancer, 129(12), pp.2905–2915.

Hancock, J.F. & Parton, R.G., 2005. Ras plasma membrane signalling platforms. Biochemical Journal, 389(Pt 1), pp.1–11.

Ilic, M. & Ilic, I., 2016. Epidemiology of pancreatic cancer. World journal of gastroenterology: WJG, 22(44), pp.9694–9705.

Infante, J.R. et al., 2014. A randomised, double-blind, placebo-controlled trial of trametinib, an oral MEK inhibitor, in combination with gemcitabine for patients with untreated metastatic adenocarcinoma of the pancreas. European journal of cancer, 50(12), pp.2072–2081.

Ji, S. et al., 2015. ERK kinase phosphorylates and destabilizes the tumor suppressor FBW7 in pancreatic cancer. Cell research, 25(5), pp.561–573.

Kawaguchi, Y. et al., 2002. The role of the transcriptional regulator Ptf1a in converting intestinal to pancreatic progenitors. Nature genetics, 32(1), pp.128–134.

Khorana, A.A., Mangu, P.B. & Katz, M.H.G., 2017. Potentially Curable Pancreatic Cancer: American Society of Clinical Oncology Clinical Practice Guideline Update Summary. Journal of oncology practice / American Society of Clinical Oncology, 13(6), pp.388–391.

Lu, P., Weaver, V.M. & Werb, Z., 2012. The extracellular matrix: a dynamic niche in cancer progression. The Journal of cell biology, 196(4), pp.395–406.

Morris, J.P., 4th, Wang, S.C. & Hebrok, M., 2010. KRAS, Hedgehog, Wnt and the twisted developmental biology of pancreatic ductal adenocarcinoma. Nature reviews. Cancer, 10(10), pp.683–695.

Olive, K.P. et al., 2004. Mutant p53 gain of function in two mouse models of Li-Fraumeni syndrome. Cell, 119(6), pp.847–860.

Paoli, P., Giannoni, E. & Chiarugi, P., 2013. Anoikis molecular pathways and its role in cancer progression. Biochimica et biophysica acta, 1833(12), pp.3481–3498.

Pontes-Júnior, J. et al., 2013. Correlation between beta1 integrin expression and prognosis in clinically localized prostate cancer. International braz j urol: official journal of the Brazilian Society of Urology, 39(3), pp.335–42; discussion 343.

Prior, I.A., Lewis, P.D. & Mattos, C., 2012. A comprehensive survey of Ras mutations in cancer. Cancer research, 72(10), pp.2457–2467.

Rahib, L. et al., 2014. Projecting cancer incidence and deaths to 2030: the unexpected burden of thyroid, liver, and pancreas cancers in the United States. Cancer research, 74(11), pp.2913–2921.

Rajalingam, K. et al., 2007. Ras oncogenes and their downstream targets. Biochimica et Biophysica Acta (BBA) - Molecular Cell Research, 1773(8), pp.1177–1195.

Roy, S.K., Srivastava, R.K. & Shankar, S., 2010. Inhibition of PI3K/AKT and MAPK/ERK pathways causes activation of FOXO transcription factor, leading to cell cycle arrest and apoptosis in pancreatic cancer. Journal of molecular signaling, 5, p.10.

dos Santos, P. et al., 2012. Beta 1 integrin predicts survival in breast cancer: a clinicopathological and immunohistochemical study. Diagnostic pathology, 7(1), p.104.

Schmick, M. et al., 2014. KRas localizes to the plasma membrane by spatial cycles of solubilization, trapping and vesicular transport. Cell, 157(2), pp.459–471.

Senthebane, D.A. et al., 2017. The Role of Tumor Microenvironment in Chemoresistance: To Survive, Keep Your Enemies Closer. International journal of molecular sciences, 18(7). Available at: http://dx.doi.org/10.3390/ijms18071586.

Smith, B.D. et al., 2009. Future of cancer incidence in the United States: burdens upon an aging, changing nation. Journal of clinical oncology: official journal of the American Society of Clinical Oncology, 27(17), pp.2758–2765.

Taddei, M.L. et al., 2012. Anoikis: an emerging hallmark in health and diseases. The Journal of pathology, 226(2), pp.380–393.

Truty, M.J. & Urrutia, R., 2007. Basics of TGF-beta and pancreatic cancer. Pancreatology: official journal of the International Association of Pancreatology ... [et al.], 7(5-6), pp.423–435.

Venning, F.A., Wullkopf, L. & Erler, J.T., 2015. Targeting ECM Disrupts Cancer Progression. Frontiers in oncology, 5, p.224.

Vincent, A. et al., 2011. Pancreatic cancer. The Lancet, 378(9791), pp.607–620.

Whyte, D.B. et al., 1997. K- and N-Ras are geranylgeranylated in cells treated with farnesyl protein transferase inhibitors. The Journal of biological chemistry, 272(22), pp.14459–14464.

Williams, T.M. et al., 2012. Cotargeting MAPK and PI3K Signaling with Concurrent Radiotherapy as a Strategy for the Treatment of Pancreatic Cancer. Molecular cancer therapeutics, 11(5), pp.1193–1202.

Yamamoto, S. et al., 2004. Prognostic significance of activated Akt expression in pancreatic ductal adenocarcinoma. Clinical cancer research: an official journal of the American Association for Cancer Research, 10(8), pp.2846–2850.

Ying, H. et al., 2012. Oncogenic Kras maintains pancreatic tumors through regulation of anabolic glucose metabolism. Cell, 149(3), pp.656–670.

Yin, X. et al., 2015. K-ras-driven engineered mouse models for pancreatic cancer. Discovery medicine, 19(102), pp.15–21.

Zent, R. & Pozzi, A., 2005. Extracellular matrix and the development of disease: The role of its components in cancer progression. In Advances in Developmental Biology. pp. 203–228.

Zhong, H. et al., 2015. Correction: Synergistic Effects of Concurrent Blockade of PI3K and MEK Pathways in Pancreatic Cancer Preclinical Models. PloS one, 10(4), p.e0127365.

Chapter 4. Investigating the Therapeutic Potential of Tank Binding Kinase-1 Blockade in Multiple Murine Models of Pancreatic Cancer

Introduction

TANK Binding Kinase 1 (TBK1) was originally identified as an integral component of innate immunity(Fitzgerald et al. 2003; Sharma et al. 2003). It acts as a nodal protein that regulates interferon and NF-kB signaling responses (Yu et al. 2012; Helgason et al. 2013).TBK1 is a cytosolic protein that is phosphorylated upon activation and in turn phosphorylates downstream target proteins, most notably interferon regulatory factor 3 (IRF3) and protein kinase B (most often referred to as AKT)(Fitzgerald et al. 2003)(Helgason et al. 2013)(Kim et al. 2013). Recently, TBK1 upregulation has been described in many forms of epithelial malignancy including lung, breast, colon, and pancreas(Kim et al. 2013; Barbie et al. 2009; Muvaffak et al. 2014; Korherr et al. 2006). This expression of TBK1 in malignant epithelial cells plays varied functional roles in cell biology. For example, TBK1 mediates mitosis of lung adenocarcinoma cells, independent of AKT or IRF3(Kim et al. 2013); whereas in breast cancer, TBK1 interacts with Estrogen Receptor α to mediate tamoxifen resistance(Wei et al. 2014). In pancreatic cancer, TBK1 overexpression is correlated with poor prognosis, and its overexpression in commercial pancreatic cancer cell lines leads to increased proliferation in vitro (Wei et al. 2014; Song et al. 2015). Although current evidence indicates that TBK1 is expressed and potentially tumor-promoting in pancreatic cancer, its mechanism of action and downstream mediators are unknown. The goal of this group

of studies was to determine whether TBK1 plays a functional role in pancreatic cancer pathogenesis, using both in vivo and in vitro model systems.

Methods

Animal Housing & Pancreatitis Induction

Animals were maintained in pathogen-free facilities of the University of Michigan Comprehensive Cancer Center as previously described(Collins, Bednar, et al. 2012). iKras* mice (p48+/Cre; Rosa26rtTa/rtTa; TRE-KrasG12D) and KC mice (p48Cre/+; LSL-KrasG12D) were housed with control littermates. Doxycycline was administered via drinking water at a concentration of 0.2g/L in a solution of 5% sucrose. To induce pancreatitis, mice were administered 2 series of 8 hourly injections of caerulein (75 µg/kg Sigma cat# 9206 diluted in 0.1% bovine serum albumin in 1x phosphate buffered saline) over a 48-hour period. Mouse pancreata and spleens were harvested for histologic analysis(Collins, Bednar, et al. 2012).

Tissue fixation and staining

Pancreata were fixed in 10% formalin formaldehyde at 22°C for at least 16 hours. At which point, tissues were processed, embedded in paraffin, and cut into 5µm-thick sections. Antigen retrieval was achieved using heated citra plus solution, and tissues were incubated with primary antibodies overnight at 4°C; after wash, tissues were incubated with secondary antibodies for 1 hour at 22°C. A heated citra antigen retrieval was then performed with “citra plus” reagent ThermoFisher Cat# NC9755543, and tissues were blocked with 1% bovine serum albumin solubilized in 1xPBS. Samples were stained

overnight at 4°C with corresponding primary antibodies. After a wash with 1xPBS, fluorophore-conjugated secondary antibodies were incubated at 22°C for 90 minutes. Slides were then mounted with Prolong gold +DAPI ThermoFisher Cat# P36931 or for immunohistochemistry, development was achieved with Vectastain elite HRP/ABC kit Cat# PK-6100.

Quantification of tissue morphology and biochemical changes

Brightfield and immunofluorescence images were acquired with Olympus BX-51 microscope and cellSens software. For quantification of PanIN progression, 6 low magnification (200x), non-overlapping images of hematoxylin/eosin-stained pancreata were taken and analyzed by a blinded observer (Yaqing Zhang). A minimum of 50 total epithelial clusters were counted from each experimental animal. Each cluster was classified as acinar, acinar-to-ductal metaplasia (ADM), PanIN1A, -1B, -2, or -3 based on classification consensus (Hruban et al. 2006). Biochemical classification of ADM was quantified similarly: 6 low magnification (200x), non-overlapping images of amylase/CK19-stained pancreata were taken and analyzed by a blinded observer (Yaqing Zhang). At least 50 epithelial clusters were counted from each experimental animal and classified as acinar (all amylase positive), ADM (positive staining for both amylase and CK19), or ductal (complete CK19 positivity).

RNA isolation and qPCR

Tissue for RNA isolation was prepared through 16-hour incubation in RNAlater Sigma Cat# R0901 at -20°C then thawed and mechanically homogenized. The RNeasy

Protect Mini Kit Qiagen Cat# 74104 was used to extract RNA. 1µg of RNA was converted to cDNA using a High-Capacity cDNA Reverse Transcription Kit ThermoFisher Cat# 4368814. Samples for qPCR were prepared with 1xSYBR Green PCR Master Mix ThermoFisher Cat# 4368577 and corresponding primers. All primers were optimized for amplification under reaction conditions: 95°C 10 minutes, then 40 cycles of 95°C 15 seconds and 60°C 1 minute. Melt curve analysis was performed following amplification. Cyclophilin was used to normalize mRNA content.

Cell culture

All cells, PDAC or Raw264.7 macrophages, were maintained in IMDM Gibco Cat# 12440053 +10% Fetal Bovine Serum, (iKras*p53* lines were maintained in 1µg/mL dox Sigma Cat# D989); media changed every 2-3 days; passaged when 85-100% confluent; all experimental cells experienced <10 passages since derivation or arrival (Raw264.7 cells were commercially ordered). “On-top” 3D culture experiments were performed as explained in Chapter 2.

Western Blot Analysis

Tissues or cell samples were homogenized in lysis buffer (Tris 50mM, NaCl 131 mM, Sodium orthovanadate 1mM, Sodium pyrophosphate tetrabasic 10mM, NaF 10mM, EDTA 1mM, Triton TX-100 1%) and dye was added (Biorad Quick Start Bradford dye reagent Cat# 5000205) for measuring protein concentration. Absorbance at 595nm was detected using a Spectra Max plate reader and VMax software was used to calculate protein concentration.15-30µg of sample protein were loaded onto Biorad gels (gradient

4-15%, 10 or 15 well-gels Cat# 4568084 or 456108) and electrophoresed, then transfered to PVDF membrane. Membranes were blocked with 5% bovine serum albumin and primary antibodies were diluted in bovine serum albumin 5% + sodium azide 0.1% for 16 hours at 4°C. After wash, HRP-conjugated secondary antibodies were diluted in milk and added to membranes for 2 hours at 22°C. Blots were developed using chemiluminescence and film exposure (Perkin Elmer Cat# NEL103E001EA).

Results

TBK1 inhibition decreases PanIN development in iKras* mice

To test the functional relevance of TBK1 in pancreatic cancer pathogenesis in vivo, we chose to pharmacologically block TBK1 in a premalignant model of pancreatic cancer wherein pancreatitis is induced in mice that express oncogenic Kras*; this protocol promotes acinar-to-ductal metaplasia and early PanIN development in a highly reproducible manner(Collins, Brisset, et al. 2012). In this set of experiments, iKras* mice were randomized into control and CYT387 treatment groups; CYT387 is a dual inhibitor of JAK and TBK1 signaling. Prior to caerulein-induced pancreatitis, Kras* expression in iKras* mice was activated by adding doxycycline to the drinking water; simultaneously, treatment with either vehicle or CYT387 (100mg/kg/day p.o.) was administered. Three days later, mice were subjected to 2 series of 8 hourly injections of caerulein (75ug/kg) over a 48-hour period to induce acute pancreatitis. 1 week following pancreatitis, pancreata were harvested and prepared for immunohistochemical analysis. Morphologic analysis via hematoxalyn/eosin staining of tissue sections revealed that mice receiving vehicle treatment developed acinar-to-ductal metaplasia in over 90% of

epithelial tissues and some development of early PanIN lesions (Fig 4.1B,C); conversely, tissue from animals treated with CYT387 showed decreased acinar-to-ductal metaplasia as well as marked increase in normal acinar tissue (50%) (Fig 4.1B,C).

To determine the degree of acinar-to-ductal metaplasia and possible difference between experimental groups, pancreas sections were stained and co-immunofluorescence-analyzed for acinar marker amylase and ductal marker cytokeratin 19 (ck19) (Fig 4.2B). Quantification analysis performed by a blinded observer showed that JAK/TBK1 inhibitor CYT387 administration led to an increase in amylase-positive epithelial cells when compared to control mice, and a decrease in cells that stained dual positive for amylase and ck19 (Fig 4.2C), indicating a decrease in acinar-to-ductal metaplasia via biochemical readout. These data taken with the above morphologic analysis suggest that JAK/TBK1 activity is pro-tumorigenic in this premalignant mouse model of PDAC.

Furthermore, upon immunohistochemical analysis, we observed presence of phosphorylated STAT3 in CYT387-treated animals (Fig 4.3), indicating active JAK/STAT signaling. This result suggests a failure of CYT387 to inhibit JAK in this model. Given 1) the phenotypic change in acinar-to-ductal metaplasia in CYT387 treated iKras* mice compared to control; 2) the fact that CYT387 has been shown to inhibit TBK1 activity; and 3) CYT387 treated iKras* mice upregulated JAK signaling, we hypothesized that phenotypic change in response to CYT387 administration was a result of TBK1 activity. To test modulation of TBK1 signaling in this system, we evaluated

activation of TBK1 targets both immunohistochemically and via gene expression analysis. We found that phosphorylated TBK1 (Ser172) was upregulated in iKras* mice 1 week following pancreatitis (Fig 4.4B), suggesting upregulation of TBK1 signaling. In contrast, pancreata from CYT387-treated iKras* mice, showed decreased staining for phosphorylated TBK1 (Fig 4.4B). Further protein and genetic analysis demonstrated that CYT387-treated iKras* mice downregulated expression of CCL5, a chemokine target of TBK1 signaling. These data in concert with mounting evidence in the field that suggests TBK1 can play a myriad of roles in malignancy and its role varies, depending on cell type and upstream signaling factors (Fig 4.5)(Helgason et al. 2013; Muvaffak et al. 2014), compelled us to investigate the role of TBK1 signaling in our system.

TBK1 expression and activation is variable in normal and iKras* pancreata following pancreatitis

In a second set of experiments, pancreatitis was induced via caerulein administration in normal or iKras* mice, and tissue was harvested immediately following cessation of the 48-hour pancreatitis protocol. Upon cell lysis and preparation for western blot performed on tissue, we found baseline expression of TBK1 in normal pancreata. Pancreatitis appeared to upregulate TBK1 activation in normal mice, indicated by a strong band at phosphorylated TBK1 (Ser172) (Fig 4.6). TBK1 activation was variable in iKras* mice following pancreatitis and not correlated with activation of STAT3, MAPK, or PI3K signaling activation (Fig 4.6). Since these results reflect signal activation of the entire tissue, which includes infiltrating immune cell populations, we sought to further

investigate TBK1 signaling and its function in PDAC in vitro, where subpopulations of cells can be separated and characterized individually.

TBK1 inhibition fails to affect PDAC 3D growth

To investigate the role of epithelial TBK1 signaling in the context of malignant PDAC, we used cell lines derived from KPC (65671) and iKras*p53* (9805) PDAC tumors. We first sought to determine the basal activation of TBK1 signaling, and if active, whether or not it could be targeted pharmacologically. To do this, we grew PDAC cells in 2D culture, serum starved them, and administered combination JAK/TBK1 inhibitor CYT387 or amlexanox, a more specific TBK1 inhibitor(Reilly et al. 2013; Oral et al. 2017). We found that both KPC and iKras*p53* PDAC cell lines expressed active, phosphorylated TBK1; however, only the KPC cell line demonstrated active, phosphorylated downstream signaling effector IRF3. In the KPC line, both administration of CYT387 as well as amlexanox were successful in decreasing phosphorylated IRF3 signaling in a dose-dependent manner (band strength was negatively correlated with drug concentration) (Fig 4.7 & 4.8). Regarding phosphorylated TBK1 activation, CYT387 and amlexanox induced a paradoxical increase in TBK1 activation, possibly due to a feedback response (Fig 4.7 & 4.8).

In iKras*p53* cells, amlexanox administration induced an increase in TBK1 phosphorylation as well. In both KPC and iKras*p53* cell lines, pharmacologic TBK1 inhibition via amlexanox decreased AKT signaling, as indicated by weaker phosphorylated AKT (Ser473) with increasing concentrations of drug (Fig 4.9). This

result is not necessarily surprising, as AKT has been shown to act as a direct substrate of TBK1(Tsichlis 2011). Amlexanox administration failed to affect MAPK or STAT3 signaling in either KPC or iKras*p53* cell lines (Fig 4.9). These results taken together suggested that TBK1 could possibly mediate signaling to AKT in PDAC cells. Since AKT signaling has been known to regulate aspects of tumorigenesis such as proliferation and apoptosis resistance in multiple types of malignancies(Testa & Tsichlis 2005; Altomare & Testa 2005), it was conceivable that TBK1 activation of AKT may play a functional, tumorigenic role in KPC and iKras*p53* cell lines. To test this question, we sought to use 3D culture to determine whether or not pharmacologic TBK1 blockade affected PDAC growth or survival.

To accomplish this, we grew PDAC cells in 3D culture for 6 days to induce formation of discrete PDAC clusters. At which point, increasing concentrations of TBK1 inhibitors CYT387 or amlexanox were added to the media. Clusters were treated for 4 days then analyzed under via brightfield microscopy to evaluate possible changes in growth. TBK1 inhibition by either compound failed to affect PDAC growth alone (Table 4.1). Furthermore, if TBK1 inhibitors were administered simultaneously with MEK inhibitor or PI3K/mTOR inhibitor, TBK1 inhibition failed to synergize with other small molecules to exacerbate PDAC death. These results taken together suggest that TBK1 function is dispensable for PDAC survival in vitro. Since our in vivo results suggest a functional, protumorigenic role for TBK1 in PDAC progression, yet TBK1 inhibition had no effect on epithelial PDAC function in vitro modeling of epithelial PDAC, we hypothesized that TBK1 may play a functional role in the immune compartment.

TBK1 inhibition disrupts PDAC epithelial-to-macrophage ccrosstalk

PDAC epithelial and stromal compartments engage in a complex exchange of signaling that has implications for tumorigenesis(von Ahrens et al. 2017; Zhan et al. 2017). For example, it has been shown in 2 separate models of murine PDAC that epithelial-cell-produced soluble GM-CSF can induce myeloid-derived cells to become immunosuppressive and halt CD8-mediated cytotoxicity(Bayne et al. 2012; Pylayeva-Gupta et al. 2012). iKras*p53* PDAC cells have the ability to secrete factors that induce macrophage polarization in vitro and increase the expression of macrophage Arginase, widely considered to be associated with the pro-tumorigenic "alternatively activated" macrophage phenotype(Rőszer 2015; Martinez & Gordon 2014) (Fig 4.10). This induction in phenotypic change is mediated by oncogenic Kras*, as cells that are deprived of doxycycline fail to induce polarization to the same degree as iKras*p53* PDAC cells wherein oncogenic Kras* expression is present for the entire experiment (Fig 4.10). We also tested transcriptional activation of growth factors and observed that conditioned media from Kras*-on iKras*p53* PDAC cells induced macrophages to increase expression of growth factors EREG and HB-EGF in vitro (Fig 4.11).

To determine whether or not TBK1 function affected the ability of macrophages to express protumorigenic genes in vitro, macrophages were administered either CYT387 or amlexanox in conjunction with conditioned media from Kras*-on iKras*p53* PDAC cells. Of the factors tested, we found that TBK1 inhibition specifically decreased expression of Monocyte Chemoattractant Protein-1 (MCP-1), a chemokine responsible

for positively regulating immune cell diapedesis and movement throughout inflamed tissue (Fig 4.12)(Deshmane et al. 2009). These results taken together suggest that TBK1 may play a protumorigenic role in PDAC in a non-cell-autonomous manner, as epithelial TBK1 blockade did not affect PDAC survival, but macrophage TBK1 blockade specifically blocked crosstalk between PDAC cells and macrophages in vitro. However, these results are not definitive and more in vivo analysis would ideally aid in uncovering the role of TBK1 in PDAC pathogenesis.

Discussion

In this set of experiments, we sought to test whether TBK1 played a functional role in PDAC pathogenesis in in vivo and in vitro models. We observed that in premalignant PDAC progression, TBK1 inhibition with JAK/TBK1 inhibitor CYT387 was successful in decreasing formation of PDAC precursor lesions following pancreatitis induction in iKras* mice, in vivo. This finding was consistent across morphologic and biochemical analysis of tissue. This finding, along with data suggesting that TBK1 expression was present and active in mouse pancreata, compelled us to determine whether TBK1 played a protumorigenic role in PDAC epithelial cells. While PDAC cells derived from KPC and iKras*p53* mice expressed active TBK1 and downstream components of the pathway, TBK1 inhibition with either CYT387 or Amlexanox was unsuccessful in abrogating PDAC growth or exacerbating growth inhibition via MAPK or PI3K inhibition in a 3D culture model. These results suggested that it is unlikely epithelial TBK1, though active, plays a significant role in tumorigenicity. Our focus then shifted to investigating the role of TBK1 activation in the stromal compartment. We

found that macrophages, activated and polarized by media from iKras*p53* PDAC cells, relied on TBK1 activity to express chemokine MCP-1 in vitro. This finding has in vivo implications, as macrophage recruitment and function has been found to be necessary for PDAC tumorigenesis(Zhang et al. 2017).

These findings suggest that TBK1 may play a role in the crosstalk between epithelial PDAC cells and macrophages; however, this relationship has yet to be tested definitively in vivo. There is mounting evidence that TBK1 plays a pro-inflammatory and pro-tumorigenic roles in epithelial malignancies, and its overexpression in PDAC is correlated with poorer prognosis(Song et al. 2015). Moreover, our findings suggest that epithelial PDAC cells express active TBK1 signaling and pharmacologic targeting of TBK1 decreases AKT activation; AKT is known to be upregulated and overactivated in PDAC, and its expression is correlated with poor patient survival(Schlieman et al. 2003; Yamamoto et al. 2004).

However, these results are eclipsed by the fact that TBK1 inhibition did not cause significant decrease in proliferation or increase in death of these cells in vitro, suggesting that while TBK1 may be active, its relative importance in terms of PDAC epithelial tumorigenesis may be minimal. This result may be due to a number of factors including: 1) intrinsic PDAC cell non-reliance on TBK1 signaling for proliferation and survival or 2) activation of compensatory signaling pathways in the context of pharmacologic TBK1 inhibition, leading to overall survival (feedback and compensatory signaling in the context of small molecule inhibition are well characterized phenomena in many

malignancies(Chen et al. 2017; Mirzoeva et al. 2009; Turke et al. 2012)). The definitive experiment to test this question in our system would be to genetically ablate TBK1 in PDAC cells in the 3D assay.

Regarding the stromal compartment, our data suggest TBK1 activation is necessary for macrophage upregulation of chemoattractant MCP-1 in response to PDAC-conditioned media. This result is interesting, as MCP-1 promotes myeloid cell recruitment, and myeloid cells seem to play a protumorigenic role in PDAC, as their ablation leads to decreased formation of PanINs (Zhang et al. 2017). These results taken together may suggest that TBK1 blockade could be beneficial in PDAC treatment. However, our experiments do not take into account other subpopulations of cells known to infiltrate PanINs and PDAC tumors (e.g. fibroblasts, cytotoxic CD8 cells). Furthermore, our in vivo data reflect TBK1's possible role in premalignant disease, and transformation may lead to a change in molecular signaling that could result in a change in the relative importance of TBK1 in PDAC pathogenesis. Regarding the therapeutic potential for TBK1 blockade in PDAC, more in vivo experimentation and analysis is needed in a malignant model.

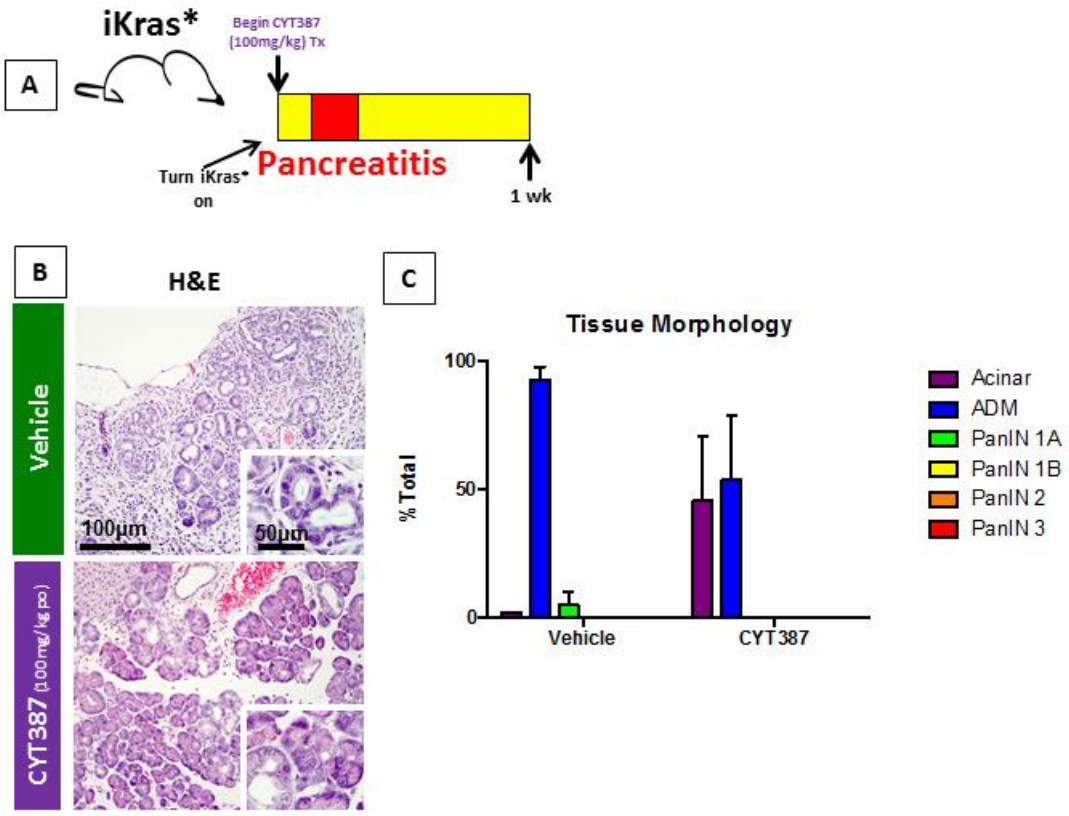

Figure 4.1 Small molecule JAK/TBK1 inhibition decreases PanIN formation in iKras* mice.

(A)Experimental mice were administered doxycycline via drinking water 72 hours prior to pancreatitis induction; concurrently, mice were randomized into vehicle and treatment experimental groups. Pancreatitis was induced via caerulein administration (75μg/kg) over a period of 48 hours. One week after, mice were randomized into vehicle or treatment groups and administered vehicle or CYT387 via daily intraperitoneal (ip) injection (10mg/kg/day) (vehicle, n=2, CYT387 n=3). (B) After 1 week, pancreata were harvested, fixed in formalin, embedded in paraffin and processed for immunohistochemical analysis. Tissue staining for hematoxylin/eosin is shown for representative mice. (C) Lesions were quantified via morphologic analysis by a blinded observer (Yaqing Zhang). (vehicle, n=2; CYT387 n=3)

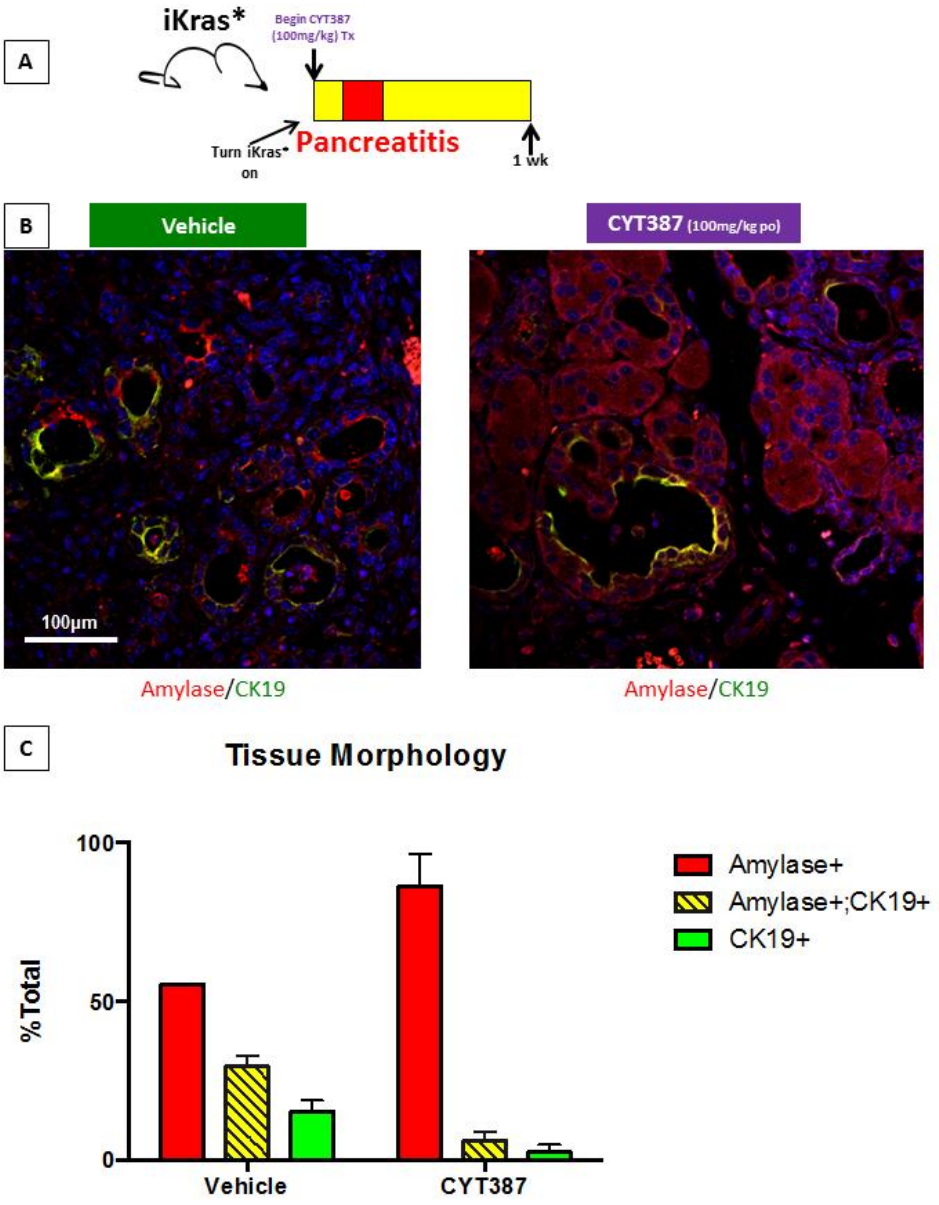

Figure 4.2 Small molecule inhibition of JAK/STAT3 decreases acinar-to-ductal metaplasia

Pancreata from experimental mice (**See Fig 4.1**) were analyzed immunofluorescently to determine the degree of acinar-to-ductal metaplasia. Amylase (expressed by normal acinar cells), is shown in red, while CK19 positivity (expressed by normal ductal cells) is shown in green. Quantification of amylase-positive and CK19-positive cells is graphed, mean±S.D. (vehicle n=2; CYT387 n=3; bars represent mean±S.D.)

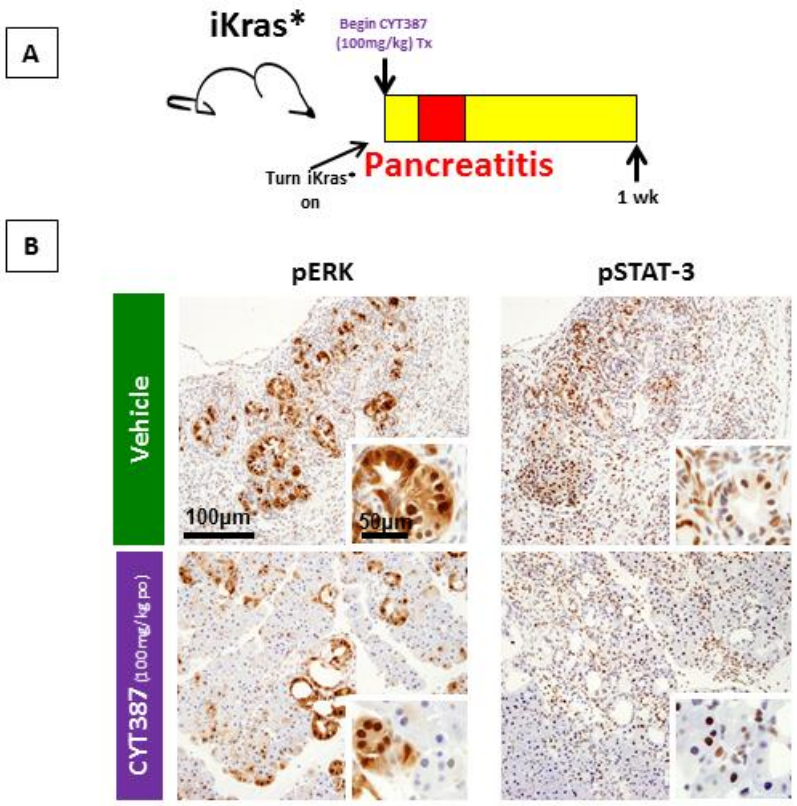

Figure 4.3 CYT387 fails to inhibit JAK/STAT signaling in iKras* mice.
Pancreata from experimental mice (**See Fig 4.1**) were analyzed by immunohistochemistry; brown staining indicates positivity. pERK=ERK1/2(pThr202/pTyr204) ; pSTAT-3= STAT-3 (pTyr705)

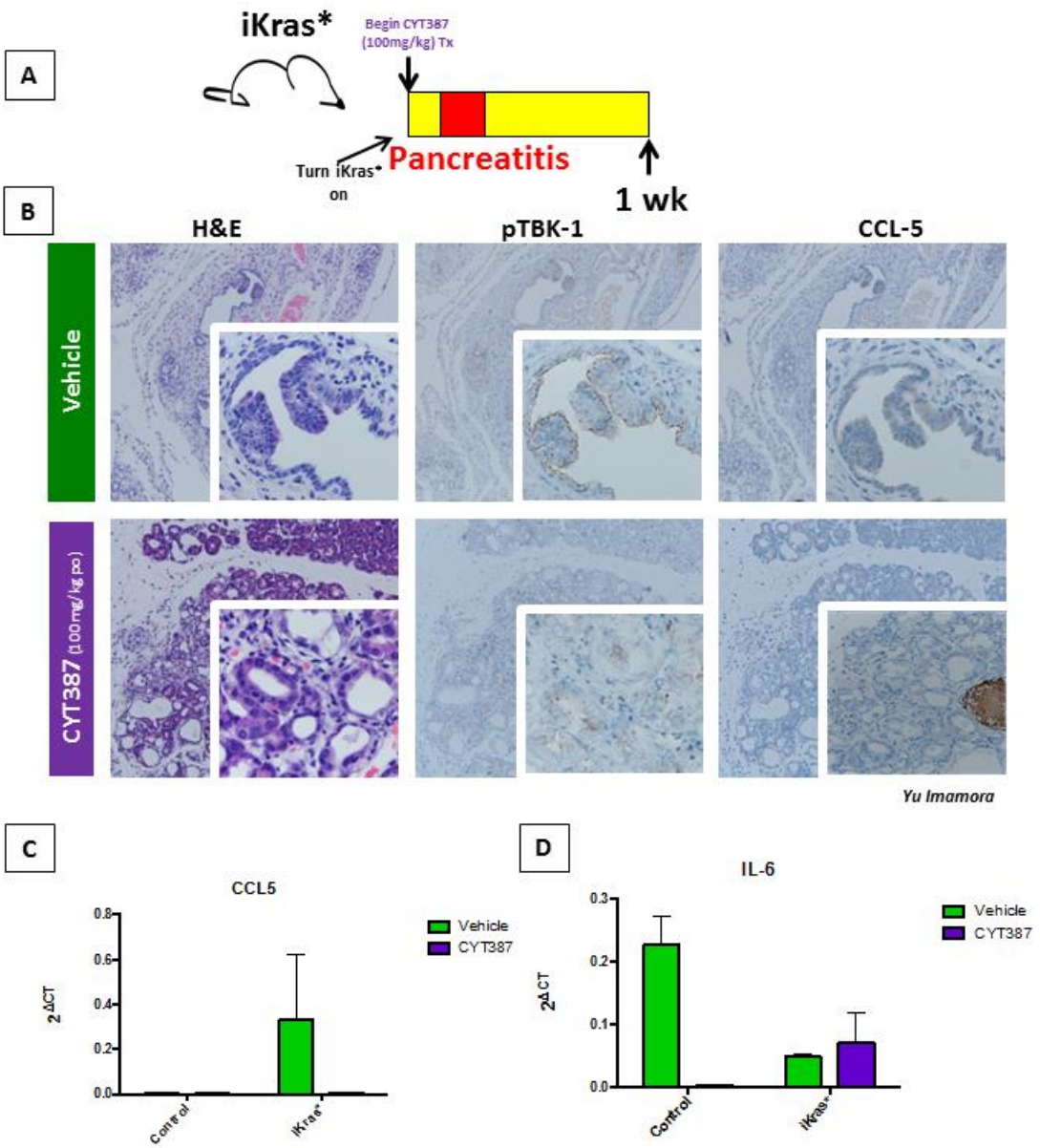

Figure 4.4 CYT387 decreases TBK1 activation and expression of target gene CCL5
(A) Pancreata harvested from iKras* mice 1 week after pancreatitis (**See Fig. 4.1**) were formalin-fixed, embedded in paraffin, sectioned and Hematoxylin/eosin stained or IHC-stained for visualization of corresponding antigens. Large panels are magnified 200x; insets 600x. pTBK1=TBK1(pSer172). CCL5=chemokine ligand 5 also known as RANTES (C) RNA was isolated from KC mouse pancreata tissue and analyzed via qPCR for corresponding gene targets. Stain credit: Yu Imamora.

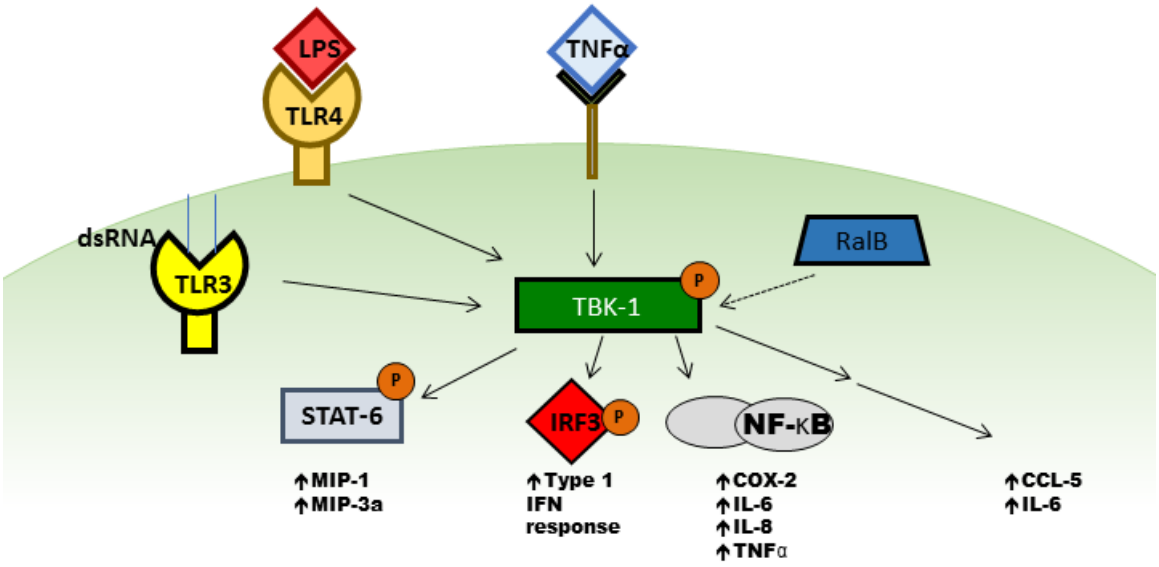

Figure 4.5 TBK-1 signaling overview.
Tank Binding Kinase 1 is a nodal protein that mediates signaling in many different contexts. Solid arrows indicate that the upstream protein mediates direct interaction, while dashed arrows indicate indirect activation. (P) indicates phosphorylation. (Helagson et. Al, 2013; Muvaffak et. Al 2014; Tsichlis, 2011)

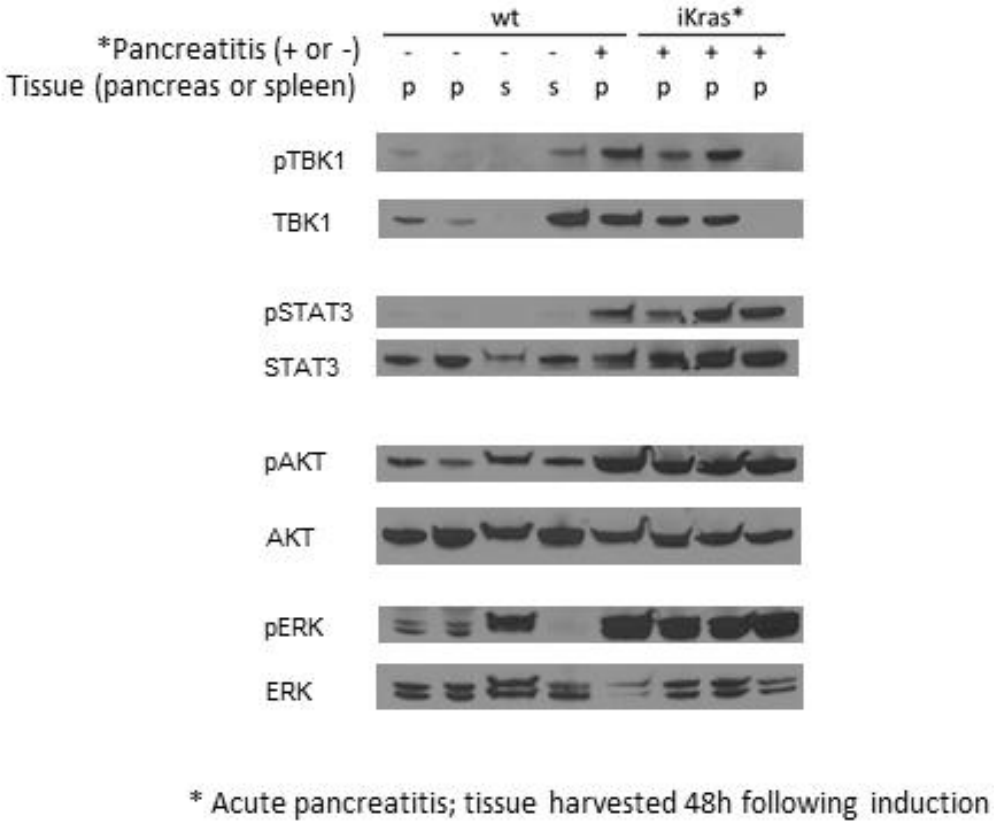

Figure 4.6 TBK1 becomes activated in normal and iKras* mice following pancreatitis.
iKras* or littermate controls were administered dox 72 hours prior to caerulein-induced pancreatitis, or 0.1% BSA in PBS vehicle (75μg/kg over 48 hours). Pancreata or spleens were harvested immediately following cessation of pancreatitis protocol, homogenized, and prepared for western blot analysis. "p" indicates phosphorylated species. pTBK1=TBK1(pSer172) pSTAT3=STAT3(pTyr705); pAKT=AKT (pSer473); pERK= ERK1/2 (pThr202/pTyr204

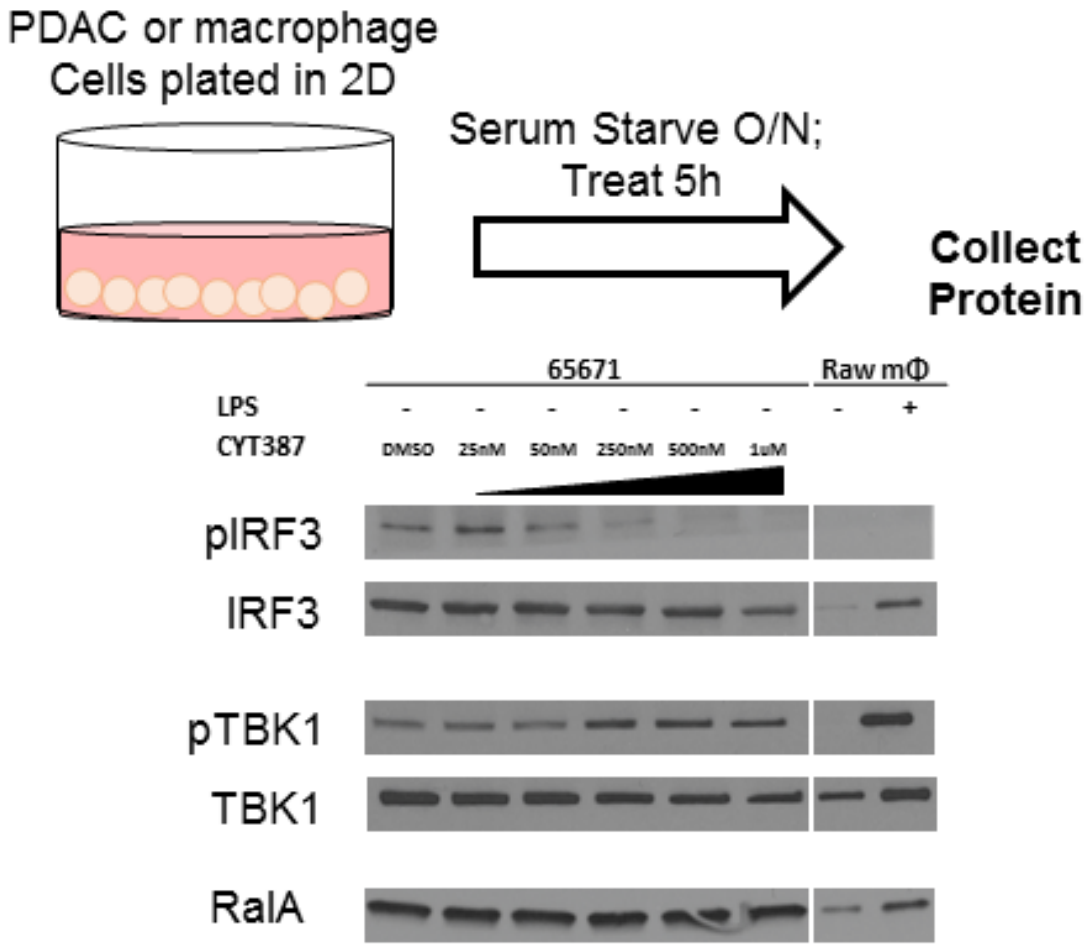

Figure 4.7 TBK1 is activated in KPC PDAC cells and CYT387 decreases activation of downstream effector IRF3 *in vitro*

PDAC (65671 cell line, derived from KPC mouse) or Raw 264.7 macrophages (positive control for TBK1 staining) were plated in 2D culture and grown to ~75% confluency in media containing full (10% FBS). At which point, cells were serum-starved (media +0.5%FBS) for 16 hours. Subsequently, cells were treated with increasing concentrations of CYT387 or Lipopolysaccharide (LPS) for 5 hours (reagents solubilized in media +0.5% FBS); then, cells were lysed and prepared for western blot. pIRF3=IRF3 (pSer396); pTBK1=TBK1 (pSer172)

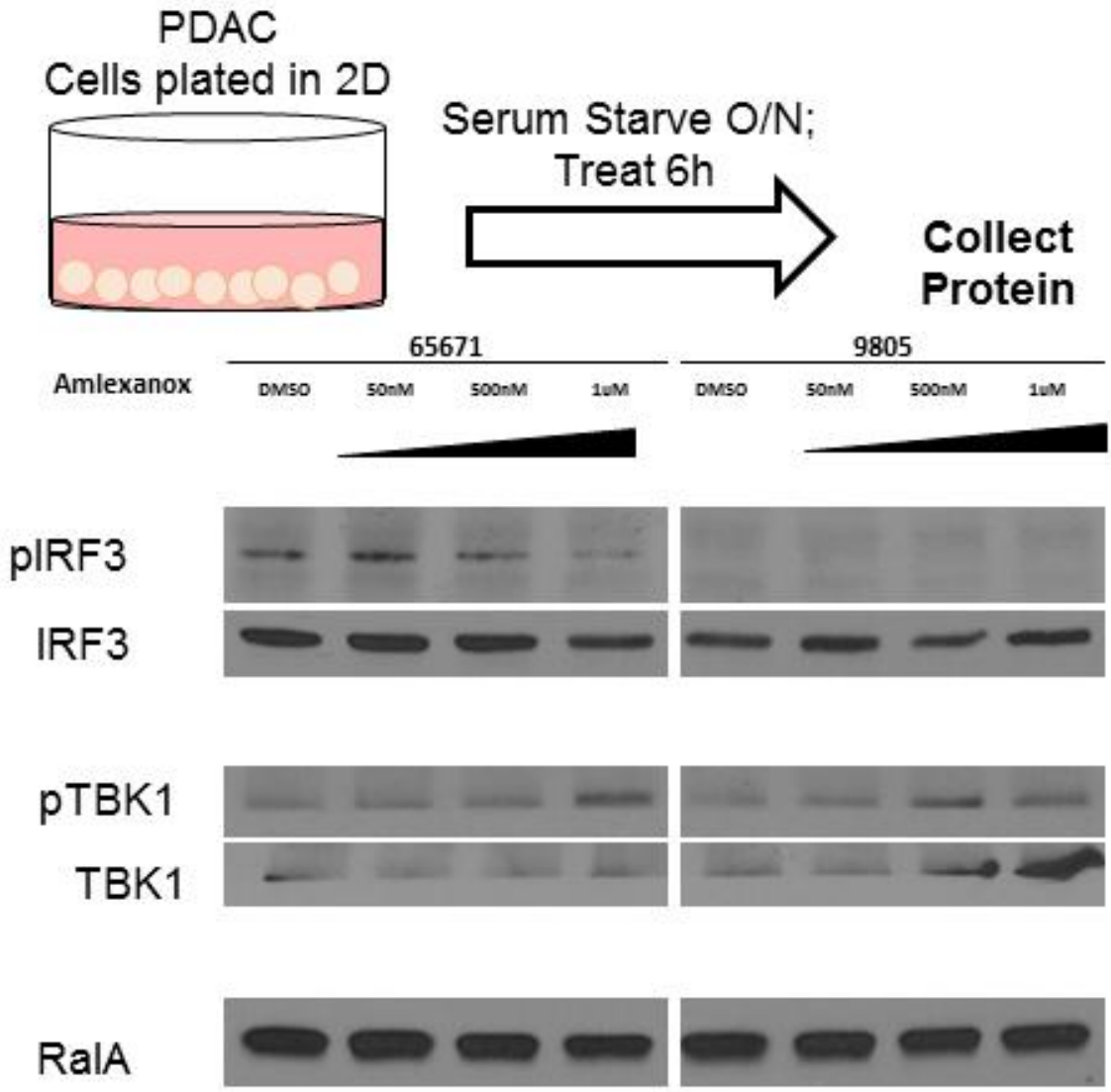

Figure 4.8 Amlexanox successfully targets TBK1 in KPC and iKras&p53* PDAC cells *in vitro*

PDAC cells from KPC mice (65671) or iKras*p53* mice (9805) were plated in 2D culture and grown to ~75% confluency in media containing full (10% FBS). At which point, cells were serum-starved (media +0.5%FBS) for 16 hours. Subsequently, cells were treated with increasing concentrations of TBK1 inhibitor Amlexanox for 6 hours (reagents solubilized in media +0.5% FBS); then, cells were lysed and prepared for western blot. pIRF3=IRF3(pSer396); pTBK1=TBK1(pSer172)

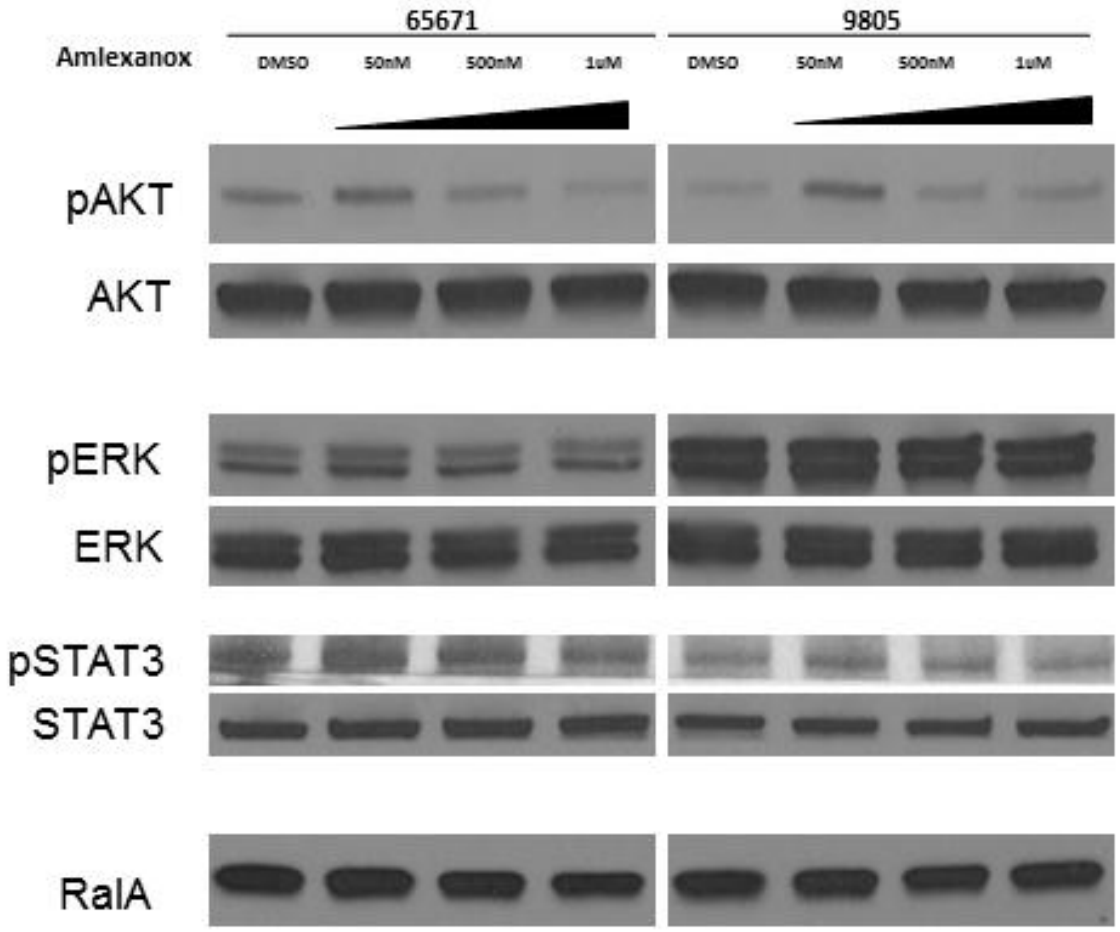

Figure 4.9 Amlexanox decreases PDAC AKT signaling *in vitro*
PDAC cells from KPC mice (65671) or iKras*p53* mice (9805) were plated in 2D culture and grown to ~75% confluency in media containing full (10% FBS) (See 4.11). At which point, cells were serum-starved (media +0.5%FBS) for 16 hours. Subsequently, cells were treated with increasing concentrations of TBK1 inhibitor Amlexanox for 6 hours (reagents solubilized in media +0.5% FBS); then, cells were lysed and prepared for western blot. pSTAT3=STAT3 (pTyr705); pAKT=AKT (pSer473); pERK=ERK1/2 (pThr202, pTyr204)

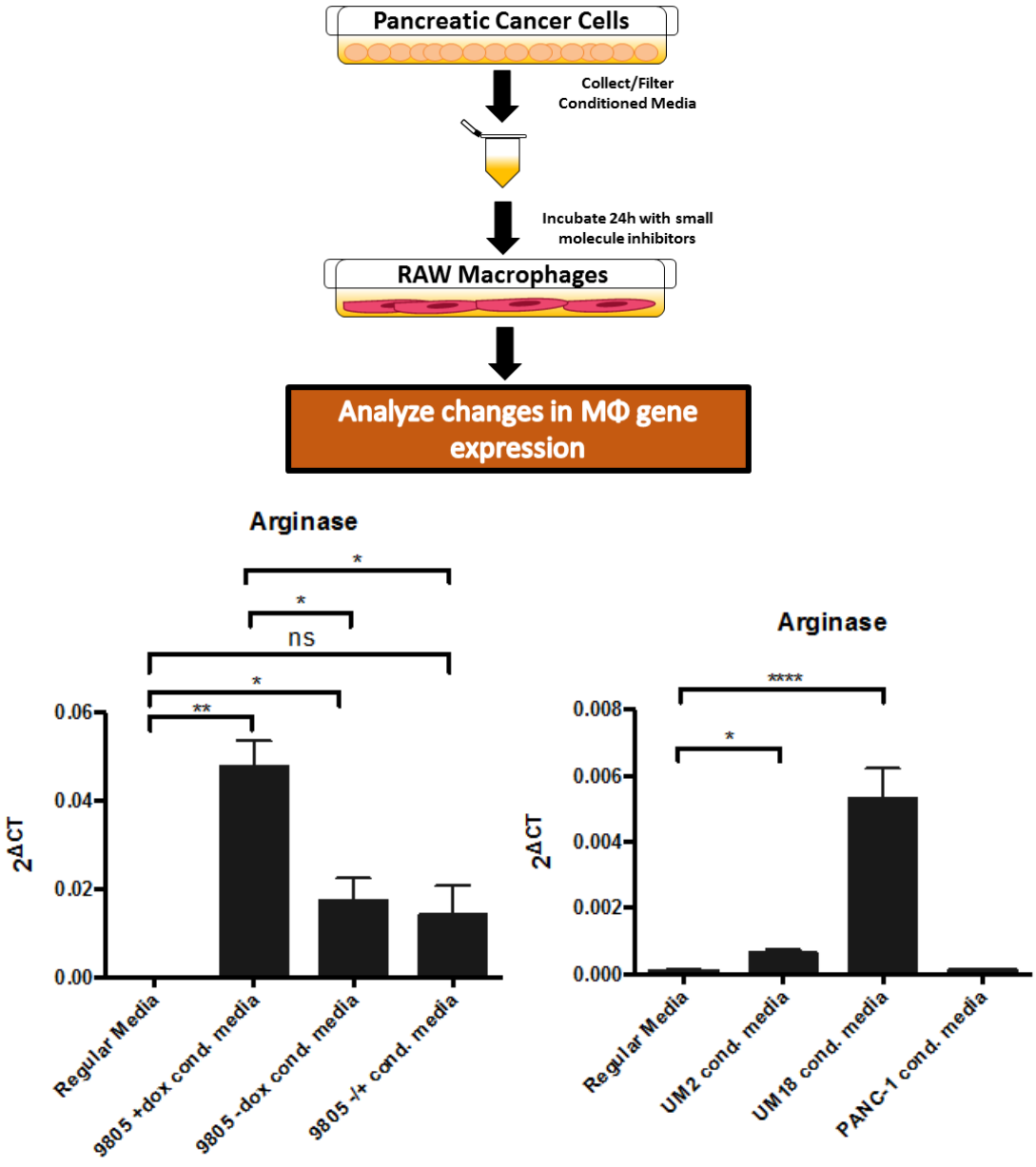

Figure 4.10 PDAC-cell conditioned media polarizes macrophages
Approximately 1x10^6 PDAC cells were seeded on 100mm plates. Either human PDAC lines or iKras*p53* PDAC cells (9805), randomized into 3 experimental groups (+doxycycline 4 days; -doxycycline 4 days; +doxycycline 2 days, then –doxycycline 2days) were used to condition culture media. On the final day, media was collected and strained using a 0.2µm strainer. Raw264.7 macrophages were grown to ~75% confluency in a 60mm cell culture dish. After, fresh media was combined with PDAC-conditioned media (1:1) and administered to Raw264.7 macrophages. After 24 hours, cells were collected, lysed, and RNA was isolated for qPCR analysis. Bars represent technical triplicate mean ± S.E.M. (n=1). Student's t test was used for statistical analysis. *=p<0.05; **=p<0.01; ****=p<0.001

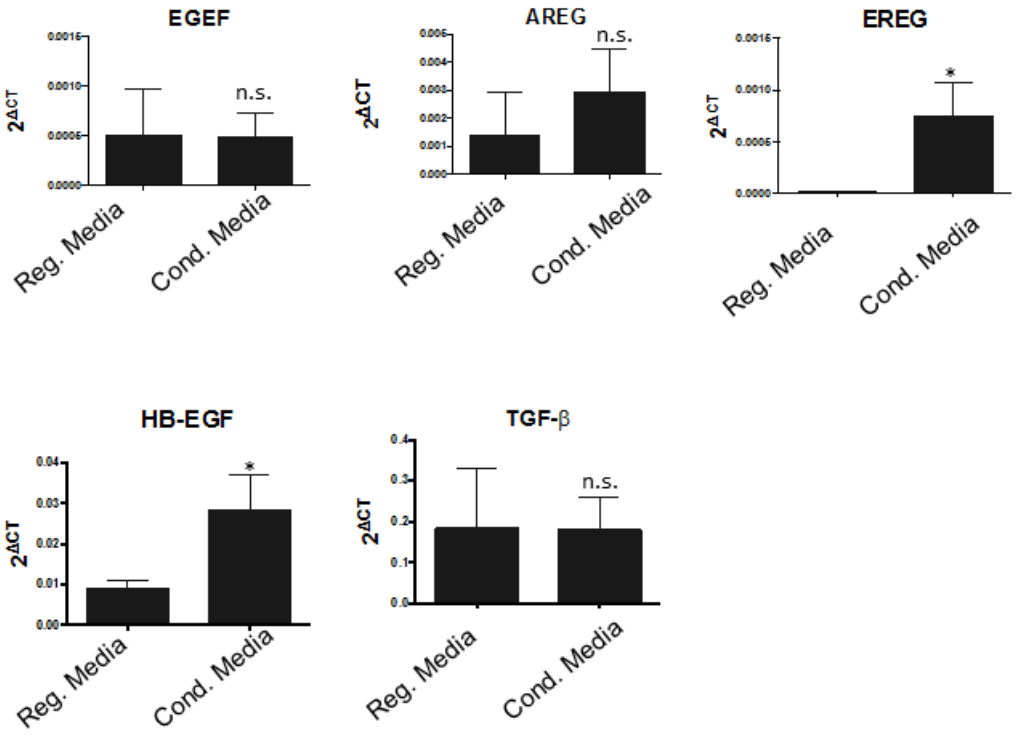

Figure 4.11 iKras*p53* PDAC conditioned media increases macrophage growth factor gene transcription

iKras*p53* PDAC cells (9805) were grown in doxycycline 4 days and conditioned media was collected and strained (**see Fig. 4.14**) Raw264.7 macrophages were grown to ~75% confluency in a 60mm cell culture dish. After, fresh media was combined with PDAC-conditioned media (1:1) and administered to Raw264.7 macrophages. After 24 hours, cells were collected, lysed, and RNA was isolated for qPCR analysis. Genes probed are listed as graph titles. Bars represent mean ± S.E.M. of technical triplicates (n=1). Student's t test was used for statistical analysis. *p<0.05; n.s. not significant

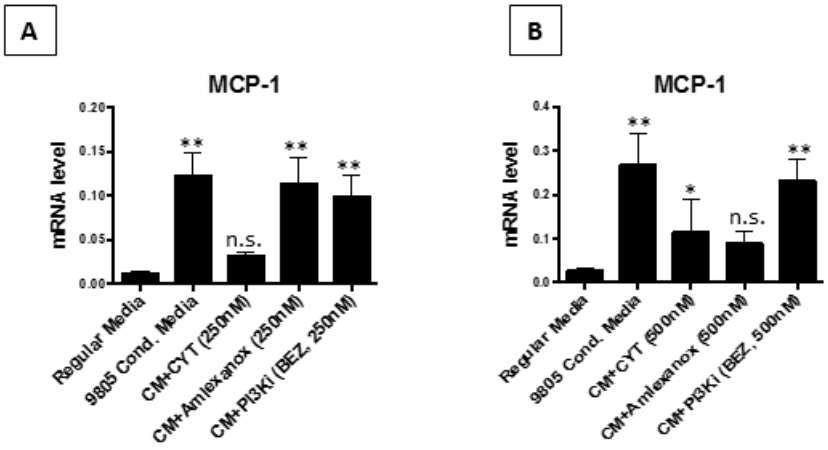

Figure 4.12 TBK1 blockade specifically decreases macrophage expression of chemoattractant MCP-1 *in vitro*

iKras*p53* PDAC cells (9805) were grown in doxycycline 4 days and conditioned media was collected and strained (**see Fig. 4.11**) Raw264.7 macrophages were grown to ~75% confluency in a 60mm cell culture dish. After, fresh media was combined with PDAC-conditioned media (1:1) and administered to Raw264.7 macrophages in conjunction with vehicle or drug (CYT=CYT387, BEZ=BEZ235). After 24 hours, cells were collected, lysed, and RNA was isolated for qPCR analysis. Bars represent mean ± S.E.M. of technical triplicates (n=1). Student's t test was used for statistical analysis. *$p<0.05$; n.s. not significant.

Chapter 4 Table

Cell line	Genotype	[TBKi] nM	[MEKi] nM	[PI3Ki] nM	Growth change compared to control
9805	iKras*;p53	25,250,500,1000	-	-	No change
9805	iKras*;p53	25,250,2500,5000	-	-	No change
8041	KPC	25,250,2500,5000	-	-	No change
13442	KPC	25,250,2500,5000	-	-	No change
Mcf7	Human breast cancer	25,250,2500,5000	-	-	No change
Mcf10a	Human breast cancer	25,250,2500,5000	-	-	No change
4T1	Murine breast cancer	25,250,2500,5000	-	-	No change
9805	iKras*;p53	CYT 25-5000	-	-	No change
9805	iKras*;p53	25,250,2500,5000	50	-	No change
9805	iKras*;p53	25,250,2500,5000	10	-	No change
9805	iKras*;p53	25,250,2500,5000	-	50	No change

Table 4.1 TBK1 inhibition fails to affect PDAC 3D growth *in vitro*
Cancer cells were grown in the "on-top" 3D culture system for 6 days and then treated with corresponding TBK1 inhibitor amlexanox for 4 days (unless otherwise noted: CYT=CYT387 JAK/TBK inhibitor). Brightfield microscopy was used to monitor cluster growth. In iKras*p53* PDAC cell lines, doxycycline was present in the media 100% of the time to induce and maintain expression of oncogenic Kas^{G12D}. MEKi=PD325901; PI3Ki=BEZ235.

References

von Ahrens, D. et al., 2017. The role of stromal cancer-associated fibroblasts in pancreatic cancer. Journal of hematology & oncology, 10(1), p.76.

Altomare, D.A. & Testa, J.R., 2005. Perturbations of the AKT signaling pathway in human cancer. Oncogene, 24(50), pp.7455–7464.

Barbie, D.A. et al., 2009. Systematic RNA interference reveals that oncogenic KRAS-driven cancers require TBK1. Nature, 462(7269), pp.108–112.

Bayne, L.J. et al., 2012. Tumor-Derived Granulocyte-Macrophage Colony-Stimulating Factor Regulates Myeloid Inflammation and T Cell Immunity in Pancreatic Cancer. Cancer cell, 21(6), pp.822–835.

Chen, C.-H. et al., 2017. MEK inhibitors induce Akt activation and drug resistance by suppressing negative feedback ERK-mediated HER2 phosphorylation at Thr701. Molecular oncology. Available at: http://dx.doi.org/10.1002/1878-0261.12102.

Collins, M.A., Brisset, J.-C., et al., 2012. Metastatic Pancreatic Cancer Is Dependent on Oncogenic Kras in Mice. PloS one, 7(12), p.e49707.

Collins, M.A., Bednar, F., et al., 2012. Oncogenic Kras is required for both the initiation and maintenance of pancreatic cancer in mice. The Journal of clinical investigation, 122(2), pp.639–653.

Deshmane, S.L. et al., 2009. Monocyte chemoattractant protein-1 (MCP-1): an overview. Journal of interferon & cytokine research: the official journal of the International Society for Interferon and Cytokine Research, 29(6), pp.313–326.

Fitzgerald, K.A. et al., 2003. IKKepsilon and TBK1 are essential components of the IRF3 signaling pathway. Nature immunology, 4(5), pp.491–496.

Helgason, E., Phung, Q.T. & Dueber, E.C., 2013. Recent insights into the complexity of Tank-binding kinase 1 signaling networks: the emerging role of cellular localization in the activation and substrate specificity of TBK1. FEBS letters, 587(8), pp.1230–1237.

Hruban, R.H. et al., 2006. Pancreatic Cancer in Mice and Man: The Penn Workshop 2004. Cancer research, 66(1), pp.14–17.

Kim, J.-Y. et al., 2013. Dissection of TBK1 signaling via phosphoproteomics in lung cancer cells. Proceedings of the National Academy of Sciences of the United States of America, 110(30), pp.12414–12419.

Korherr, C. et al., 2006. Identification of proangiogenic genes and pathways by high-throughput functional genomics: TBK1 and the IRF3 pathway. Proceedings of the National Academy of Sciences of the United States of America, 103(11), pp.4240–4245.

Martinez, F.O. & Gordon, S., 2014. The M1 and M2 paradigm of macrophage activation: time for reassessment. F1000prime reports, 6. Available at: http://dx.doi.org/10.12703/p6-13.

Mirzoeva, O.K. et al., 2009. Basal subtype and MAPK/ERK kinase (MEK)-phosphoinositide 3-kinase feedback signaling determine susceptibility of breast cancer cells to MEK inhibition. Cancer research, 69(2), pp.565–572.

Muvaffak, A. et al., 2014. Evaluating TBK1 as a therapeutic target in cancers with activated IRF3. Molecular cancer research: MCR, 12(7), pp.1055–1066.

Oral, E.A. et al., 2017. Inhibition of IKKε and TBK1 Improves Glucose Control in a Subset of Patients with Type 2 Diabetes. Cell metabolism, 26(1), pp.157–170.e7.

Pylayeva-Gupta, Y. et al., 2012. Oncogenic Kras-induced GM-CSF production promotes the development of pancreatic neoplasia. Cancer cell, 21(6), pp.836–847.

Reilly, S.M. et al., 2013. An inhibitor of the protein kinases TBK1 and IKK-ε improves obesity-related metabolic dysfunctions in mice. Nature medicine, 19(3), pp.313–321.

Rőszer, T., 2015. Understanding the Mysterious M2 Macrophage through Activation Markers and Effector Mechanisms. Mediators of inflammation, 2015, p.816460.

Schlieman, M.G. et al., 2003. Incidence, mechanism and prognostic value of activated AKT in pancreas cancer. British journal of cancer, 89(11), pp.2110–2115.

Sharma, S. et al., 2003. Triggering the interferon antiviral response through an IKK-related pathway. Science, 300(5622), pp.1148–1151.

Song, B. et al., 2015. miR-429 determines poor outcome and inhibits pancreatic ductal adenocarcinoma growth by targeting TBK1. Cellular physiology and biochemistry: international journal of experimental cellular physiology, biochemistry, and pharmacology, 35(5), pp.1846–1856.

Testa, J.R. & Tsichlis, P.N., 2005. AKT signaling in normal and malignant cells. Oncogene, 24(50), pp.7391–7393.

Tsichlis, P., 2011. Faculty of 1000 evaluation for IkappaB kinase epsilon and TANK-binding kinase 1 activate AKT by direct phosphorylation. F1000 - Post-publication peer review of the biomedical literature. Available at: http://dx.doi.org/10.3410/f.10579957.11681056.

Turke, A.B. et al., 2012. MEK inhibition leads to PI3K/AKT activation by relieving a negative feedback on ERBB receptors. Cancer research, 72(13), pp.3228–3237.

Wei, C. et al., 2014. Elevated expression of TANK-binding kinase 1 enhances tamoxifen resistance in breast cancer. Proceedings of the National Academy of Sciences of the United States of America, 111(5), pp.E601–10.

Yamamoto, S. et al., 2004. Prognostic significance of activated Akt expression in pancreatic ductal adenocarcinoma. Clinical cancer research: an official journal of the American Association for Cancer Research, 10(8), pp.2846–2850.

Yu, T. et al., 2012. The pivotal role of TBK1 in inflammatory responses mediated by macrophages. Mediators of inflammation, 2012, p.979105.

Zhang, Y. et al., 2017. Myeloid cells are required for PD-1/PD-L1 checkpoint activation and the establishment of an immunosuppressive environment in pancreatic cancer. Gut, 66(1), pp.124–136.

Zhan, H.-X. et al., 2017. Crosstalk between stromal cells and cancer cells in pancreatic cancer: New insights into stromal biology. Cancer letters, 392, pp.83–93.

Chapter 5. Discussion and Perspectives on Future Directions

Summary and Discussion

The major findings of my work implicate novel roles for cell adhesion and β1 integrin signaling in PDAC pathophysiology and resistance to small molecule inhibition. I found that in a 3D culture system, PDAC cells derived from iKras*p53* mice 1) recapitulated oncogenic Kras* dependency and Kras* effector activation (Chapter 2); relied on β1 integrin signaling for survival in the context of MEK inhibition (Chapter 3); and were dependent upon β1 integrin signaling to activate oncogenic Kras* effector signaling when physically separated from the ECM (Chapter 3). Moreover, in vivo and in vitro results suggest that TBK1 inhibition has minimal effect on PDAC cell function but may modulate epithelial:immune crosstalk (Chapter 4).

My findings suggest that PDAC cells show disparate reliance on MAPK signaling for survival, depending on whether or not they are in contact with ECM components (Fig 3.4). Cells lacking a physical interface with ECM components rely on MAPK signaling for anoikis resistance and are thus more sensitive to MEK inhibition via small molecule administration. Cells in contact with ECM components display a survival advantage in the context of MEK inhibition and form single-layered ductal structures, which have the morphologic appearance of polarized epithelia (though attempts to stain PDAC clusters for apical markers such as GM130 and αPKC were unsuccessful, data not shown).

At this point, the mechanism by which these cells resist anoikis is unclear. We have demonstrated that β1 integrin signaling is necessary, as ductal organization and survival were both inhibited upon co-administration of a β1 integrin neutralizing antibody (Fig 3.8-3.10). However, the distinct survival advantage of ECM-adjacent cells could reflect a number of biological processes, untested in this model. Namely, PDAC cell survival in the context of MAPK inhibition could be a reflection of 1) PDAC tumor cell heterogeneity: perhaps a subpopulation of PDAC cells are intrinsically resistant to MAPK inhibition; or 2) an adaptive response wherein the vast majority of PDAC cells possess the capability of forming lumen to maximize ECM contact/signaling, and the cells that happen to be adjacent to the ECM preferentially receive survival signaling (in this theoretical scenario, any PDAC cell has the intrinsic ability to resist MAPK inhibition, and survival is a reflection of a cell's happenstance--being in the right place at the right time).

This distinction, though nuanced, is an important one, as it has major implications for how we understand PDAC pathophysiology and the function of the ECM. If a subpopulation of cells is intrinsically more resistant to MAPK inhibition, the morphologic change and formation of ducts by these cells may have more relative importance than their interaction with ECM. For example, PDAC cells may change expression of membrane proteins, allowing for active excretion of drug, and morphologic change may manifest as a non-functional result. Drug efflux is a well-known characterized mechanism of cancer cell resistance, and it possibly accounts for resistance

in our 3D model(Gottesman et al. 2002; Fletcher et al. 2010). If PDAC cells were able to actively exclude drug, they may be able to continue to activate and rely on MAPK signaling. This scenario is unlikely, as IF analysis of pERK staining demonstrates complete blockade; however, it is possible that remaining PDAC cells upregulate MAPK signaling to a degree that is functionally relevant though undetectable by current tools. In this case, targeting interaction with the ECM in conjunction with Kras* effector blockade may fail to be an effective strategy in generating synthetic lethality.

Addressing the question of whether PDAC cell heterogeneity is the primary contributing factor to PDAC survival in the context of MAPK inhibition is theoretically relatively simple in this 3D culture setup. MEK inhibition can be used to select for surviving cells, and subsequently, I could trypsinize, isolate, and replate PDAC cells into the 3D culture system. After, I would essentially repeat the MEK inhibition assay, using the subpopulation of previously surviving cells as the seeding population in a second, tandem assay (as well as vehicle-treated PDAC cells as a control). These seeding populations differ in that vehicle-treated PDAC clusters would be comprised of ECM-adjacent and non-ECM-adjacent cells, whereas MEK-inhibited PDAC clusters would be comprised of significantly more ECM-adjacent cells. These cell populations would be seeded at equal density, grown into clusters, then re-treated with vehicle or MEK inhibitor. If tumor heterogeneity accounts for MEK resistance, then in this assay, previously MEK inhibited cells would show increased survival following a second round of MEK inhibition, compared to previously vehicle-treated cells.

Alternatively, the first step to determine whether or not ECM signaling plays a functional role in PDAC survival in the context of MEK inhibition would be deep characterization of ECM signaling machinery in our model. We have already explored small molecule blockade of focal adhesion kinase (FAK, Fig 3.6) and integrin-linked kinase (ILK, data not shown) in conjunction with MEK inhibitor administration and observed no difference when compared to singular MEK inhibition, suggesting that these popular mediators of ECM signaling do not play a functional role in PDAC survival in the context of MAPK inhibition (a genetic approach to knockdown either FAK or ILK would be needed to definitively confirm these findings and could be easily incorporated into the 3D assay). So, characterization of the ECM signaling machinery in vehicle-treated versus MEK-inhibited clusters would provide insight into possible mechanism; this could be achieved by transcriptional and protein expression characterization. The most attractive gene targets for qPCR analysis in PDAC cell clusters would be the integrin family of proteins, as β1 integrin represents only a fraction of integrin family proteins. These integrins may co-associate in alternative binding patterns, and it has been shown that distinct heterodimers play multifaceted roles in cell:cell and cell:adhesion signaling in a context dependent manner. Characterizing the integrin expression profile in these cells would provide insight into the cell's ability to interpret and transmit ECM signaling. Given the efficiency of the 3D culture model, it is possible to perform the proposed experiments in parallel.

A major finding described in this study is that non-ECM-adjacent PDAC cells rely on β1 integrin signaling in order to activate Kras* downstream effector signaling

(both MAPK and PI3K)(Fig 3.9). This observation is novel and counter-intuitive, as the vast majority of characterized substrates that activate β1 integrin signaling are ECM components. Further, PDAC cells that remain in contact with the ECM are able to upregulate oncogenic Kras* effector signaling, independent of β1 integrin activity. These results taken together confer a novel, protumorigenic role for β1 integrin in PDAC pathophysiology as well as the ECM. The molecular reasoning behind this differential reliance on β1 integrin signaling in the absence or presence of the ECM may be attributed to the importance of both upstream signaling and membrane dynamics, regarding Kras* activation. While mutated Kras* has decreased intrinsic GTPase ability, effectively locking the signaling molecule in the "on" state, it has been shown that some growth factor signaling is necessary to maintain oncogenic Kras* signaling and induce a positive feedback signaling loop that leads to growth factor synthesis and release(Ardito et al. 2012). It has also been shown that β1 integrin signaling can mediate growth factor signaling, and its inactivation can decrease Ras-mediated activation of downstream effector pathways(Bhowmick et al. 2001). Thus, it is conceivable that β1 integrin may mediate PDAC cell interpretation and propagation of growth factor signaling in non-ECM-adjacent cells.

Interestingly, I found in preliminary experiments that Kras* inactivation in the context of MAPK inhibition failed to exacerbate death (data not shown), suggesting that ECM-adjacent cells are able to survive MEK inhibition, independent of Kras* signaling. This finding has some precedence in the literature, as multiple groups, including ours, have shown that a subset of PDAC cells is able to escape "oncogene addiction" and

survive despite Kras* inactivation (Collins et al. 2012; Kapoor et al. 2014). Researchers found that in one model, survival in the context of Kras* inactivation relied on Hippo-pathway signaling; this pathway utilizes cell adhesion and interaction with the ECM to regulate organ size, cell proliferation, and anoikis(Zhao et al. 2012; Yu et al. 2015; Zeng & Hong 2008). These results taken with the observations in this study suggest that PDAC cell:cell adhesion and interaction with ECM components likely plays an important, formerly unrealized role in PDAC pathogenesis.

Major limitations

A major drawback to the group of experiments performed is that the vast majority of these assays were performed in a murine model of disease, which may not accurately reflect human disease. In fact, many treatments, including Kras* effector blockade with a MEK or PI3K inhibitor, yield tumor regression in mice but fail to be effective in eradicating human PDAC. To address this concern, human patient lines (commercial and primary) may be incorporated into the 3D model of PDAC growth. iKras*p53* PDAC cells were used here, as these cells allow for easily modifiable oncogenic Kras* expression, which can be used to test the necessity of Kras* in a variety of ways.

Another limitation in this model is failure to include stromal elements of PDAC disease which may contribute substantially to pathogenesis. Human PDAC tumors can be comprised of >50% nonneoplastic, stromal elements, including infiltrating fibroblasts, immune cells and vascular components(Waghray et al. 2013; Whatcott et al. 2013; Bijlsma & van Laarhoven 2015). Many models of disease have shown that these factors

can contribute to disease by affecting tumorigenicity. Moreover, the crosstalk between epithelial cells and other subpopulations in the stroma can play a significant role in PDAC pathogenesis. Our 3D model of PDAC, though it contains ECM components commonly found to be abundant in PDAC tumors, does not include immune cells. Thus, the results of MEK inhibition in vitro may not accurately reflect the effects of MEK inhibition in vivo in mice or humans. Global inhibition of MAPK signaling that would result from systemic small molecule treatment could potentially affect behavior of normal, stromal cells. Specifically, it has been shown that global MAPK inhibition prevents recovery from pancreatitis in the normal and non-malignant, neoplastic pancreas. Even if we were to discover a drug combination that would achieve synthetic lethality in PDAC epithelial cells, the presence of systemic MEK inhibitor may prevent tissue repair and lead to exacerbated disease(Halbrook et al. 2017; Collins et al. 2014).

References

Ardito, C.M. et al., 2012. EGF receptor is required for KRAS-induced pancreatic tumorigenesis. Cancer cell, 22(3), pp.304–317.

Bhowmick, N.A. et al., 2001. Integrin beta 1 signaling is necessary for transforming growth factor-beta activation of p38MAPK and epithelial plasticity. The Journal of biological chemistry, 276(50), pp.46707–46713.

Bijlsma, M.F. & van Laarhoven, H.W.M., 2015. The conflicting roles of tumor stroma in pancreatic cancer and their contribution to the failure of clinical trials: a systematic review and critical appraisal. Cancer metastasis reviews, 34(1), pp.97–114.

Collins, M.A. et al., 2014. MAPK signaling is required for dedifferentiation of acinar cells and development of pancreatic intraepithelial neoplasia in mice. Gastroenterology, 146(3), pp.822–834.e7.

Collins, M.A. et al., 2012. Metastatic pancreatic cancer is dependent on oncogenic Kras in mice. PloS one, 7(12), p.e49707.

Fletcher, J.I. et al., 2010. ABC transporters in cancer: more than just drug efflux pumps. Nature reviews. Cancer, 10(2), pp.147–156.

Gottesman, M.M., Fojo, T. & Bates, S.E., 2002. MULTIDRUG RESISTANCE IN CANCER: ROLE OF ATP-DEPENDENT TRANSPORTERS. Nature reviews. Cancer, 2(1), pp.48–58.

Halbrook, C.J. et al., 2017. Mitogen-activated Protein Kinase Kinase Activity Maintains Acinar-to-Ductal Metaplasia and Is Required for Organ Regeneration in Pancreatitis. Cellular and molecular gastroenterology and hepatology, 3(1), pp.99–118.

Kapoor, A. et al., 2014. Yap1 activation enables bypass of oncogenic Kras addiction in pancreatic cancer. Cell, 158(1), pp.185–197.

Waghray, M. et al., 2013. Deciphering the role of stroma in pancreatic cancer. Current opinion in gastroenterology, 29(5), pp.537–543.

Whatcott, C. et al., 2013. Tumor-stromal interactions in pancreatic cancer. Critical reviews in oncogenesis, 18(1-2), pp.135–151.

Yu, F.-X., Zhao, B. & Guan, K.-L., 2015. Hippo Pathway in Organ Size Control, Tissue Homeostasis, and Cancer. Cell, 163(4), pp.811–828.

Zeng, Q. & Hong, W., 2008. The Emerging Role of the Hippo Pathway in Cell Contact Inhibition, Organ Size Control, and Cancer Development in Mammals. Cancer cell, 13(3), pp.188–192.

Zhao, B. et al., 2012. Cell detachment activates the Hippo pathway via cytoskeleton reorganization to induce anoikis. Genes & development, 26(1), pp.54–68.